Solid State Nuclear Magnetic Resonance Spectroscopy of Polymer Thin Films: Chain conformation, Dynamics, and Morphology

by

Victor Fuad Nasreddine

A thesis submitted to the Faculty of Graduate Studies and Research in partial fulfillment of the requirements for the degree of

Doctor of Philosophy

Department of Chemistry
McGill University
Montreal, Quebec
Canada, H3A 2K6

November 2002

National Library
of Canada

Acquisitions and
Bibliographic Services

395 Wellington Street
Ottawa ON K1A 0N4
Canada

Bibliothèque nationale
du Canada

Acquisisitons et
services bibliographiques

395, rue Wellington
Ottawa ON K1A 0N4
Canada

Your file Votre référence
ISBN: 0-612-88538-0
Our file Notre référence
ISBN: 0-612-88538-0

Canada

Abstract

This dissertation presents solid-state NMR studies of the chain conformation, dynamics and morphology of three adsorbed polymer systems: two random semi-crystalline copolymers, poly(ethylene-co-acrylic acid) (PEA) and poly(propylene-co-acrylic acid) (PPA), and an amorphous homopolymer, poly(n-butyl methacrylate) (PnBMA). Zirconia (ZrO_2) was chosen as the substrate for all three polymers since the binding of carboxylic acids to this metal oxide is well understood. The choice of polymers was based on their particular bulk conformational and dynamic properties as well as their common use in polymer coatings. These studies are motivated by the general lack of a microscopic picture of adsorbed polymers, which can be provided by NMR, and the relevance of chain conformation and dynamics to important polymer film properties such as adhesion.

First the chain conformation and surface binding of adsorbed PEA as a function of acrylic acid content are characterized by ^{13}C cross polarization - magic angle spinning (CP-MAS), 2D ^{1}H-^{13}C wideline separation (WISE) and ^{1}H spin diffusion NMR experiments and FTIR-PAS (Fourier transform infrared photoacoustic spectroscopy) measurements. The most important finding is that the chain conformation of adsorbed PEA is determined primarily by the sticker group density rather than the surface coverage. The second study of PEA concerns the chain dynamics in the bulk and adsorbed states. Variable temperature NMR experiments provide evidence that ethylene segments of adsorbed PEA form partially folded loops rather than flat extended trains.

Finally ^{129}Xe NMR studies, used to probe the morphology of adsorbed PEA, show a bulk-like signal only for the highest loadings.

The second system investigated, PPA, is another semi-crystalline random copolymer which binds to zirconia via carboxylate linkages. The ^{13}C CP-MAS NMR spectra of adsorbed PPAC unexpectedly show splittings normally associated with chain-chain packing in the crystalline regions of bulk polypropylene (PP). The splittings in the spectra of adsorbed PPAC, which are more resolved than in bulk PPA, are proposed to arise from recrystallization of the PP segments between sticker groups.

Finally the interfacial properties of an amorphous homopolymer, PnBMA were studied using ^{13}C and ^{129}Xe NMR to characterize adsorbed and filled samples. PnBMA binds to zirconia via the partial hydrolysis of the ester side chains. The remaining ester chains of adsorbed PnBMA are found to segregate to the polymer/air interface. Both adsorbed and ZrO_2-filled PnBMA show enhanced local segmental mobility. However, the ^{129}Xe NMR measurements of the filled samples are consistent with restricted motion on a larger length scale which may be due to particle bridging.

Résumé

Dans cette thèse, nous avons étudié par RMN de l'état solide la conformation des chaînes, la dynamique et la morphologie de trois systèmes de polymères adsorbés: deux copolymères semi-cristallins aléatoires, poly(éthylène-co-acide acrylique) (PEAA) and poly(propylène-co-acide acrylique (PPAA), et un homopolymère amorphe, poly(methacrylate de n-butyle) (PMnBu). La zircone (ZrO_2) a été choisie comme substrat pour les trois polymères car la liaison des acides carboxyliques à cet oxyde métallique est bien comprise. Ces recherches ont été motivées par le manque général d'une image microscopique des polymères adsorbés, laquelle est fournie par la RMN, ainsi que par la pertinence de la conformation des chaînes et de leur dynamique dans des propriétés importantes des films polymériques, comme l'adhésion.

Premièrement, la conformation des chaînes et la morphologie du PEAA brut et adsorbé, en fonction de la teneur en acide acrylique, ont été caractérisées par plusieurs expériences RMN : ^{13}C CP-MAS, 2D WISE et diffusion de spin ^{1}H. Des mesures de FTIR-PAS (spectroscopie infrarouge photoacoustique par transformée de Fourier) ont montré que le PEAA est chimisorbé à la zircone par les groupes liants acide carboxylique. Le résultat le plus important est que la conformation de la chaîne du PEAA adsorbé est principalement déterminée par la densité de groupes liants plutôt que par la quantité adsorbée. La seconde étude avec le PEAA concerne la dynamique des chaînes dans les états bruts et adsorbés. Des expériences RMN à température variable ^{13}C CP-MAS, de relaxation spin-réseau et d'échange 2D apportent la preuve que les segments éthylène du PEAA adsorbé forment ,de façon préférentielle, des boucles repliées plutôt

que des structures planes, déployées. Enfin, la RMN du ^{129}Xe a été utilisée pour étudier la morphologie du PEAA adsorbé. En RMN du ^{129}Xe, un signal correspondant à la présence de polymère dans l'état brut est détecté seulement pour les densités de charge les plus élevées.

Le second système étudié, PPAA, est un autre copolymère semi-cristallin aléatoire qui se lie à la zircone par les groupes acide carboxylique. Les spectres ^{13}C CP-MAS du PPAA adsorbé montrent des dédoublements de lignes inattendus pour les carbones des groupes méthyles et méthylènes qui sont normalement associés avec l'empilment des chaînes dans les régions cristallines du polypropylène (PP) à l'état brut. Nous avons proposé que les dédoublements dans les spectres du PPAA adsorbé, qui sont mieux résolus que pour le PPAA brut, proviennent de la recristallisation des segments PP entre les groupes liants.

Enfin, les propriétés interfaciales de l'homopolymère amorphe, PMnBu ont été étudiées par RMN du ^{13}C et ^{129}Xe pour caractériser les échantillons adsorbés et chargés. Le PMnBu se lie à la zircone par hydrolyse partielle des chaînes latérales esters. Les chaînes esters restantes du PMnBu adsorbé se ségrègent à l'interface air/polymère. Le PMnBu adsorbé et le PMnBu chargé de ZrO_2 montrent une mobilité segmentaire locale accrue. Cependant, les mesures de RMN du ^{129}Xe NMR des échantillons chargés sont compatibles avec une liberté de mouvement restreinte à longue distance . La coexistence d'une mobilité locale accrue et d'une mobilité restreinte des chaînes à longue distance est peut-être dûe au pontage des particules.

Foreword

In accordance with guideline C of the "Guidelines for Thesis Preparation" (Faculty of Graduate Studies and Research), the following text is cited:

> "As an alternative to the traditional thesis format, the dissertation can consist of a collection of papers of which the student is an author or co-author. These papers must have a cohesive, unitary character making them a report of a single program of research. The structure for the manuscript-based thesis must conform to the following:
>
> Candidates have the option of including, as part of the thesis, the text of one or more papers submitted, or to be submitted, for publication, or the clearly-duplicated text (not the reprints) of one or more published papers. These texts must conform to the "Guidelines for Thesis Preparation" with respect to font size, line spacing and margin sizes and must be bound together as an integral part of the thesis. (Reprints of published papers can be included in the appendices at the end of the thesis.)
>
> The thesis must be more than a collection of manuscripts. All components must be integrated into a cohesive unit with a logical progression from one chapter to the next. In order to ensure that the thesis has continuity, connecting texts that provide logical bridges preceeding and following each manuscript are mandatory.

As manuscripts for publication are frequently very concise documents, where appropriate, additional material must be provided (e.g., in appendices) in sufficient detail to allow a clear and precise judgement to be made of the importance and originality of the research reported in the thesis.

In general, when co-authored papers are included in a thesis the candidate must have made a substantial contribution to all papers included in the thesis. In addition, the candidate is required to make an explicit statement in the thesis as to who contributed to such work and to what extent. This statement should appear in a single section entitled "Contributions of Authors" as a preface to the thesis. The supervisor must attest to the accuracy of this statement at the doctoral oral defence. Since the task of the examiners is made more difficult in these cases, it is in the candidate's interest to clearly specify the responsibilities of all the authors of the co-authored papers.

When previously published copyright material is presented in a thesis, the candidate must include signed waivers from the publishers and submit these to the Graduate and Postdoctoral Studies Office with the final deposition, if not submitted previously."

The thesis consists of seven chapters and include five papers (Chapters 2, 3, 4, 5, and 6) with a general introduction in Chapter 1 and conclusions and future work in Chapter 7. The papers have either been published in, submitted to, or to be submitted to scientific journals. A list of the papers is given below:

Chapter Two: "Conformation of Adsorbed Random Copolymers: A Solid-State NMR and FTIR-PAS Study" Nasreddine, V.; Halla, J.; Reven, L. *Macromolecules* **2001**, *34*, 7403-7410.

Chapter Three: "Dynamics of Adsorbed Polyethylene-Acrylic Acid Copolymers: A Solid-State NMR Study" Nasreddine, V.; Morin, F.; Reven, L. *submitted to Polymer*.

Chapter Four: "Probing the Morphology of Adsorbed Random Copolymers: A ^{129}Xe NMR study" Nasreddine, V.; Chijiwa, S.; Reven, L. *submitted to Langmuir*.

Chapter Five: "^{13}C Solid-State NMR of Adsorbed Polypropylene-Acrylic acid Copolymers" Nasreddine, V.; Morin, F.; Reven, L. *to be submitted*.

Chapter Six: "Dynamics and Morphology of Poly(n-butyl methacrylate) Films: A ^{13}C and ^{129}Xe Solid-state NMR study" Nasreddine, V.; Genereux-Vincent, T.; Reven, L. *to be submitted.*

Chapter Four consists of a paper to be submitted: "Probing the Morphology of Adsorbed Random Copolymers: A ^{129}Xe NMR study". All the results and experiments are performed by myself. Sachiko Chijiwa has helped me with setting up the Xenon gas loading apparatus and starting up this project. She also ran some experiments on the Unity 500 NMR spectrometer and helped me start those experiments on this spectrometer. This work has been already been published in *Polymer Preprints*.

I hereby give copyright clearance for the inclusion of the following papers, of which I am co-author, in the dissertation of Victor Nasreddine.

"Probing the Morphology of Adsorbed Random Copolymers: A ^{129}Xe NMR study"

Date: August 2, 2002

Ms. Sachiko Chijiwa

Chapter Five consists of a paper to be submitted: “Chain Conformation and Dynamics of Adsorbed Poly(propylene-co-acrylic acid) Random Copolymers”. All the CP-MAS and the FTIR experiments as well as all samples prepared are carried out by myself under the supervision of Prof. Linda Reven. Dr. Fred Morin has contributed to this work through his helpful suggestions as well as for critical reading of the manuscript. This work has already been published in *Polymer Preprints.*

I hereby give copyright clearance for the inclusion of the following papers, of which I am co-author, in the dissertation of Victor Nasreddine.

“^{13}C Solid-State NMR of Adsorbed Polypropylene-Acrylic acid Copolymers”

Date: 2003/1/10

Dr. Fred Morin
Manager of Solid-State NMR Facility
Department of Chemistry
McGill University

Acknowledgements

I am very grateful to Professor Linda Reven for the opportunity to work in her laboratory, for her supervision and expertise, as well as for her guidance and patience throughout my graduate study and writing my thesis and for financial support to attend several local and international conferences. Her passion and dedication to her work and research and her attention towards her students has inspired me. She has been a great advisor and mentor.

I am also indebted to Dr Fred Morin, the manager of the Solid-State NMR facility, for his help and guidance and for all the insightful discussions especially when Prof. Reven was away on sabbatical. I am very grateful for his expertise in Polymer Science and NMR Spectroscopy and for technical assistance and tips on using different NMR spectrometers and for critical reading of chapters 1, 3, 5, and 6 of my thesis. I would also like to thank Dr. Paul Xia, the manager of the Solution NMR facility, for his help on using the Unity 500 NMR spectrometer.

I would also like to thank all my coworkers in the lab past and present especially Shane Pawsey for his help and feedback about the NMR instrumentation and Andrew O'Donnell for buying equipment for the xenon gas loading apparatus and for proofreading chapter five of my thesis. I am also indebted to Sachiko Chijiwa for her help on starting up the demanding Xenon NMR project, for her dedication, and for all her work on running some of my samples and training me on the Unity 500 NMR spectrometer. I am very grateful for her assistance and wish her the best of luck for her career endeavors. I would like to thank Valerie Gandubert for the French translation of the abstract and Felaniaina Rakotondradany for the French translation of polymer names.

I would also like to thank all the faculty and staff at the Chemistry Department at McGill and especially the former Chairman and Director of Graduate Studies, Professors David Harpp and Bruce Lennox, and currently Professors Bruce Lennox and Masad Damha for their hard work, dedication, and for their continuous efforts for the well-being of graduate students. I would also like to thank Professor David Ronis, Robert Marchessault, Adi Eisenberg, and Chris Barrett for insightful scientific and career discussions and for being great mentors and all the members of my PhD thesis defense committee for their advice and for critical reading of my dissertation.

I greatly enjoyed my teaching assignments at the Chemistry Dept. especially the two years during which I gave the tutorials for the general chemistry course. I would like to thank Professors: Bryan Sanctuary, Masad Damha, Ariel Fenster, Joe Schwarz, and Chris Barrett for their help and guidance and for a very rewarding teaching experience.

I would like to thank Renee Charron and Chantal Marotte for their assistance and for always making sure that students are paid on time. For technical support I would like to thank: Rick Rossi, George Kopp for his glass blowing expertise for preparing Xenon NMR samples, Fred Kluck for his help with the Xenon gas loading apparatus, Intisar Hlil for DSC analysis, Prof. Alan Hay for helpful discussions, and Graig Hyett at the University of Montreal for using the FTIR spectrometer.

I would like to thank Prof. Hanadi Sleiman for her help, advice, and letters of recommendations when applying to graduate school at McGill as well as my Masters thesis advisor Prof. Rabih Sultan for his continuous guidance and letters of recommendations.

I would like to thank the Arndsten Group for being such good neighbors and the Barrett group as well as all my friends in the chemistry department, in McGill, and in Montreal. I hope I did not forget anyone.

I am deeply indebted and grateful for the financial support and recognition from the Chemistry Department, McGill University, FCAR Quebec, and NSERC Canada in the form of graduate scholarships and awards. These scholarships and awards had a profound effect on my well-being, my work and productivity, as well as on my career advancement.

Finally I dedicate this thesis to *my parents* for their love, encouragement, and for their financial and moral support throughout my education, without which this would not have been possible.

Table of Contents

Chapter One: Introduction

Chapter Two: Conformation of Adsorbed Random Copolymers: A Solid-State NMR and FTIR-PAS Study

Chapter Three: Dynamics of Adsorbed Polyethylene-Acrylic Acid Copolymers: A Solid-State NMR Study

Chapter Four: A ^{129}Xe NMR study of Adsorbed Polyethylene-co-Acrylic Acid Random Copolymers

Chapter Five: ^{13}C Solid-State NMR of Adsorbed Polypropylene-Acrylic acid Copolymers

Chapter Six: Dynamics and Morphology of Poly(n-butyl methacrylate) Films: A ^{13}C and ^{129}Xe Solid-state NMR study

Chapter Seven: Conclusions, Contributions to Knowledge, and Future Work

List of Abbreviations

Acronym	**Abbreviation**
2D-WISE	Two Dimensional Wideline Separation
ACQ	Acquisition
CH	Cyclohexane
CP	Cross Polarization
CP-MAS	Cross Polarization-Magic Angle Spinning
CSA	Chemical Shift Anisotropy
DD-MAS	Dipolar Decoupled- Magic Angle Spinning
DSC	Differential scanning calorimetry
FID	Free Induction Decay
FTIR-PAS	Fourier Transform Infra Red-Photoacoustic Spectroscopy
i-PP	Isotactic-Polypropylene
KHz	Kilohertz
LDPE, LLDPE, PE	Low density polyethylene, Linear Low density polyethylene, Polyethylene
MHz	Megahertz
NMR	Nuclear Magnetic Resonance
PEA	Poly(ethylene-co-acrylic acid)
PMMA	Poly(methyl methacrylate)

PnBMA	Poly(n-butyl methacrylate)
PPA	Poly(propylene-co-acrylic acid)
ppm	Parts per million
PS	Polystyrene
psi	Pound per square inch
SAM	Self-Assembled Monolayer
t_1	NMR evolution time
T_1, T_2	Spin-lattice, Spin-spin relaxation times in the laboratory frame
$T_{1\rho}$	Spin-lattice relaxation time in the rotating frame
t_2	NMR detection time
T_g	Glass Transition temperature
THF	Tetrahydrofuran
TOSS	Total Suppression of Spinning Side bands
Xe	Xenon
ZrO_2	Zirconia
$\Delta\upsilon_{1/2}$	Linewidth at half height
δ	Chemical shift
τ_m	Mixing time
τ, τ_c	Time delay or correlation time
ω	Larmor frequency

List of Tables

List of Figures

"Try not to become a man of success but rather to become a man of value"

Albert Einstein

"Science is organized knowledge. Wisdom is organized life"

Immanuel Kant

Dedicated to My Parents

* * *

Chapter One

Introduction

1.1 Preface

This chapter is a general introduction and consists of five main sections. The first is a brief introduction of polymers at surfaces and interfaces; the second, third, and fourth sections present the relevant theory and experiments of solid-state NMR, Xenon NMR spectroscopy, and FTIR-PAS and the last section is the objectives and scope of the thesis.

1.2 Polymers at surfaces and interfaces

Polymers are a very important class of materials whose properties and applications can be tailored by changing their structure and chemical composition. The wide interest in polymers and especially in polymer films and coatings stems from the significance of these materials in the fields of colloids and surface chemistry, protective coatings, adhesion, gas permeability, microelectronics, as well as polymer composites.

Polymer adsorption has been studied at the solid/liquid interface[1-4], and at the polymer/polymer and polymer/solid interfaces[5] and the latter include polymer adsorption at the interface between dissimilar polymer phases, and adsorption at planar or curved polymer/solid interfaces. Generally, interfaces involving polymers can be classified into five categories[6]:

(1) polymer/air interface

(2) polymer solution-colloid interface

(3) a symmetric polymer-polymer interface, which involves two similar polymers in contact with each other

(4) an asymmetric polymer interface, involving two different polymers

(5) a composite interface between a polymer and a non-polymer solid phase such as glass or inorganic particles. In this case the polymer adheres to the surface via physical or chemical bonding modes.

The way a polymer adsorbs on the surface, the total adsorbed amount, configuration, and mobility of the chains near the interface determine the properties and applications of a particular film. The simplest case involves the adsorption of a polymer from a dilute solution.[6,7a] Homopolymers and random copolymers adsorb randomly on a surface and adsorption is altered by the presence of certain functional groups. In general, polymer chains can adopt different configurations: trains with segments directly or nearly directly attached to the interface; loops that are unbound and connect trains, as well as tails, which are non-adsorbed chain ends (Figure 1.1). In the limit of a very low surface coverage, chains have the tendency to lie flat on the surface in a pancake configuration because this lowers the free energy. Terminally attached polymers adsorb via a single group or a block of segments resulting either in a brush or a mushroom conformation.

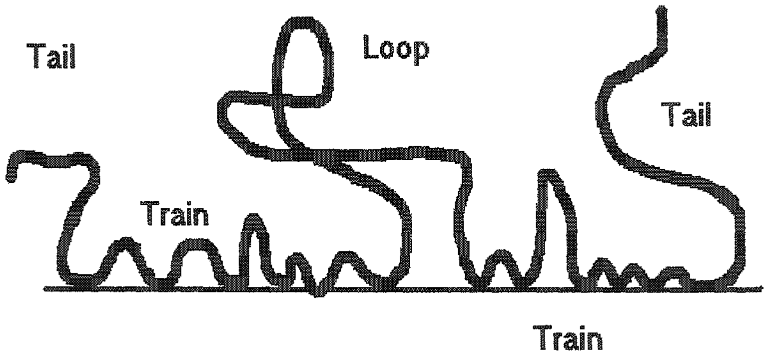

Figure 1.1 Schematic representation of a randomly adsorbed polymer.[7a]

Random (statistical) copolymers are widely used in many commercial applications such as adhesives, adhesion promoters, and dispersion stabilizers. They are usually not very different from homopolymers, with their average thermodynamic and structural properties being intermediate between those of the corresponding homopolymers with the different surface affinities of the monomer units affecting the chain configurations adopted at surfaces. The adsorption of random copolymers AB, with A having a higher surface affinity[4], can be classified into four classes:

(1) chains with a narrow molecular weight distribution but heterodisperse in composition. This will lead to segregation of A near the surface,

(2) chains heterodisperse in both aspects: Chains richer in A will adsorb unlike homopolymers in dilute solutions where longer chains adsorb preferentially. Chain composition is more important than that of chain length,

(3) blocky copolymers: This is the case when the monomer units are not distributed statistically but occur in sequences (blocks). This blockiness might lead to preferential adsorption of longer blocks,

(4) aggregation effects due to poorly soluble segments. In the limit of high concentrations, the solution may become a gel and the surface structure may become continuous with the bulk making it difficult to differentiate between chains in direct contact with the surface and those trapped in an adsorbed aggregate.

The mobility of polymers at surfaces and the glass transition temperature of polymer thin films[7b] are significant from a fundamental point of view, to investigate how mobility in thin films differs from the bulk, as well as from a practical perspective, since these properties are important in understanding properties such as adhesion and friction. The T_g of a polymer film is associated with discontinuities in quantities that are second derivatives of the free energy, such as the heat capacity or expansivity. In ellipsometry or X-ray reflectivity, the sharp change in the derivative of the thickness-temperature curve is associated with the T_g of the film and studies have shown that it can be lower or higher than the bulk T_g depending on the thickness, polymer/substrate interaction, and whether the film is freely standing or supported.

The relation between the microscopic properties of polymer films and their applications leads to the need of characterizing these materials and understanding their properties at the microscopic level. The methods generally used for interface characterization are mainly scattering techniques such as: Electron Spectroscopy for Chemical Analysis (ESCA), Auger Electron Spectroscopy (AES), Scanning Tunneling Microscopy (STM), Transmission Electron Microscopy (TEM), surface force techniques such as: Atomic Force Microscopy (AFM), as well as vibrational spectroscopy, typically in the ATR (Attenuated Total Reflection) mode.

Solution NMR techniques, based primarily on relaxation measurements, have been used to estimate the fraction bound to a surface, the chain conformation, and the mobility of polymers at the solid-liquid interface.[4,8] For example, Cosgrove and Barnett[8] used a combined NMR pulse sequence to simultaneously monitor solid and liquid spins. Recently Schonhoff et al.[9] used ^1H NMR to study the coil-to-globule transition of thermoreversible polymers adsorbed on colloidal silica and were able to distinguish between polymer chains adsorbed as trains or loops. Blum et al.[10a] studied the adsorption of poly(methyl methacrylate)-d (PMA) to silica from toluene solutions and used spin-lattice (T_1) and spin-spin (T_2) liquid state relaxation experiments to elucidate the structure of the adsorbed polymer as well as probe loops and tails. They performed solution ^2H NMR relaxation experiments to study the adsorption of block copolymers of polystyrene-vinylpyridine (PS-b-VP), deuterated in the backbone of the styrene block, onto colloidal silica.[10b,c] They used the variation in the ratio T_1/T_2 to compare dynamics of solvated polymer to the polymer adsorbed at the solid-liquid interface.

A large number of solid-state NMR techniques have been utilized to investigate chain conformation, dynamics, and morphology of bulk polymers[11] since structure over a wide range of length scales from nanometers to micrometers and dynamics from picoseconds to seconds can be probed. In contrast to its extensive use to characterize bulk polymers, solid state NMR has not been used frequently in the characterization of polymer interfaces for two major reasons[12]:

(1) it lacks the sensitivity of other spectroscopic techniques,

(2) it is difficult to differentiate between the interface and the large signals from the bulk material.

The first problem can be overcome by using samples having a very large surface area while the second can be addressed by performing specific NMR experiments that selectively observe signals from the interface while suppressing those outside the interface. Thus under these conditions multidimensional solid state NMR can give more insight into the nature of polymers at interfaces at the molecular level.

Some of the few NMR studies carried out for adsorbed polymers at the solid/air interface are those of Blum and coworkers[10d-f]. They observed that the peaks in the ^{13}C CP-MAS NMR spectrum of rubbery poly(isopropyl acrylate) (PIPA)[10f] narrowed upon adsorption onto silica. They attributed the broad lines in the bulk due to the interference of the motional frequencies with those of magic angle spinning or dipolar decoupling. Blum et al. have used solid-state ^{2}H NMR spectroscopy to study the adsorption of PMA-d at the silica/air interface and observed a mobility gradient as a function of the distance from the silica surface with the least mobile component located at the polymer/silica interface. ^{1}H to ^{29}Si CP-MAS has also been used to study the adsorption of poly(vinyl alcohol) (PVA). Upon deuteration of the exchangeable PVA and silanol protons, the efficiency of polarization transfer decreased indicating that the hydroxyl groups in PVA are the driving mechanism for the interaction of PVA with the silica.[13]

^{1}H solid-state NMR has recently been used to probe polymers at interfaces. Mirau et al.[14] have used fast magic-angle spinning solid-state proton NMR and multiple-quantum NMR to study the structure and dynamics of poly(ethyl acrylate) in bulk and polymerized in Vycor glass with 40 Å pores. While the polymer in the center of the pore has bulk-like mobility, it is motionally restricted at the surface of the pore. These techniques as well as ^{1}H-^{29}Si two-dimensional heteronuclear correlation and wideline separation NMR were also applied[14b] to probe the polymer-glass interface in the same system where they showed that the polymer fills the central 30 Å of the pore, and that the remaining volume is filled with surface hydroxyl groups and water. These studies demonstrate that these techniques can be applicable to a wide variety of low surface area materials because of the high sensitivity of proton NMR. Finally, solid-state multipulse ^{1}H NMR has also been used to study the morphology of poly(styrene-b-isoprene-b-styrene) triblock copolymers in clear and self-assembled polymer films and to measure domain sizes from ^{1}H spin diffusion experiments.[14c]

1.3 Solid State NMR and FTIR Spectroscopy

1.3.1 Overview

NMR spectroscopy is one of the most important techniques used to investigate the structure, dynamics, and morphology of polymers. The NMR spectra of solid polymers are different from polymers in solution because local interactions such as the chemical shift anisotropy (CSA) and dipolar couplings are not averaged to zero by molecular motion. Bond rotations and other motions in the chain backbone and side groups may partially average these interactions. For solid polymers the extent and nature of the averaging of these broadening interactions determines the techniques used to obtain high-resolution spectra. One needs to consider the nuclear spin Hamiltonian of the system in order to understand how nuclear spins interact with each other and with their surroundings to interpret solid-state NMR spectra. The Hamiltonian describing the spin system is[15,16]:

$$\mathbf{H} = \mathbf{H}_Z + \mathbf{H}_{RF} + \mathbf{H}_D + \mathbf{H}_{CS} \qquad 1.1$$

where $\mathbf{H}_Z$ is the Zeeman interaction (10^6-10^9 Hz) and is due to the coupling of the nuclear spins with the external static magnetic field $\mathbf{B}_0$; $\mathbf{H}_{RF}$ corresponds to the coupling of nuclear spins with the applied radiofrequency field $\mathbf{B}_1(t)$; $\mathbf{H}_D$ (0-10^5 Hz) is the dipole-dipole interaction of nuclear spins through their magnetic moments; $\mathbf{H}_{CS}$ (0-10^5 Hz) describes the chemical shift due to the screening of nuclei from B_0 by surrounding electrons, and is usually anisotropic. Three interactions have been omitted from Equation

1.1: $\mathbf{H_Q}$ (0-10^9 Hz) which represents the coupling of nuclear spins with quadrupole moments (I > ½) and electric field gradients. This is neglected since only NMR experiments of spin ½ nuclei are performed. $\mathbf{H_J}$ (0-10^4 Hz) the indirect electron-coupled nuclear spin interaction (scalar coupling) is negligible in the solid state. $\mathbf{H_{SR}}$ which describes the spin-rotation interaction and corresponds to the coupling nuclear spins and magnetic moments associated with molecular angular momentum is also neglected.

The Zeeman interaction occurs for all nuclei with nuclear spin I different than zero, resulting in 2I +1 energy levels. The Hamiltonian is

$$\mathbf{H_Z} = -\gamma \hbar B_0 I_Z \quad = \quad -g_N \beta_N B_0 I_Z \qquad 1.2$$

where γ is the magnetogyric ratio, g_N the nuclear g factor, and β_N the Bohr magneton of the nucleus. At higher magnetic fields, larger separations occur, resulting in an increase in the population difference between nuclear energy levels and an increase in sensitivity. The dipolar Hamiltonian expression for a solid with two unlike spins I and S is:

$$\mathbf{H_D} = \mathbf{H_{IS}} = \frac{\gamma_I \gamma_S \hbar^2}{r_{IS}^3} \vec{I} \bullet \hat{D} \bullet \vec{S} \qquad 1.3$$

where r_{IS} is the internuclear separation and $\hat{D}$ the dipolar coupling tensor. This interaction depends on the magnitude of the magnetic moments and it falls off rapidly as

($1/r^3$) with internuclear distance. Linewidths are broadened by this interaction in the solid state and it can go up to 190 kHz for a ^{1}H-^{1}H pair in a H_2 molecule.

The chemical shift interaction is due to the shielding effect on the nucleus of the fields created by the surrounding electrons and is expressed as

$$\mathbf{H}_{CS} = \gamma_I \hbar \vec{I} \bullet \hat{\sigma} \bullet \vec{H} \qquad 1.4$$

The interaction is stronger at higher magnetic fields and since it is very sensitive to the geometry of neighboring atoms. $\hat{\sigma}$ is the chemical shift tensor and is expressed in terms of a 3 x 3 matrix which by choosing the correct choice of co-ordinate system can be diagonalized. The remaining diagonal elements are used to determine the isotropic chemical shift δ_{ISO}.

$$\begin{bmatrix} \sigma_{11} & \sigma_{12} & \sigma_{13} \\ \sigma_{21} & \sigma_{22} & \sigma_{23} \\ \sigma_{31} & \sigma_{32} & \sigma_{33} \end{bmatrix} \rightarrow \begin{bmatrix} \sigma_{xx} & & \\ & \sigma_{yy} & \\ & & \sigma_{zz} \end{bmatrix}$$

The average or isotropic shift is

$$\delta_{ISO} = \frac{\sigma_{xx} + \sigma_{yy} + \sigma_{zz}}{3} \qquad 1.5$$

1.3.2 Experiments

1.3.2.1 One Pulse/Cross-Polarization (CP):

The single pulse NMR experiment[15] is the simplest single-resonance experiment. Its pulse sequence consists of a single pulse applied at the ^{13}C frequency which transforms the magnetization along the z-axis into the x-y plane creating transverse magnetization. A Free Induction Decay (FID) is then acquired during irradiation of the ^1H resonance frequency to eliminate heteronuclear coupling between ^1H and ^{13}C. The FIDs are accumulated from a large number of scans and are then Fourier transformed to give the NMR spectrum. To obtain NMR spectra with good signal to noise, the time between pulses (recycle delay *rd*) should be five times or at least three times the spin-lattice relaxation time T_1 so that the magnetization has enough time to return to equilibrium (along z-axis). The experiment is very similar to the one used in solution NMR except that the decoupling field used is much stronger for solids. In some solid polymer samples for example, the T_1 can be very long making the recycle delay very long and the experiments become very time consuming. This makes the experiment particularly useful for observing mobile and disordered components that have a short T_1. The pulse sequence is shown in Figure 1.2.

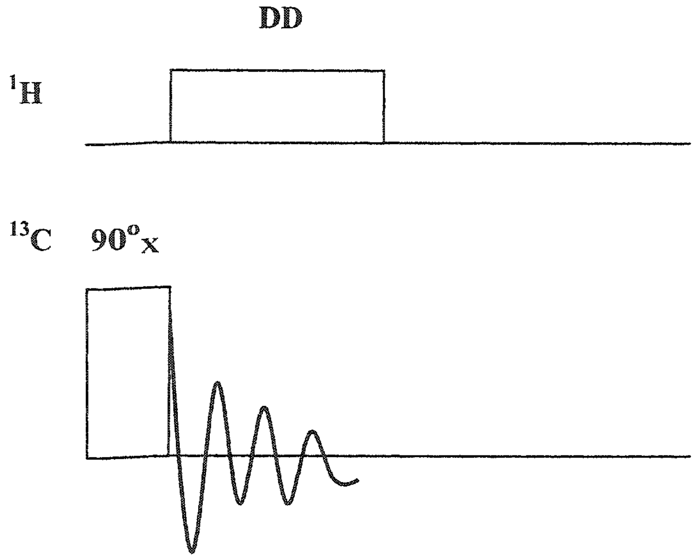

Figure 1.2 The pulse sequence of a single pulse NMR experiment with decoupling.[15]

To overcome the drawback of long T_1 values, which render the single pulse experiment inefficient, the abundant ^{1}H spin system is used as the source of magnetization for the ^{13}C signal. The process is called cross-polarization (CP) and is usually used to increase the signal of rare, low γ (magnetogyric ratio) nuclei such as ^{13}C, ^{31}P, ^{29}Si by transferring magnetization from abundant, high γ nuclei, such as ^{1}H or ^{19}F. The recycle delay in a ^{1}H-^{13}C CP experiment is five times the proton spin-lattice relaxation time thus making the experiment much shorter and the signal is enhanced in the ratio of the resonance frequencies ^{1}H/^{13}C ~ 4. CP is a double resonance experiment where the ^{1}H spins are initially spin locked in the rotating frame. Cross-polarization is achieved by switching on a resonant ^{13}C rf field with an amplitude satisfying the Hartmann-Hahn[17] matching condition

$$\gamma_H B_{1H} = \gamma_C B_{1C} \quad \textbf{1.6}$$

^1H and ^{13}C spins now have the same effective precession frequency around their respective B_1 fields, and they can exchange energy via their dipolar interactions. The ^{13}C magnetization builds up initially with a time constant T_{CH} which is characteristic of the strength of the dipolar coupling between protons and carbons. As the cross-polarization time, t_{CP}, increases the magnetization passes through a maximum and then diminishes due to the influence of the spin relaxation processes in the rotating frame ($T_{1\rho H}$ and $T_{1\rho C}$).[18,19] The pulse sequence of a CP experiment is shown in Figure 1.3. The ^{13}C magnetization $M(t_{CP})$ builds up according to the following expression:

$$M(t_{CP}) = (M_0/\lambda)[1 - \exp\{-\lambda t_{CP}/T_{CH}\}]\exp\{-t_{CP}/T_{1\rho H}\} \quad \textbf{1.7}$$

where $\lambda = 1 + (T_{CH}/T_{1\rho C}) - (T_{CH}/T_{1\rho H})$.

Multiple homonuclear dipole-dipole couplings among ^1H usually result in one $T_{1\rho H}$ for the sample. $T_{1\rho C}$ and T_{CH} are different for different carbons of the molecule and an estimate of their values is needed for a quantitative analysis of CP signals.[20] For rigid systems, carbons bonded directly to protons can cross polarize more rapidly than those not bonded to protons or those bonded to protons in mobile systems where dipole-dipole couplings are weak and motionally averaged. CP experiments are usually performed with magic angle spinning (MAS), which reduces the chemical shift anisotropy as well as the dipolar couplings, giving rise to higher resolution spectra.

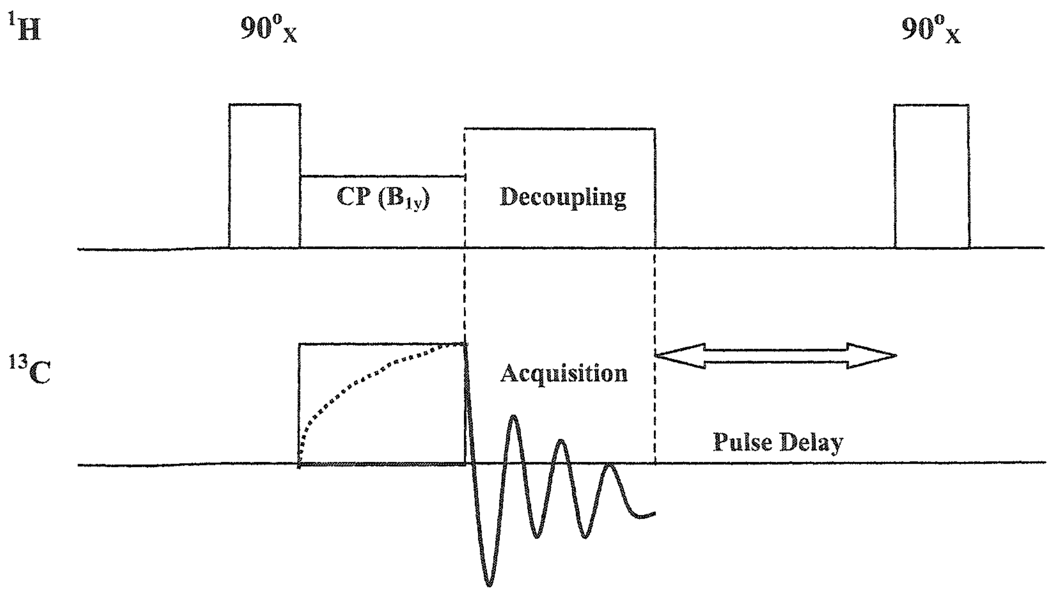

Figure 1.3 The sequence of the Cross-Polarization (CP) experiment.[15]

MAS is the mechanical spinning of the sample around an axis making an angle of 54.7° with the direction of the magnetic field B_0. The angle is called the "magic angle" since it results in narrowing of NMR lines of solids. The technique was introduced by E.R. Andrew[21] in 1954 as a method to obtain high resolution NMR spectra of solids by averaging out interactions in solids like chemical shift anisotropy (CSA) and dipolar coupling that lead to line broadening. At the magic angle, $\theta = 54.7^{\circ}$ and the term $(3\cos^2\theta - 1)$ in the dipolar and CSA Hamiltonians is zero thus eliminating the CSA and dipolar couplings.

If the rotor spinning frequency is less than the anisotropy interaction, spinning side bands are obtained. Although these spinning side bands provide information about the anisotropies of the spin interactions, they might overlap with the isotropic chemical shifts complicating the interpretation of spectra. The most commonly used pulse sequence used to modulate or suppress these spinning side bands is the TOSS (Total Suppression of Spinning Sidebands) sequence.[22] It consists of a set of four 180° pulses at well defined times t_1, t_2, t_3, and t_4 before the acquisition period. The timing of these pulses is selected so that the magnetization giving rise to the sidebands is eliminated resulting in a spectrum that only contains peaks at the isotropic chemical shifts.

1.3.2.2 2D Wide line Separation Experiment (2D-WISE):

^{1}H homonuclear dipolar couplings in rigid solids give rise to broad and featureless lines making it difficult to resolve the resonances corresponding to different components of the system. Molecular motion narrows these broad lines and in the limit of extremely fast isotropic motion, the lines resemble those in solution spectra. Schmidt-Rohr et al.[23] have designed a two-dimensional heteronuclear solid state NMR experiment that overcomes this problem via ^{13}C isotropic chemical shifts. The simplest version of this experiment is derived from the standard CP-MAS experiment by placing an incremented delay t_1 after the initial ^{1}H 90° pulse. This makes it possible to detect the decay of proton magnetization through amplitude modulation of the ^{13}C signal generated by CP. Fourier transformation over t_1 and t_2 yields a 2D dimensional spectrum correlating mobility (^{1}H linewidth) to structure (^{13}C chemical shift). The sequence is shown in Figure 1.4. After a 90° ^{1}H pulse, transverse magnetization is created which then decays during the incremented evolution time t_1 due to dipolar couplings with the rigid components decaying faster than mobile ones. The extent of this decay is monitored by cross-polarization to ^{13}C and acquiring the FID during t_2 under decoupling conditions.

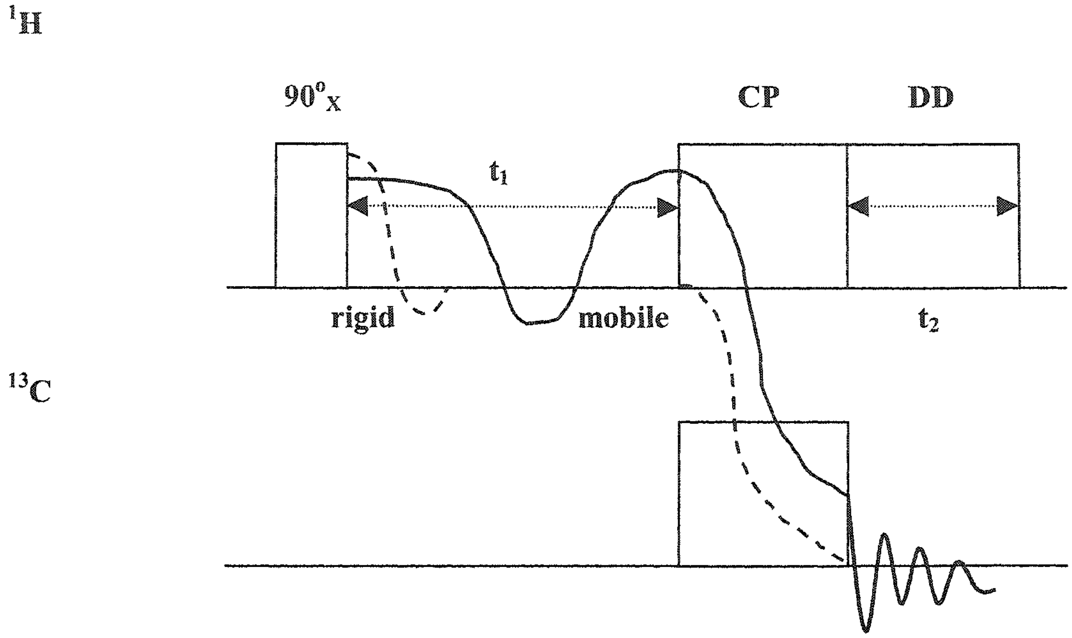

Figure 1.4 The basic pulse sequence of a 2D-WISE NMR experiment.[23]

1.3.2.3 NMR Relaxation parameters:

Spin-lattice relaxation or longitudinal relaxation (T_1) corresponds to the process in which the spins exchange magnetization with their surroundings, the lattice. There are several ways to measure T_1. In the inversion recovery experiment, the system is initially at equilibrium with the spins occupying levels according to the Boltzmann distribution resulting in a net magnetization vector, M_0, along the z-axis (B_0 direction). After applying a 180° pulse, transverse magnetization is inverted. Before applying the second pulse, we have to wait a certain time till the magnetization has relaxed back to the z-axis. Plotting the variation of the population difference (M_z) as a function of time τ, we obtain an exponential curve starting at $-M_0$ and increasing towards the Boltzmann equilibrium value with a time constant T_1, the spin-lattice relaxation time. The Boltzmann equilibrium nuclear magnetization is M_0, and the actual longitudinal magnetization M_Z rises back to the M_0 value exponentially according to this equation[24]:

$$M_Z = M_0[1 - 2\exp(-\tau / T_1)] \qquad \textbf{1.8}$$

The inversion-recovery pulse sequence 180°-τ-90° is shown in Figure 1.5. The whole pulse sequence is repeated for different values of τ and the plot of M_Z as a function of τ yields an exponential curve according to equation 1.8. The value at which M_Z equals zero is called the null point at which $\tau = \tau_n$ where

$$\tau_n = 0.693\ T_1 \qquad \textbf{1.9}$$

and this gives an estimate of the T_1 value.

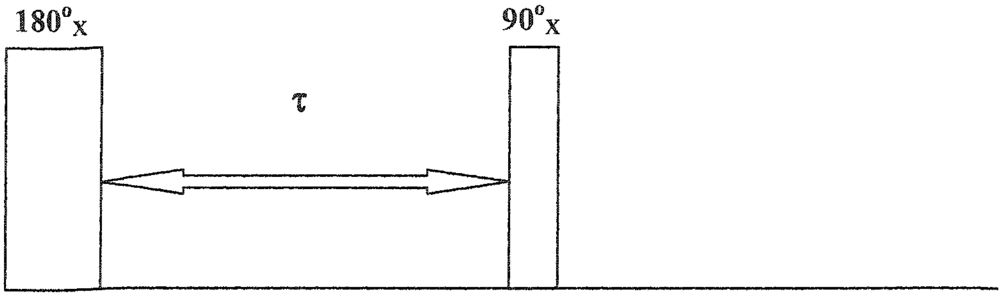

Figure 1.5 The inversion-recovery pulse sequence.

Spin-lattice relaxation times can also be measured by other techniques. Two other techniques are: i) saturation-recovery, and the ii) Torchia[25] experiment.

The first technique for measuring spin-lattice relaxation times is the saturation-recovery method and is more practical than the inversion recovery method when measuring very long spin-lattice relaxation times. An inversion-recovery experiment can be time consuming since the waiting time between each pulse sequence should be 4-5 T_1 to allow for the establishment of equilibrium. In the saturation-recovery experiment, $(90^o)_n$-τ-90^o, instead a sequence of 90^o pulses is applied that saturates the equilibrium magnetization which is then allowed to evolve during a delay τ, and then detected by a 90^o pulse. The signal intensity is given by

$$M_Z = M_0[1 - \exp(-\tau / T_1)] \qquad \textbf{1.10}$$

The plot of the logarithm of M_Z versus τ yields a straight line whose slope is $1/T_1$.

Another technique that is suitable for measuring long T_1 values typical of organic solids and semi-crystalline polymers is the Torchia pulse sequence[25] with the inversion-recovery method being useful for measuring short T_1's typical of mobile solids. The pulse sequence is a modification of the cross-polarization (CP) pulse sequence (see Figure 1.3) and allows the determination of T_1 of rigid polymers whose spectra are usually acquired under CP conditions by inserting a variable delay τ between the spin locking and decoupling of the proton spins and then repeating the pulse, but this time using a 90^o proton pulse of opposite phase in the second sequence. When the signal derived from the second sequence is subtracted from that of the first sequence, the net signal will not depend on: M_O (the equilibrium longitudinal magnetization), the residual carbon magnetization due to spin-lattice processes at the beginning of the sequence or during a long delay τ, and on artifact transients. The sequence retains the enhancement obtained in the normal cross-polarization experiment and the net signal I after N scans (N is even) will be proportional to $NM_{CP}(0)exp(-t/T_1)$, where $M_{CP}(0)$ is the initial proton-enhanced longitudinal magnetization. Spin-lattice relaxation can also be measured in the rotating frame. The pulse sequence for proton spin-lattice relaxation in the rotating frame ($T_{1\rho H}$) includes the CP sequence but with leaving the ^{1}H rf field on for a time delay t before the cross polarization step.[26]

One of the reasons as previously mentioned for line broadening of NMR lines in solids and polymers in their crystalline or glassy states is the dipolar interaction with the major interaction occurring between protons and to a lesser extent between protons and carbons, with carbon-carbon interactions being negligible due to low abundance, large internuclear distances, and a smaller magnetic moment. Dipolar interaction operates through space and depends on the orientation of the internuclear vector relative to the magnetic field as well as on the distance between the dipoles. The dipolar Hamiltonian for two spins I and S has the following expression[27]:

$$\mathbf{H_D} = \mathbf{H_{II}} + \mathbf{H_{SS}} + \mathbf{H_{IS}} \qquad 1.11$$

where

$$H_{II} = \frac{1}{2}\gamma_I^2 \hbar^2 \sum_{i<j}^{N_I}\sum^{N_I} r_{ij}^{-3}\,(3\cos^2\theta_{ij} - 1)(\vec{I}_i \bullet \vec{I}_j - 3I_{iz}\,I_{jz}) \qquad 1.12$$

$$H_{IS} = -\gamma_I \gamma_S \hbar^2 \sum_i^{N_I} \sum_k^{N_S} r_{ik}^{-3} (3\cos^2\theta_{ik} - 1)(I_{iz} I_{kz}) \quad \textbf{1.13}$$

r is the internuclear separation and θ is the angle the I-S vector makes with the external magnetic field.

As the I-S internuclear vector undergoes motion, magnetic dipole interactions provide a mechanism for relaxation. The relaxation rate $R_1 = 1/T_1$ where T_1 is the spin-lattice relaxation time, has the following expression for two unlike spins[28]:

$$R_1 = \frac{\gamma_I^2 \gamma_S^2 \hbar^2}{10 r_{IS}^6} \left[\frac{\tau_C}{1 + (\omega_I - \omega_S)^2 \tau_C^2} + \frac{3\tau_C}{1 + \omega_I^2 \tau_C^2} + \frac{6\tau_C}{1 + (\omega_I + \omega_S)^2 \tau_C^2} \right] \quad \textbf{1.14}$$

where ω_I and ω_S are the Larmor frequencies of the two spins and τ_c is the correlation time.

The variation of T_1 with the correlation time τ_c and temperature gives information about the dynamics of the system. In the fast motional regime or extreme narrowing condition, T_1 usually decreases as τ_c increases and temperature decreases then it passes through a minimum at which the larmor frequency equals the reciprocal of τ_c. The higher the temperature at which the T_1 minimum occurs, the more restricted the mobility. Above the minimum, T_1 increases as τ_c increases and temperature decreases. This is called the slow motional regime.

1.3.2.4 Spin diffusion:

Spin diffusion is the spatial migration of magnetization through zero-quantum flip-flop transitions in a homonuclear spin system and is important for spins of high abundance and large γ values and is mediated by dipolar couplings. For solids $T_1 >> T_2$ (spin-spin lattice relaxation time), and thus energy can remain in the spin system for a certain time which is long relative to T_2 before being transferred to the lattice. Spin diffusion eliminates the spatial magnetization gradient that is usually observed in heterogeneous polymers. The time needed to reach equilibrium in a spin system provides a measure of the length scale of the system by determining sizes of domains and hence the extent of heterogeneity. This is especially significant for industrial materials which are multi-component systems such as polymer blends and copolymers.[11, 29]

Spin diffusion experiments are performed by utilizing selective techniques where magnetization is built up selectively in one component of a heterogeneous system while suppressed in the other resulting in a non-equilibrium distribution of nuclear magnetization. A variable delay usually called the mixing time (τ_m) is incorporated in the pulse sequence during which the spatial migration of magnetization is monitored. Eventually equilibrium is attained and the magnetization gradient is eliminated. The migration of magnetization is described by Fick's law of diffusion:

$$\dot{M}(r,t) = \nabla \bullet \left[D(r)\, \nabla M(r,t) \right] \qquad 1.15$$

where D is the spin-diffusion coefficient, r is the space vector and t is the diffusion time.

A technique where the selection is based on proton chemical-shift differences is called the chemical-shift filter and more commonly CRAMPS[30] (Combined Rotation and Multiple Pulse Sequence). The rotation refers to spinning the sample at the magic angle (MAS), which removes chemical shift anisotropy. The multiple pulse refers to a train of closely spaced very short 90° pulses (~ 1.5 μs) which eliminate proton-proton dipolar couplings because this series of pulses places the proton magnetization for equal times on the x, y, and z axes, resulting in a net magnetization directed at the magic angle with respect to B_0 (along the z-axis). This corresponds to averaging in spin space rather than in real space, meaning that the spins are manipulated and not the sample as in MAS.

A second spin diffusion experiment is the dipolar filter[31] or the "mobility filter" where the selection technique is based on the motional heterogeneity of the system. Initially magnetization is built in the mobile component and suppressed in the rigid or crystalline component (short T_2) where dipolar couplings are strong; then a waiting time, the mixing time, is incorporated during which the initial magnetization gradient diminishes until equilibrium is reached. The pulse sequence is shown in Figure 1.6. The initial train of pulses represents the selection step, where strong dipolar couplings, typical of rigid domains, are eliminated and magnetization is suppressed. The weak dipolar couplings, on the other hand, are retained and their magnetization is refocused at the end of the selection step.

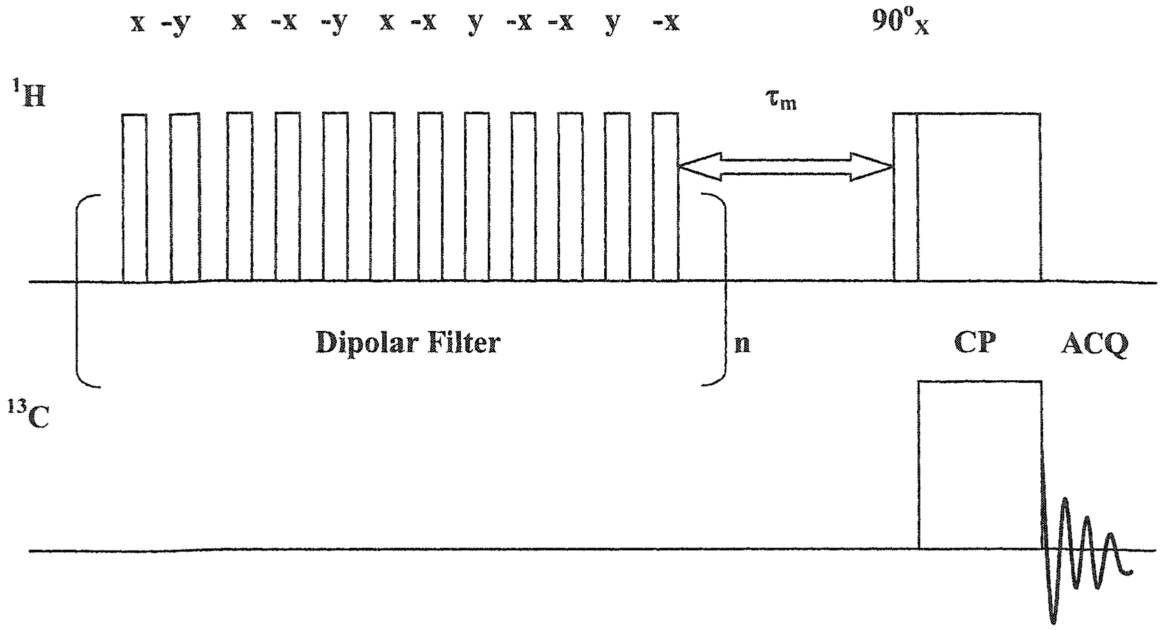

Figure 1.6 The Dipolar-filter pulse sequence.[31]

After the mobile component has been selected, its magnetization is restored to the z-axis. A mixing time t_m is incorporated where spin diffusion occurs and a build up of magnetization of the rigid or crystalline component and a decrease in the amorphous component and at equilibrium a plateau is reached. By plotting the magnetization build-up versus the square root of t_m, the domain sizes of the crystalline and amorphous components can be calculated.[29] The magnetization of the rigid component usually reaches a maximum and then decreases with no plateau observed. This decrease is attributed to spin-lattice relaxation for long mixing periods ($\tau_m \sim T_1$). This problem is overcome by phase cycling of the pulses before the mixing time and this is achieved by applying a 180° phase correction during alternate acquisition cycles compensating for longitudinal relaxation for long mixing times. When multiplying the build-up magnetization curve by a correction factor $\exp(t_m/T_1)$, a magnetization recovery curve with a plateau is obtained from which domain sizes can be extracted using the initial rate approximation.[29]

The spin diffusion coefficients are needed to evaluate the domain sizes and morphology from the spin diffusion data. Two methods will be presented. In the first method the spin diffusion coefficient D is expressed as a function of the local dipolar field[32] and for a powder sample it is expressed by

$$D=\sqrt{\frac{\pi}{6}}\left\langle r^2\right\rangle B_L \tag{1.16}$$

where $\langle r^2 \rangle$ is the average square distance between the nearest spins and B_L is the local magnetic field in the laboratory frame[33] and for purely dipolar spin interactions the local field is:

$$B_L^2=\frac{5}{3}\overline{M}_2 \tag{1.17}$$

where $\overline{M}_2$ is the second moment of the NMR absorption line for a powder sample in the high magnetic field and for a Gaussian absorption line shape it has the following expression:

$$(\overline{M}_2)^{1/2}=\frac{1}{2\sqrt{2\ln 2}}\Delta\upsilon_{1/2} \tag{1.18}$$

and for Lorentzian line shapes

$$\overline{M}_2=\frac{\alpha\Delta\upsilon_{1/2}}{\pi} \tag{1.19}$$

where $\Delta\upsilon_{1/2}$ is line width at half intensity and α is a cut-off parameter for the Lorenztian line shape.[33]

The diffusion coefficients D_M and D_R of the mobile and rigid components respectively can be determined by combining equations 1.16-1.19 resulting in the following expressions:

$$D_R = \frac{1}{12}\sqrt{\frac{\pi}{2\ln 2}}\left\langle r^2 \right\rangle \Delta\upsilon_{1/2} \qquad \mathbf{1.20}$$

and

$$D_M = \frac{1}{6}\left\langle r^2 \right\rangle [\alpha\, \Delta\upsilon_{1/2}]^{1/2} \qquad \mathbf{1.21}$$

$\langle r^2 \rangle$ is determined from nearest-neighbor proton-proton distances, smaller than 3 Å and are obtained from crystal structure data.

The second method to calculate spin diffusion coefficients is based on the experimentally measured spin diffusion coefficient for a polymer with well-defined morphology like a symmetric diblock copolymer of poly(styrene) and poly(methyl methacrylate) (PS-b-PMMA) which has a spin diffusion coefficient of $D_{PS\text{-}PMMA} = (8 \pm 2) \times 10^{-16}$ m^2/s.[29] The spin diffusion coefficient[27] for a rigid spin distribution is proportional to the strength of the dipolar coupling as well as to the mean square of the distance, r, among nearest-neighbour protons and is described by:

$$D = k\langle r^2\rangle \Delta\upsilon_{1/2} \qquad \textbf{1.22}$$

This relation is only valid for Gaussian NMR lines and for $\Delta\upsilon_{1/2} > 5$ kHz.

Spin diffusion in solid polymers is very effective due to strong dipolar coupling between protons but this complicates the analysis of different relaxation processes. This can be overcome by probing ^{13}C spin diffusion, but this nucleus has very weak homonuclear dipolar couplings and low abundance that render spin diffusion negligible. Using ^{13}C-enriched polymers provides a way to detect ^{13}C spin diffusion and is useful in probing extremely short length scales between labeled sites.[34] Another method to enhance ^{13}C spin diffusion without resorting to labeling, is to adjust the MAS rotor frequency to be an integer fraction of the chemical shift difference of the spins.[35] The previous discussion shows the importance of spin diffusion in providing valuable morphological information for heterogeneous polymer systems, nevertheless spin diffusion can interfere with other dynamic processes taking place and can complicate the interpretation of relaxation data. For this reason, it is sometimes necessary to suppress spin diffusion. This can be achieved by applying the rf field at the magic angle eliminating dipolar coupling and spin diffusion.[36]

1.3.2.5 2D Exchange NMR:

The 2D Exchange NMR experiment is a two-dimensional experiment which can probe relatively slow motions. The experiment used for solids is a CP-MAS analog of the two-dimensional experiment introduced by Ernst et al.[37] to study exchange and spin diffusion. The basic principle of the experiment is measuring the NMR frequency of one nucleus at two different times and detecting the slow dynamics through the change in NMR frequency if the nucleus has changed its orientation. Chemical exchange corresponding to reorientation of molecules or molecular segments in space, spin diffusion, or sample rotation and flipping can lead to exchange peaks. The pulse sequence is shown in Figure 1.7. The pulse sequence[38] is different from that of liquids in that the initial 90° pulse is replaced with a cross-polarization sequence. The pulse sequence can be divided into four parts:

(1) The preparation period during which ^{1}H magnetization is transferred to the ^{13}C spins through cross polarization.

(2) The evolution period (t_1), during which the dilute ^{13}C spins are subjected to Zeeman interaction under the influence of the ^{13}C chemical shift Hamiltonian and under strong proton decoupling and MAS. At the end of this period a 90° pulse is applied on the ^{13}C spins to convert all magnetization into z-magnetization just before the third period.

(3) The mixing period during which exchange might occur between z-magnetization of the ^{13}C spins. Proton decoupling is turned off during this period to eliminate residual transverse components of the ^{13}C magnetization.

(4) The fourth and final period is the detection period (t_2), which occurs after a 90° pulse on the ^{13}C spins to re-establish transverse magnetization. Fourier transformation of the data in the t_2 dimension yields a set of spectra having modulation of peak amplitudes that reflect chemical shifts and processes that took place during the mixing period. A second Fourier transform in the t_1 dimension gives the 2D NMR spectrum. If no exchange occurs, peaks are only observed along the diagonal and in the case of exchange off-diagonal peaks are observed.

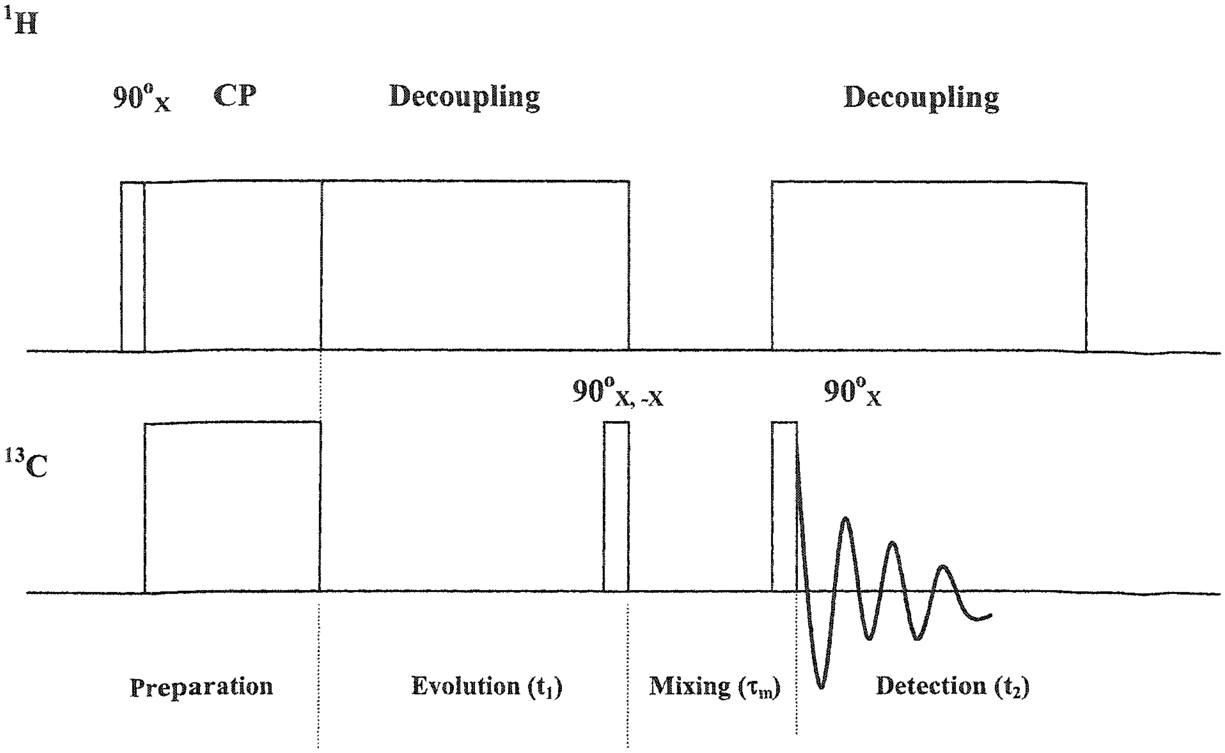

Figure 1.7 The 2D Exchange NMR pulse sequence.[38]

In addition to providing dynamics information, 2D exchange experiments can provide T_2 information from linewidths of diagonal peaks in contour plots as well as distinguish between homogeneously and inhomogeneously broadened NMR lines. Lines broadened by a homogenous mechanism are due to insufficient decoupling, efficient T_2 due to paramagnetic species, or molecular motions whose frequency interferes with decoupling. Inhomogeneously broadened lines are due to different environments that give rise to a chemical shift distribution. Zemke et al.[39] have used 2D exchange NMR experiments to show that NMR lines in atactic polypropylene are inhomogeneously broadened due to the absence of circular or star-shaped humps at the diagonal peaks in the contour plot. Instead the contour plot at $t_m = 5$ ms was extended along the diagonal with little homogenous broadening as indicated by the small width perpendicular to the diagonal.

1.4 Xenon NMR Spectroscopy

1.4.1 Overview

Xenon has a wide variety of applications in chemistry, physics and in the field of material science. It is a noble gas, and being inert makes it a an appropriate probe since it does not modify its environment. It also has a wide chemical shift range from -40 ppm for Xe adsorbed on AgX to about 7500 ppm in the compound XeO_6^{-4}. Most of its adsorption properties stem from its large polarizable electron cloud which is very sensitive to its local environment. There are two xenon NMR active isotopes: ^{129}Xe, spin = 1/2, 26.44% natural abundance; ^{131}Xe, spin = 3/2, 21.18% natural abundance. ^{129}Xe NMR, usually used without MAS, has been applied to solutions, polymers, clathrates, porous materials and various surfaces were it probes structure, morphology and pore size distribution.[40] The ^{129}Xe chemical shift consists of two parts: a diamagnetic part arising from the interaction of the electron orbitals with applied fields and a paramagnetic part which depends on the excited states and on the symmetry of the valence orbitals. It expresses the deviation from spherical symmetry and is zero for the isolated Xe atom and is responsible for shifts to higher frequencies of the xenon nucleus.[41] Jameson et al.[42] expressed the ^{129}Xe chemical shift in the gas phase as a virial expansion in the gas density

ρ

$$\sigma = \sigma_0 + \sigma_1\rho + \sigma_2\rho^2 + \ldots.. \qquad \textbf{1.23}$$

where the σ values are virial coefficients. The nonlinearity at higher xenon pressures is due to contributions from three-body or higher collisions and is neglected for pressures less than 50 atm. While the spin-lattice relaxation time is very short for the quadropolar isotope (^{131}Xe), that of ^{129}Xe is very long and it was shown[43] that $T_1(^{129}Xe)$ decreases with increasing gas density or decreasing temperature.

^{129}Xe NMR has been used as a tool for the structural and morphological characterization of zeolites[44] in which the xenon chemical shift is expressed as a virial expansion of terms representing different interactions

$$\delta = \delta_{ref} + \delta_s + \delta_{Xe} + \delta_{SAS} + \delta_E + \delta_M \qquad \textbf{1.24}$$

where δ_{ref} is the reference shift corresponding to the chemical shift of xenon gas extrapolated to zero pressure. δ_s is the shift due to the adsorbed gas. δ_{Xe} is due xenon-xenon interactions and varies linearly with gas density in the limit of low pressures. δ_{SAS} corresponds to the interaction of xenon with strong absorption sites (SAS). δ_E is a term introduced by Fraissard to account for the effect of cations in zeolites on the xenon chemical shift, and δ_M describes the magnetism created by the charge and paramagnetism of the cations. The ^{129}Xe NMR chemical shift is an average of all chemical shifts in all the environments xenon is exposed to, and is weighted by the fraction of time spent by xenon at each location during the time frame of the NMR experiment. The chemical shift increases with decreasing void size. Lines are expected to be anisotropic if the xenon atoms are static but this is rare since xenon is usually exchanging among different sites. Being similar in size to CH_4, xenon serves as a model for the study of the diffusion of small organic molecules in porous materials.

1.4.2 Applications to Polymers

Besides the significance of ^{129}Xe NMR for structural and morphological elucidation of porous materials and in probing microvoid and pore structure, there has been a wide variety of applications to polymer systems.[45] While in porous materials there have been many models as well as empirical expressions relating xenon's chemical shift with pore size and dimensions. In polymers this is usually not possible, but the chemical shift does vary inversely to the free volume. Xenon readily dissolves in a polymer above its T_g due to the free volume created by chains mobility. The chemical shift is also described here as a virial expression and is similar to that of xenon dissolved in liquids

$$\delta = \delta_W + \delta_r + \delta_b + \delta_a + \delta_E^2 \qquad \mathbf{1.25}$$

where δ_W and δ_r are the van der waals dispersion and repulsion interactions which dominate the shift observed for xenon dissolved in liquids. δ_b is the term associated with bulk susceptibility and is neglected for polymers. δ_a and δ_E^2 terms have small contributions and are due to magnetic anisotropy and permanent electric dipole moment of the solvent and are also neglected.

The ^{129}Xe chemical shift δ is characteristic of a particular polymer and ranges from 152 to 250 ppm with the majority of polymers having chemical shifts in the 200-

230 ppm region at room temperature.[46] δ and the xenon linewidth ($\Delta\upsilon_{1/2}$) increase with decreasing temperature due to densification of the polymer and diminishing free volume. Above T_g lines are narrow and isotropic due to the enhanced mobility of polymer chains in the rubbery state. For glassy polymers, chains are restricted and lines are broad due a chemical shift heterogeneity resulting from a distribution of sites not averaged out by the xenon's dynamic exchange.

The chemical shift is also sensitive to the macroscopic heterogeneity in polymers such as rubbers. Uncrosslinked EPDM (a terpolymer of ethylene, propylene, and ethylidenenorbornene)[47] has a ^{129}Xe spectrum consisting of four overlapping peaks corresponding to four different amorphous regions in the sample with sites of different size or density. Upon crosslinking, fewer peaks are observed and peaks shifted down field due to the densification of the polymer upon crosslinking. Brownstein et al.[48] investigated a block copolymer of polystyrene (PS) ($T_g \sim 100^\circ$C) and polyisoprene (PI) ($T_g \sim -63^\circ$C) where two xenon lines were observed, a broad one for PS, and a narrow one for PI. The peaks were broader than in the homopolymers due to lifetime broadening resulting from xenon exchange between the two phases. Wang et al.[49] have used xenon as a probe to study the mobility of xenon and to characterize the sorption sites on a series of poly(2,6-dimethyl-1,4-phenylene oxide) (PXE) samples. They observed that the chemical shift in a dense cast film of PXE is smaller than that observed for typical glassy polymers indicating a larger free volume in the films. When PXE was antiplasticized, the shift was higher and the lines became broader due to diminishing mobility of polymer chains.

The technique has also been used to measure domain sizes and probe the extent of homogeneity for polymer mixtures and blends based on differences in xenon chemical shifts. De Souza et al.[50] have used ^{129}Xe NMR to probe the homogeneity of poly(ethylene-co-vinyl acetate) (EVA)/poly(vinyl acetate) blends and showed that EVA with a higher vinyl acetate content makes the two components more miscible and the blend more homogeneous. Mansfield and Veeman[51] studied a blend of polypropylene (T_g ~ 0°C) and polyethylene-polypropylene copolymer (T_g ~ -50°C to -60°C). From ^{1}H-^{129}Xe cross-polarization and 2D heteronuclear correlation spectra at -30°C, they deduced that there was no magnetization transfer occurring in the copolymer but only in glassy PP. At room temperature, no CP signal was observed from either material due to enhanced mobility above T_g for both components. Simpson et al.[52] developed a method for determining diffusion coefficients using polymer microspheres of well-defined size. Using polystyrene beads of sizes 10, 18, and 64 mm, they observed resonances of xenon in the gas and in the polymer and by monitoring the intensity of the ^{129}Xe resonance as a function of saturation time they determined the values of diffusion coefficients which when measured at different temperatures, yielded the activation energy for diffusion in glassy PS.

1.5 Photoacoustic Fourier Transform Infrared Spectroscopy (PAS-FTIR)

This FTIR technique was used to acquire IR spectra of bulk and adsorbed samples, to monitor the binding of the anchor groups to the surface of zirconia, to probe changes in order upon adsorption of polymer chains, as well as to gain insight into the binding mechanism. Photoacoustic spectroscopy[53] is based on the detection of an acoustic signal emitted from a sample due to modulated radiation. A sample is placed in a chamber that is isolated acoustically where a microphone is attached. Upon absorption of modulated radiation, heat is generated in the sample, and causes pressure changes in a surrounding gas. This generates acoustic waves in the sample chamber and the changes in gas pressure are detected by a sensitive microphone and the electrical signal is then Fourier transformed.

1.6 Scope of the thesis

A better understanding into the nature of adsorbed polymers is needed at the molecular level to optimize their macroscopic properties. In this work, we utilize a range of solid-state ^{13}C NMR techniques to probe the chain conformation, dynamics, and morphology of polymers adsorbed on zirconia (ZrO_2). ^{129}Xe NMR is also used to probe the morphologies of adsorbed polymers and the dynamics around the glass transitions of bulk and filled polymers. The surface bonding is monitored by FTIR-Photoacoustic spectroscopy. We compare the behavior of bulk and adsorbed polymers and investigate the effect of polymer loading and chain composition on adsorption. The thesis consists of seven chapters:

* ***Chapter One*** consists of a general introduction and a literature review of polymers at surfaces and interfaces, solid-state NMR, ^{129}Xe NMR and FTIR-PAS.

* ***Chapter Two*** consists of the study of the chain conformation and morphology of a semi-crystalline random copolymer of ethylene and acrylic acid (PEA) in the bulk state and adsorbed on zirconia using ^{13}C CP-MAS, 2D-WISE, and ^{1}H spin diffusion NMR experiments. We chose this copolymer first because of its importance as an adhesion promoter for polymer coatings. Secondly, we were motivated to investigate the adsorption of semi-crystalline polymers since most studies in the literature deal with amorphous polymers. This study focused on the effect of the sticker group density and adsorbed amount on chain conformation at the metal oxide surface.

* ***Chapter Three*** consists of the NMR study of the dynamics of bulk and adsorbed PEA using variable temperature ^{13}C CP-MAS, ^{13}C spin-lattice relaxation, and 2D Exchange NMR experiments. The objective of this study is to use the dynamics information obtained from NMR experiments to distinguish between possible surface chain configurations (trains versus loops and tails) of adsorbed PEA.

* ***Chapter Four*** consists of a ^{129}Xe NMR study of bulk and adsorbed PEA. The xenon chemical shift and spin-lattice relaxation measurements are used to probe the morphology of the adsorbed copolymer. Variable temperature experiments are performed to measure the glass transition temperature of the bulk copolymers.

* ***Chapter Five*** consists of a solid-state ^{13}C NMR study of the chain conformation and dynamics of a semi-crystalline random copolymer of polypropylene and acrylic acid (PPAC). We investigate how the polymer chain configuration and mobility are altered upon adsorption and how these properties vary as a function of adsorbed amount.

* ***Chapter Six*** consists of solid-state ^{13}C and ^{129}Xe NMR studies of the dynamics and morphology of bulk, adsorbed, and zirconia filled poly(n-butyl methacrylate) (PnBMA). ^{13}C NMR is used to characterize the binding, mobility and conformation of adsorbed PnBMA as a function of coverage and deposition solvent. Variable temperature ^{129}Xe NMR experiments are performed on bulk and zirconia-filled PnBMA to probe the dynamics in the temperature range where thermal transitions are observed by differential scanning calorimetry.

* ***Chapter Seven*** is the last chapter of the thesis and consists of the conclusions, contributions to knowledge, suggestions for future work and a list of publications and conferences.

1.7 References

(1) Lipatov, Y.S.; Sergeeva, L.M. *Adsorption of Polymers*, John Wiley, New York, 1974.

(2) Fleer, F.J.; Lyklema, J. *Adsorption from Solution at the Solid/Liquid Interface*, Eds. Parfitt, G.D. and Rochester, C.H., Academic Press, London, 1983; pg: 153.

(3) Fleer, F.J.; Scheutjens, J.M.H.M., *Coagulation and Flocculation: Theory and Applications*, Surfactant Science Series, Vol. 47, Ed. Dobais, B., Marcel Dekker, New York, 1993; pg: 209.

(4) Fleer, F.J.; Cohen-Stuart, M.A.; Scheutjens, J.M.H.M.; Cosgrove, T.; Vincent, B. *Polymers at Interfaces*, Chapman & Hall, London, 1993.

(5) Oslanec, R.; Composto, R.J. Polymer Adsorption at polymer/solid interfaces, pg: 181 in *Polymer Surfaces, Interfaces and Thin Films*, Eds. Karim, A. and Kumar, S., World Scientific Publishing Co. Pte. Ltd., 2000.

(6) Wool, R.P. *Polymer Interfaces: Structure and Strength*, Hanser/Gardner: New York, 1995.

(7) (a) Blum, F.D. *Colloid-Polymer Interactions: From Fundamentals to Practice*, Ed. Farinato, R.S., Dubin, P.L., John Wiley & Sons, Inc., 1999; pg: 207. (b) Jones, R.A.L. *Current Opinion in Colloid and Interface Science* **1999**, *4*, 153.

(8) (a) Cosgrove, T.; Barnett, K.G. *J. Mag. Res.* **1981**, *43*, 15. (b) Cosgrove, T.; Griffiths, P.C. *Advances in Colloid and Interfaces* **1992**, *42*, 175.

(9) Schonhoff, M.; Larsson, A.; Welzel, P.B.; Kuckling, D. *J. Phys. Chem. B* **2002**, *106*, 7800.

(10) (a) Liang, M.; Blum, F.D. *Macromolecules* **1996**, *29,* 7374. (b) Blum, F.D.; Sinha, B.R.; Schwab, F.C. *Macromolecules* **1990**, *23,* 3592. (c) Xie, M.; Blum, F.D. *Langmuir* **1996**, *12,* 5669. (d) Lin, W.Y.; Blum, F.D. *Macromolecules* **1998**, *31,* 4135. (e) Blum, F. *Ann. Rep. NMR Spectroscopy* **1994**, *28*, 277. (f) Blum, F.D. *Colloids and Surfaces* **1990**, *45*, 361.

(11) Schimdt-Rohr, K.; Spiess, H.W. *Multidimensional Solid-State NMR and Polymers*, Academic Press, New York, 1994.

(12) Zumbulyadis, N.; Landry, C.J.T. Solid State NMR of Polymer Interfaces, Ed. Lohse et al.; Interfacial Aspects of Multicomponent Polymer Material. Plenum Press, New York, 1997; pg: 73.

(13) Zumbulyadis, N.; O'Reilly, J.M. *Macromolecules* **1991**, *24,* 5298.

(14) (a) Mirau, P.A.; Heffner, S.A. *Macromolecules* **1999**, *32,* 4912. (b) Mirau, P.A.; Heffner, S.A.; Schilling *Solid State NMR* **2000**, *16,* 47. (c) Marjanski, M.; Srinivasarao, M.; Mirau, P.A *Solid State NMR* **1998**, *12,* 113.

(15) McBrierty, V.J.; Packer, K.J. *Nuclear Magnetic Resonance in Solid Polymers*, Cambridge University Press, Cambridge, 1993.

(16) Fyfe, C.A. *Solid-State NMR For Chemists*, CFC Press, Guelph, Ontario, Canada, 1983.

(17) Hartmann, S.R.; Hahn, E.L. *Phys. Rev.* **1962**, *128*, 2042.

(18) Mehring, M. *Principles of High Resolution NMR in Solids*, 2nd Ed. Springer, Berlin, Heidelberg, New York, 1980.

(19) Slichter, C.P. *Principles of Magnetic Resonance*, 3rd Ed. Springer, Berlin, Heidelberg, New York, 1989.

(20) Voelkel, R. *Angew. Chem. Int. Ed. Eng.* **1988**, *27*, 1468.

(21) Andrew, E.R.; Bradbury, A.; Eades, R.G. *Nature* **1958**, *182*, 1659.

(22) (a) Dixon, W.T. *J. Chem. Phys.* **1982**, *77*, 1800. (b) Titman, J.J.; Feux de Lacroix, S.; Spiess, H.W. *J. Chem. Phys.* **1993**, *98*, 3816.

(23) Schmidt-Rohr, K.; Clauss, J.; Spiess, H.W. *Macromolecules* **1992**, *25*, 3273.

(24) Freeman, R. *A Hanbook of Nuclear Magnetic Resonance*, 2nd Ed. Addison Wesley Longman Limited, Essex, England, 1997.

(25) Torchia, D.A. *J. Magn. Reson.* **1978**, *36*, 91.

(26) Sullivan, M.J.; Maciel, G.E. *Anal. Chem.* **1982**, *54*, 1615.

(27) Abragam, A. *The Principles of Nuclear Magnetism*, Clarendon Press, Oxford, 1961.

(28) (a) Becker, E.D. *High Resolution NMR: Theory and Chemical Applications*, Academic Press, London, 2000. (b) Farrar, T.C.; Becker, E.D. *Pulse Fourier Transform NMR: Introduction to Theory and Methods*, Academic Press, New York, 1971.

(29) Clauss, J.; Schimdt-Rohr, K.; Spiess, H.W. *Acta Polymer* **1993**, *44*, 1.

(30) Clauss, J.; Schimdt-Rohr, K.; Blumich, B.; Spiess, H.W. *Magn. Res. in Chem.* **1990**, *28*, 3.

(31) Clauss, J.; Schimdt-Rohr, K.; Blumich, B.; Spiess, H.W. *Polym. Prepr.* (Am. Chem. Soc., Div. Polym. Chem.) **1990**, *31(1)*, 172-3.

(32) (a) Cheung, T.T.P. *Phys. Rev.* **1981**, *B23*, 1404. (b) Cheung, T.T.P.; Gerstein, B.C. *J. Applied Phys.* **1981**, *52*, 5517.

(33) Goldman, M. *Spin Temperature and Nuclear Magnetic Resonance in Solids*, Clarendon Press, Oxford, 1970.

(34) (a) Henrichs, P.M.; Linder, M. *J. Magn. Res.* **1984**, *58*, 458. (b) Linder, M.; Henrichs, P.M.; Hewitt, J.M.; Massa, D.J. *J. Chem. Phys.* **1985**, *82*, 1585.

(35) Colombo, M.G.; Meier, B.H.; Ernst, R.R. *Chem. Phys. Letters* **1988**, *146*, 189.

(36) Lee, M.; Goldburg, W.I. *Phys. Rev.* **1965**, *140(4A)*, A1261.

(37) Jeener, J.; Meier, B.H.; Bachmann, P.; Ernst, R.R. *J. Chem. Phys.* **1979**, *71*, 4546.

(38) Szeverenyi, N.M.; Sullivan, M.J.; Maciel, G.E. *J. Magn. Res.* **1982**, *47*, 462.

(39) Zemke, K.; Chmelka, B.; Schimdt-Rohr, K.; Spiess, H.W. *Macromolecules* **1991**, *24*, 6874.

(40) Springuel-Huet, M.A. ^{129}Xe NMR of Physisorbed Xenon, in Fraissard, J. (Ed.) *Physical Adsorption: Experiment, Theory and Applications*, Kluwer Academic Publishers, Netherlands, 1997. pgs: 331-348.

(41) Ramsey, N.F. W.I. *Phys. Rev.* **1950**, *78*, 699.

(42) Jameson, A.K.; Jameson, C.K. Gutowsky, H.S. *J. Chem. Phys.* **1970**, *53*, 2310.

(43) Streever, R.L.; Carr, H.W. *Phys. Rev.* **1961**, *121*, 20.

(44) (a) Fraissard, J.; Ito, T. *Zeolites* **1998**, *8*, 350. (b) Barrie, P.J.; Kinowski, J. *Prog. Nucl. Magn. Res. Spectrosc.* **1992**, *24*, 91.

(45) Walton, J.H. *Polym. Polym. Compos.* **1994**, *2*, 35.

(46) (a) Raftery, D; Chmelka, B.F. *NMR Basic Principles and Progress* **1994**, *30*, 111. (b) Ratcliffe, C.I. *Annual Reports on NMR Spectroscopy* **1998**, *36*, 124.

(47) Kennedy, *J. Polym. Bull.* **1990**, *23*, 605.

(48) Brownstein, J.E.; Roovers, L.; Worsfold, D.J. *Magn. Reson. Chem.* **1988**, *26*, 392.

(49) Wang, Y.; Inglefield, P.T.; Jones, A.A. *J. Polym. Sci., Part B: Polym. Phys.* **2002**, *40*, 1965.

(50) De Souza, C.M.G.; Tavares, M.B. *J. Appl. Polym. Sci.* **2002**, *86*, 116.

(51) (a) Mansfield, M.; Veeman, W.S. *Chem Phys. Lett.* **1993**, *213*, 153. (b) Mansfield, M.; Veeman, W.S. *Chem Phys. Lett.* **1994**, *222*, 422.

(52) (a) Simpson, J.T.; Wen, W.Y.; Jones, A.A.; Inglefield, P.T.; Bendler, J.T. *Appl. Magn. Reson.* **1995**, *8*, 349. (b) Simpson, J.T.; Wen, W.Y.; Jones, A.A.; Inglefield, P.T. *Macromolecules* **1996**, *29*, 2138.

(53) Urban, M.W. *Vibrational Spectroscopy of Molecules and Macromolecules on Surafces*, Wiley-Interscience, New York, 1993.

Chapter Two

Conformation of Adsorbed Random Copolymers: A Solid-State NMR and FTIR-PAS Study

---

2.1 Preface

In this chapter we investigate the chain conformation and morphology of bulk and zirconia-adsorbed polyethylene-co-acrylic acid (PEA) random copolymers using ^{13}C CP-MAS, 2D WISE, ^{1}H spin diffusion NMR experiments and FTIR-PAS. We compare how bulk properties are altered upon adsorption and study the effect of copolymer loading and sticker concentration on chain conformation and how this affects polymer adhesion.

2.2 Introduction

Polymer/solid interfaces are key to industrial applications ranging from protective coatings to photoresists.[1] The relationship between the conformational and dynamic features of adsorbed polymers to surface properties such as adhesion and wettability is of interest to these applications. Although vibrational spectroscopy has been commonly employed to investigate the conformational properties of polymers at interfaces, this technique does not provide dynamic information. Solution NMR techniques, based primarily on relaxation measurements, have been used to estimate the fraction of polymer bound to a surface.[1a, 2] Although a large number of solid-state NMR techniques have been developed to probe polymer dynamics,[3] relatively few NMR studies have been carried out for adsorbed polymers at the solid/air interface due to sensitivity problems. A notable exception has been the solid-state NMR studies of adsorbed polymers and copolymers by Blum and coworkers[4] where they used ^{2}H NMR lineshapes to probe the dynamics of bulk and adsorbed polymers.

Copolymers containing acrylic acid have been used for many years to increase the adhesion of polymer films to metals. Most studies have focused on the mechanical properties (peeling tests, thermal stability) rather than the molecular level structure.[5] Gong et al. showed that a critical concentration of carboxylic acid sticker groups is required for optimal chain connectivity near the surface and a maximum in the fracture energy.[6] Theoretical studies of adsorbed random copolymers predict that the maximum fracture energy is associated with the chain conformation at the interface.[7] It was recently reported that the bonding of fatty acids and acrylic acid copolymers to alumina can be enhanced by pretreating the surface with zirconium alkoxides.[8] Likewise, we have found that whereas long chain carboxylic acids adsorb weakly to alumina, highly ordered self-assembled monolayers form on zirconia.[9] The high surface area zirconia substrate used in this study provided sufficient signal to noise for even 2D solid-state ^{13}C NMR experiments. Furthermore, the nature of the metal carboxylate surface bond could be easily determined by vibrational spectroscopy.[8, 9]

In view of these results, as well as the wide industrial use of acrylic acid containing copolymers, we have chosen polyethylene-co-acrylic acid (PEA) random copolymers deposited on nonporous zirconia as a convenient system for a detailed solid-state NMR study of a strongly adsorbed polymer. The chain conformation of the polyethylene segments, determined from the ^{13}C chemical shifts, can be correlated with the interaction of the polyacrylic acid groups with the surface, as detected by infrared spectroscopy. Solid-state 2D wideline separation (WISE) and ^{1}H spin diffusion NMR experiments are applied to probe the chain motion and morphology in the bulk and adsorbed states. The effect of copolymer loading and acrylic acid content on surface bonding, the chain order, mobility and morphology are reported.

2.3 Experimental Section

Sample preparation. Random polyethylene-co-acrylic acid (PEA) copolymers were used as received (Scientific Polymer Products, Inc.). The two copolymers used (5% PEA and 15% PEA) contain 5% and 15% acrylic acid by weight respectively. Nonporous zirconia (ZrO_2) powder (monoclinic, VP zirconium dioxide, Degussa Corp.) was calcinated at 400°C to eliminate any residual organic impurities. The reported average primary particle size of this ZrO_2 is 30 nm, and the BET surface area is 40 m^2/g. Zirconia powder (2 grams) was dispersed in 250 ml xylene by sonication for 15 minutes. The copolymer solutions were prepared by dissolving the appropriate amount of polymer in 50 ml of warm xylene. A total of 7 samples were prepared for each copolymer using 30, 60, 120, 200, 300, 600, and 900 mg of polymer. The copolymer solutions were added to the dispersed zirconia powder under stirring. The resulting mixture was refluxed with stirring for one day. The samples were washed a total of six times each by redispersing the powder in 40 ml xylene with gentle heating, filtering, and then drying under vacuum after the final washing step. The samples studied along with the carbon content in percent weight (%C) determined from elemental analysis are summarized in Table 2.1.

Table 2.1 Samples, preparation loadings and adsorbed amounts of PEA.

Sample Name	**Preparation loadings mg polymer/g ZrO_2**	**Adsorbed amount % C***
5%PEA bulk	-	-
15% PEA bulk	-	-
15PEA5%	15	2.4
15PEA15%	15	2.2
30PEA5%	30	3.1
30PEA15%	30	3.2
60PEA5%	60	4.8
60PEA15%	60	4.5
100PEA5%	100	6.4
100PEA15%	100	5.6
150PEA5%	150	6.0
150PEA15%	150	6.6
300PEA5%	300	15.4
300PEA15%	300	15.0
450PEA5%	450	18.9
450PEA15%	450	17.8

*%C : is the percentage of carbon in an adsorbed polymer sample = [(wt C)/(wt polymer + wt zirconia)] x 100%.

Gel Permeation Chromatography (GPC). The molecular weights of the copolymers were determined by GPC. For the 5% PEA, $M_w \sim 7900$, and the polydispersity index is $M_w/M_n \sim 1.8$. For 15% PEA, $M_w \sim 1300$, and the polydispersity index is $M_w/M_n \sim 1.1$. The measurements were done at 135 °C in trichlorobenzene and PS standards were used for calibration. The flow rate was 1.000 ml/min. A refractive index detector and two Styragel HT6E L columns in series were used.

Differential Scanning Calorimetry (DSC). The crystallinity of the 5% and 15% PEA were 24% and 8% respectively, as determined by using a Perkin-Elmer differential calorimeter, DSC-7 with a heating rate of 15 °C/min under N_2 at a flow rate of 200 ml/min. The crystallinities were determined by determing the enthalpy of fusion by integrating the melting peak and comparing it to that of a PE crystal (290 J/g).

NMR. Solid-state ^{13}C NMR spectra (67.92 MHz) were recorded on a Chemagnetics CMX-270 NMR spectrometer with a 7 mm double-tuned fast magic angle spinning (MAS) Doty probe. Samples were spun at a rate of 3 kHz. A pulse delay of 3 s for both bulk (100 scans) and loadings (8000 scans) was used to acquire the ^{13}C CP-MAS spectra. For the ^{1}H-^{13}C cross polarization (CP) experiments, ^{1}H 90° pulse widths between 3 and 4 μs and a contact time of 3 ms were used. Fully relaxed dipolar decoupled magic angle spinning (DD-MAS) ^{13}C NMR spectra were also acquired for the bulk polymers using a pulse delay of 600 s.

For the 2D wide-line separation experiments (WISE),[10] a ^{1}H 90° pulse was followed by a proton evolution period, t_1, consisting of 128 increments of 5 μs. After each t_1 period, cross polarization followed by carbon detection with proton decoupling gives a carbon spectrum that is modulated as a function of t_1 by the free induction decay of the associated protons. 1024 scans were required for each t_1 evolution period. A short contact time of 0.5 ms was used to minimize proton spin diffusion, which will equalize the proton linewidths. The processed data sets contained 512 points in the F_2 (^{13}C) dimension and 1024 points in the F_1 (^1H) dimension. 2D WISE measurements with a spin diffusion mix time incorporated before the cross polarization step were also carried out.

The dipolar filter[11] (spin diffusion experiment) destroys the magnetization of the rigid phase (at 33 ppm) in a manner similar to the classic Goldman-Shen experiment.[12] The magnetization of the more mobile component (at 31 ppm) is retained. Eight cycles of the dipolar filter with 10 μs delays between the pulses were used. After application of the dipolar filter the residual magnetization was stored on the ± Z axis (parallel to the magnetic field B_o) for a mixing time t_m, during which spin diffusion occurs and eventually equilibrates the inhomogeneous distribution of magnetization. The intensities of the peaks were taken for each mixing time and corrected for longitudinal relaxation by measuring the signal decay for the same mixing time without the application of the dipolar filter.

FTIR-PAS. All spectra were run on powder samples of bulk and adsorbed polymers using a Fourier transform Mattson Research series 1 spectrometer equipped with a photoacoustic spectroscopy cell (MTEC model 300) at 1.0 cm^{-1} nominal resolution.

2.4 Results

2.4.1 ^{13}C CP-MAS NMR and FTIR-PAS Spectroscopy

The ^{13}C CP-MAS NMR and FTIR-PAS spectra of the bulk and adsorbed 5% and 15% polyethylene-co-acrylic acid random copolymers are shown in Figures 2.1 and 2.2. The ^{13}C CP-MAS NMR spectrum of polyethylene consists of a sharp peak at 33 ppm arising from all-trans polymer chains with restricted mobility within the crystalline regions and a broader peak at 31 ppm due to more mobile chains within the amorphous regions which contain gauche defects. The methylene carbon in this conformation is shielded relative to the all-trans one due to the γ-gauche effect.[13] The relative integrated intensities of the crystalline and amorphous components, I(33)/I(31) were 2.7 and 2.0 for PEA5% and PEA15% respectively. Fully relaxed ^{13}C DD-MAS NMR spectra were also acquired for the bulk polymers. The relative integrated intensities of the 33, 30 and 15 ppm peaks were 1.0, 0.89, 0.036 for 5% PEA and 1.0, 1.14, 0.049 for 15% PEA. The different relative intensities in the ^{13}C DD-MAS NMR spectra as compared to the spectra acquired with cross polarization is due to the different cross polarization efficiencies of the 33 and 31 ppm components. No quantitative analysis of the relative amounts of the two components was performed. The intensities of the methyl peaks at 15 ppm reflect the low molecular weights of these copolymers (M_w ~1300 and 8000). The lower crystallinity of the copolymer with higher acrylic acid content has been reported[14] and is due to disrupting the efficiency of chain packing.

The spectra of the adsorbed 5% PEA samples prepared with low loadings (15PEA5% to 150PEA5%) display resonances at 33 and 31 ppm which are of comparable relative intensities. Fully relaxed ^{13}C DD-MAS NMR spectra of the adsorbed samples showed similar relative intensities to the ^{13}C CP-MAS NMR spectra. Although these two peaks are assigned to chains in the crystalline and amorphous regions in bulk polyethylene, the 33 and 31 ppm resonances of the adsorbed copolymers are more properly described as arising from chain segments with a high trans content (transoid) and conformationally disordered chain segments containing a higher population of gauche defects (gauchoid). This distinction is important since we cannot refer to crystallinity (long range order) in the case of the adsorbed polymers.

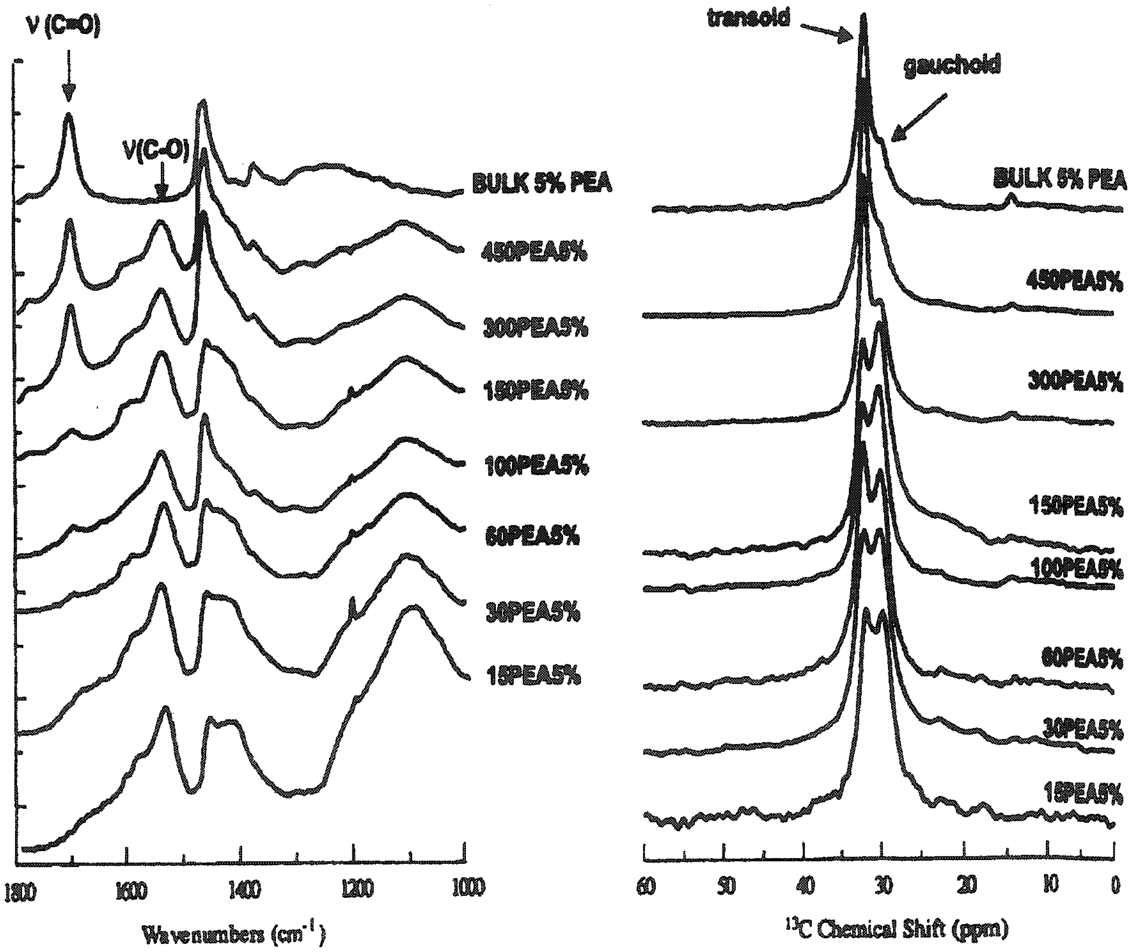

Figure 2.1 67.9 MHz ^{13}C CP-MAS NMR and FTIR-PAS spectra of the 5% polyethylene-co-acrylic acid copolymer in the bulk state and adsorbed on zirconia. See Table 2.1 for the loading amounts in the adsorbed polymer samples. A contact time of 3 ms, a spinning

speed of 3 kHz, and 100 and 8000 acquisitions were used for the bulk and adsorbed polymer samples respectively.

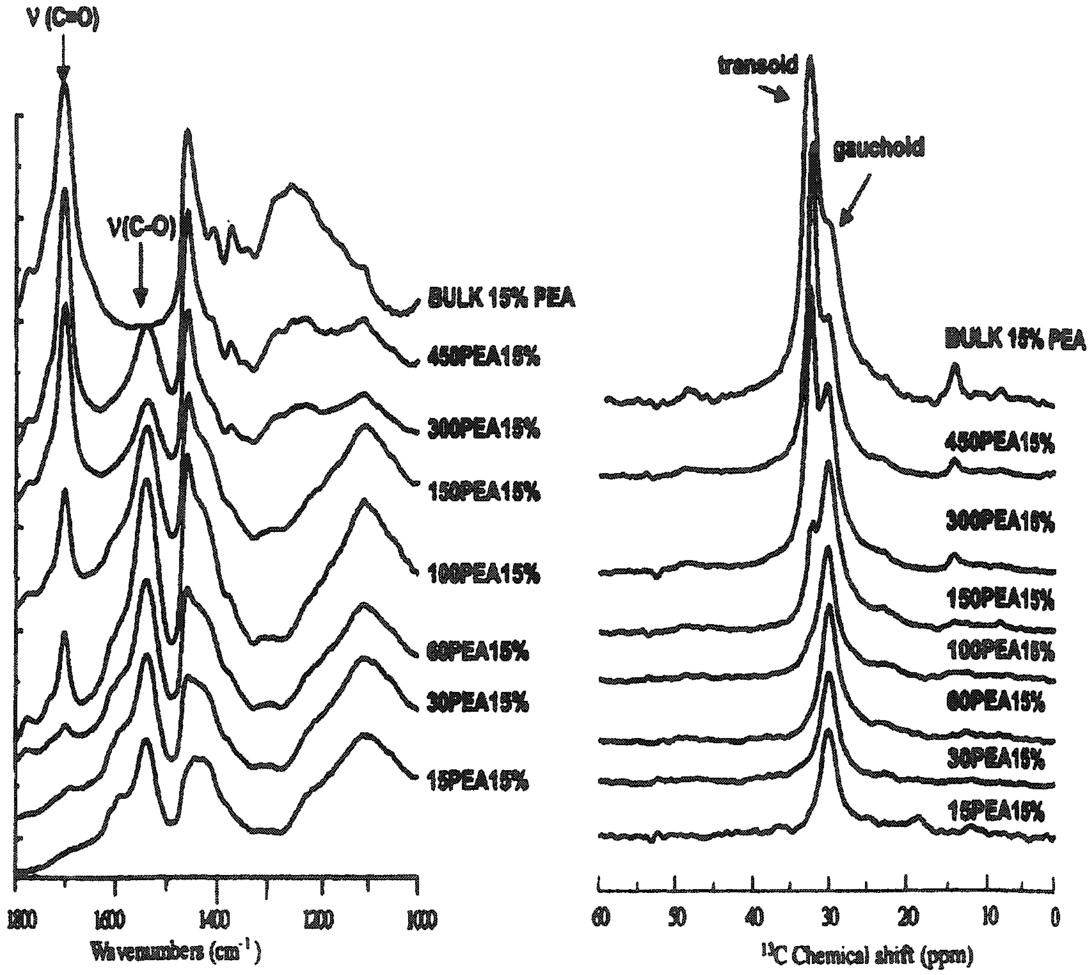

Figure 2.2 67.9 MHz ^{13}C CP-MAS NMR and FTIR-PAS spectra of the 15% polyethylene-co-acrylic acid copolymer in the bulk state and adsorbed on zirconia. See Table 2.1 for the loading amounts in the adsorbed polymer samples.

The absence of a free acid C=O band at ~1700 cm^{-1} in the FTIR-PAS spectra with the simultaneous appearance of new bands in the carboxylate region indicates that all the carboxylic acid groups are bound to the surface in the samples with the lowest copolymer loadings. The chemisorption of the acid groups is indicated by the appearance of two broad intense bands in the C-O stretching region at ~1540 and ~1460 cm^{-1}, which are assigned to the asymmetric and symmetric C-O stretches of a chelating bidentate zirconium carboxylate surface bond.[8] These bands were assigned previously from isotopically labeled fatty acids on zirconia.[9] Note that the CH_2 scissoring band at 1470 cm^{-1} overlaps with the symmetric C-O stretch at ~1460 cm^{-1}.

In the 100PEA15% and 300PEA5% samples, a strong peak at 1704 cm^{-1} appears which is assigned to the C=O stretch of unbound carboxylic acid groups. Weak broad peaks for unbound acid groups may also be present in the lower loadings, 60PEA15% and 150PEA5%. The appearance of a strong free acid peak for adsorbed PEA5% at a loading which is 3 times higher than when it appears for adsorbed PEA15% reflects the relative acrylic acid contents of the two copolymers. The FTIR-PAS spectra of the highest loadings are similar to those of the bulk copolymers with the additional presence of the 1540 cm^{-1} asymmetric C-O stretching band due the chemisorbed polymer segments. Likewise in the ^{13}C CP-MAS NMR spectra, the relative intensities of the transoid and gauchoid peaks at 33 and 31 ppm of the two highest loadings approach those of the bulk copolymers. In contrast to the 5% PEA samples, the ^{13}C CP-MAS NMR spectra of samples prepared with 15% PEA contain only one peak at 31 ppm when low loadings are used (15PEA15% to 100PEA15%). A 33 ppm transoid component first appears in 150PEA15%, a loading above which a free acid peak is present in the FTIR spectra. A similar correlation between the FTIR-PAS and ^{13}C CP-MAS NMR spectra is also evident for the 5% PEA. The intensity of the 33 ppm peak relative to that of the 31 ppm peak only increases in the 300PEA5% sample, the same loading at which a strong free acid peak appears in the IR spectra.

2.4.2 2D wideline separation (WISE) NMR

Qualitative information concerning the chain dynamics can be obtained from the WISE experiment which provides a correlation between chemical structure (^{13}C dimension) and mobility (^{1}H dimension).[10] In this 2D heteronuclear NMR experiment, each resolved ^{13}C resonance yields a proton wideline spectrum which reflects the dipolar couplings of the protons in the proximity of the respective ^{13}C nuclei. Since the ^{13}C chemical shift is sensitive to conformation, slices taken in the ^{1}H dimension in a 2D WISE spectrum allow separation of the broad proton resonances for ordered and disordered regions, which would completely overlap in the 1D ^{1}H NMR spectrum. In addition, the contributions from the protons associated with the metal oxide substrate are suppressed. In the WISE NMR spectrum of bulk polyethylene, the dipolar slice of the ^{13}C signal arising from the crystalline domains is a broad Gaussian peak with a typical linewidth of 50-70 kHz, whereas the slice corresponding to amorphous regions displays a motionally narrowed lineshape with widths between 5 and 20 kHz .[10]

Figure 2.3 shows the 33 and 31 ppm dipolar slices extracted from the 2D WISE NMR spectra of 100PEA5%, 450PEA5%, and the bulk copolymers and the linewidths are listed in Table 2.2. Relatively short contact times (0.5 ms) were used to

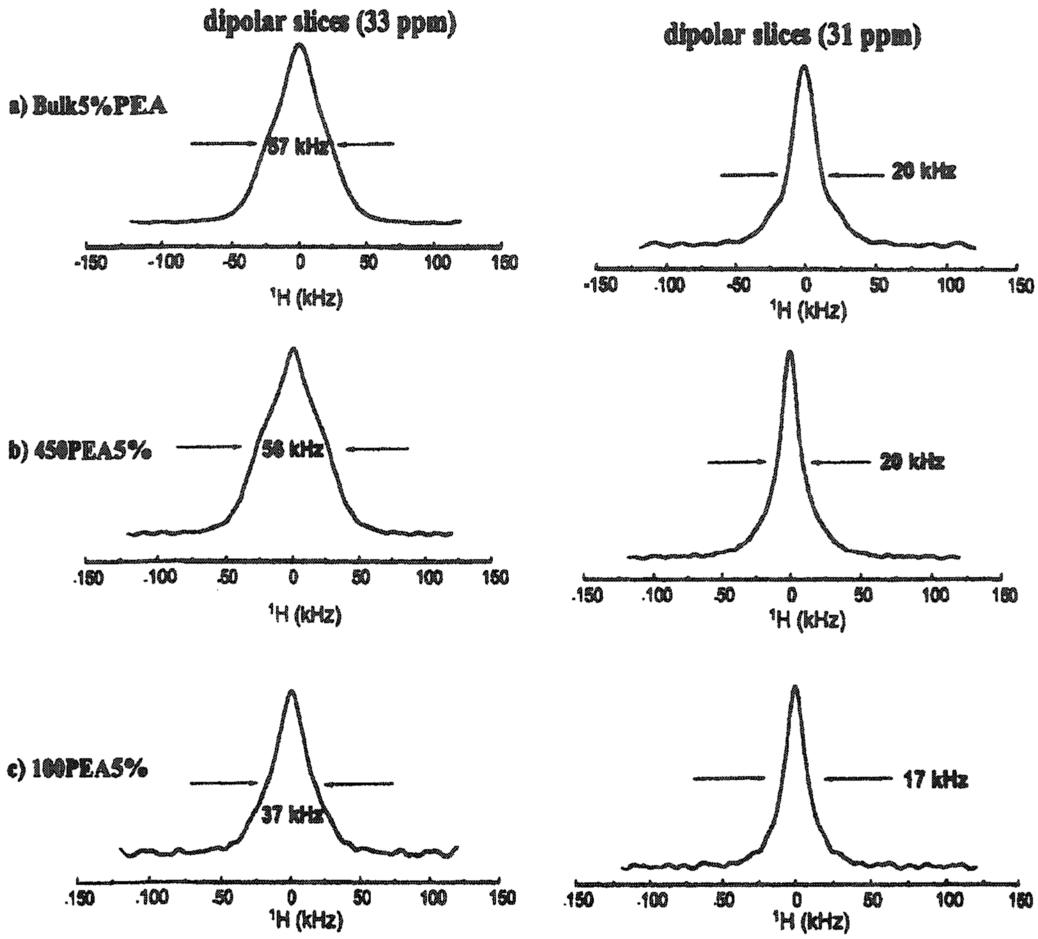

Figure 2.3 ^{1}H wide-line spectra for (a) 5% PEA, (b) 450PEA5% and (c) 100PEA5%. The ^{1}H wideline spectra shown correspond to the ^{1}H slices of the gauchoid and transoid components at 31 ppm and 33 ppm in the ^{13}C dimension in the 2D wide-line separation (WISE) NMR experiments.

minimize spin diffusion which will tend to equalize the linewidths. The WISE spectra indicate that the acrylic acid content affects the morphology and mobility of the copolymer. The width at half height of the crystalline (33 ppm) dipolar slice of the bulk 5% PEA was found to be 57-60, similar to bulk polyethylene. The dipolar slice of the crystalline component of the 15% PEA is 43 kHz.

The linewidths of the highest loading, 450PEA5%, and bulk 5% PEA are comparable, reflecting a similar dynamic state. In 100PEA5%, the reduced linewidth of the 33 ppm transoid component (38 kHz) shows that the dipolar couplings of the transoid chain segments of the adsorbed copolymer is less than the crystalline regions of the bulk copolymer. However, the linewidth of the 31 ppm component indicates that the gauchoid chain segments of the adsorbed polymers experience dipolar couplings similar to the chains in the amorphous regions of the bulk copolymer. A similar trend is observed for the 15% PEA samples.

2.4.3 Spin Diffusion Experiments

^{1}H spin diffusion experiments were used to determine the domain sizes of the crystalline and amorphous phases in the two copolymers and the ordered and disordered regions in the 100PEA5% and 450PEA5% adsorbed copolymer samples. Spin diffusion is the process by which nuclear magnetization is transported spatially through a solid sample via flip-flop transitions among dipolar coupled protons. In general, the first step of a spin diffusion experiment is to select the magnetization of one component and suppress the others via differences in mobilities or chemical shifts. The copolymer has two components of differing mobilities arising from the crystalline and amorphous regions. The dipolar filter experiment was used to select the magnetization of the more mobile amorphous component by suppressing the signal of the rigid component. Monitoring the transfer of magnetization from the mobile to the rigid component makes it possible to determine the length scales in polymers[15-20] and other heterogeneous materials.[21]

The spin diffusion experiment used consisted of four steps: (a) Selection of the more mobile proton component via the dipolar filter, (b) a mixing step of variable duration, τ_m, in which the remaining magnetization spreads into neighboring spins, (c) transfer of the ^1H magnetization to ^{13}C spins via cross polarization and (d) a detection period in which the resolved ^{13}C signals are recorded. The domain size is proportional to the square root of the product of the spin diffusion constant and the time for spin diffusion to eliminate the initial polarization gradient. The plot of the intensity of the more rigid component, I(33 ppm), versus $(\tau_m)^{1/2}$, Figure 2.4, confirms that spin diffusion occurs between the amorphous (mobile) and crystalline (rigid) regions. In many polymer studies of this kind, a sigmoidal shape is observed due to the presence of a significant interphase. However, this was not the case for our data. Using the initial rate approximation,[16] the domain sizes of the mobile region were calculated using the following equation:

$$d_{mobile} = 2\varepsilon(D_{eff}\,\tau^{s}{}_{m}/\pi)^{1/2}/F_{rigid} \qquad \text{where } F_{rigid} = 1 - F_{mobile} \qquad \textbf{2.1}$$

In the initial rate approximation, the parameter $(\tau^{s}{}_{m})^{1/2}$ is determined from a fit of the points in the initial linear range and extending this line to find the value of $(\tau_m)^{1/2}$ where the line intersects with I = 100%, at $\tau_m \to \infty$. The parameter ε in the equation designates the number of orthogonal directions relevant for the diffusion process.

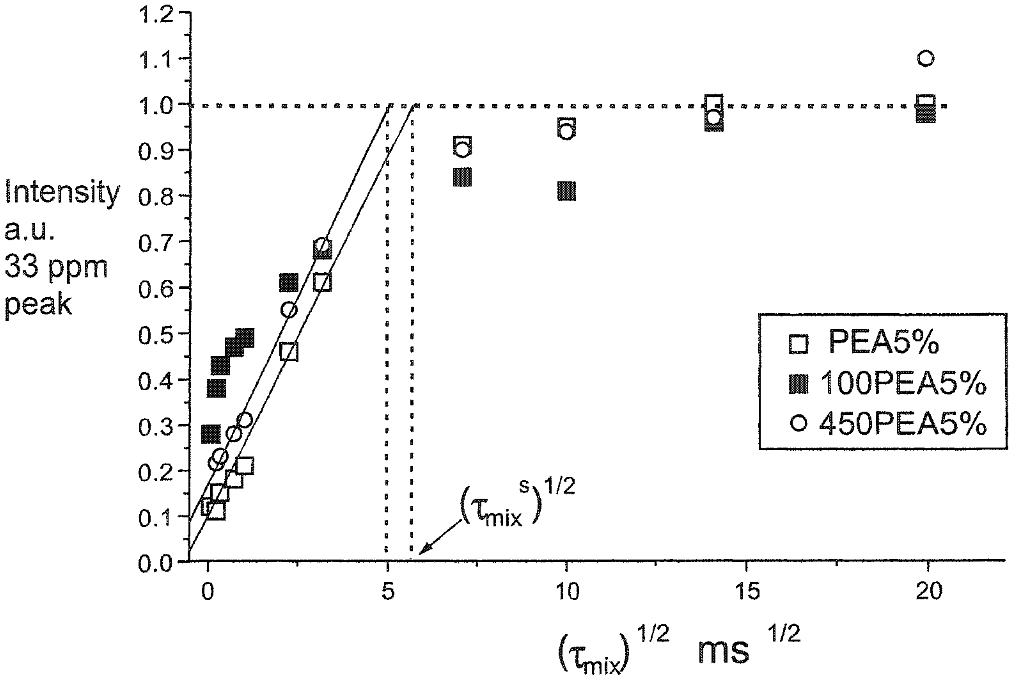

Figure 2.4 Plot of the peak intensity of the rigid peak at 33 ppm (corrected for T_1 relaxation) against the square root of the mixing time for the bulk 5% PEA and the adsorbed copolymer samples 450PEA5% and 100PEA5%. The build up signal is normalized against the average of the points in the plateau region.

Its value depends on the morphology and is 1 for polymers with lamellar morphology as is the case for polyethylene and which was assumed for the copolymers. It is justifiable to use a value of 1 for 450PEA5% since it is the bulk-like. As for 100PEA5%, this would be a crude approximation but is more likely than cylindrical ($\varepsilon = 2$) or spherical ($\varepsilon = 3$) morphologies. The square root of the effective spin diffusion coefficient is defined as:

$$\sqrt{D_{eff}} = \frac{\sqrt{D_{mobile}\, D_{rigid}}}{(\sqrt{D_{mobile}} + \sqrt{D_{rigid}})/2} \qquad \textbf{2.2}$$

The diffusivity D is proportional to the strength of the dipolar couplings and to the square of the average distance among nearest protons r_{HH}. The strength of the dipolar coupling is proportional to the full width at half height $\Delta\nu_{1/2}$ of a proton in a ^{1}H wideline spectrum. For $\Delta\nu_{1/2} > 5$ kHz, the spin diffusion coefficient can also be estimated using the following equation:

$$D = \frac{\Delta\nu_{1/2}\,(r_{HH})^2}{3} \qquad \textbf{2.3}$$

with the linewidth being in kHz and the separation in nm. For $\Delta\nu_{1/2} < 5$ kHz, a relationship between the spin-spin relaxation time, T_2, and the diffusion coefficient has been established.[19] Other useful formula for the diffusion coefficients of the rigid and mobile components have been discussed by Demco and coworkers.[19b]

In addition to the diffusion coefficients, the estimate of the domain sizes from spin diffusion experiments depend strongly on the assumed values for the volume fractions, F_{mobile} and $F_{rigid.}$ For polyethylene, the volume fractions are normally found from the crystallinity as measured by X-ray diffraction, DSC or a fully relaxed DD-MAS ^{13}C NMR spectrum. However, the crystallinities of the polyethylene-co-acrylic acid random copolymers, as measured by DSC versus the fully relaxed DD-MAS ^{13}C NMR spectra differ greatly. Whereas DSC measurements gave crystallinities of 24% and 8% for the 5% and 15% PEA respectively, the integrated intensities of the transoid and gauchoid components from the fully relaxed DD-MAS ^{13}C NMR spectra yielded much larger crystallinities of 52% and 47% respectively. A source of error is that the ^{13}C chemical shifts are due to conformational differences, which are not necessarily correlated with crystallinity. However, a 2D WISE experiment with a mix time incorporated, which takes into account both conformation and mobility, gave a similar result. This large discrepancy may be due to the presence of the acid groups which hinder the formation of large crystalline domains combined with the fact that DSC will only detect crystalline domains greater than 2 to 5 nm, depending on the polymer.[22a] A similar situation was reported for a closely related random copolymer, 20% poly(ethylene-co-methacrylic acid).[22b] Whereas the WISE experiment detected 50% crystallinity, X-ray diffraction indicated a 25% crystallinity in a poly(ethylene-co-methacrylic acid) with a 20 % methacrylic acid content. The large difference between these two techniques was attributed to the diffraction limit of ca. 1.5 nm for polyethylene.[22] Since the spin diffusion experiment is actually probing the transfer of magnetization from the mobile gauchoid chains to the less mobile transoid chain segments which may be located in very small crystalline domains not detected by DSC, it is more appropriate to use the volume fractions as derived from NMR. Using the volume fractions from the fully relaxed DD-MAS ^{13}C NMR spectra, the domain sizes of the 5% PEA are 6 and 7 nm for the rigid and mobile components respectively, and 8 nm and 7 nm for the rigid and mobile components of the 15% PEA. Although we would expect larger crystalline domains for the copolymer with the lower acrylic acid content, the rigid component domain sizes for 5%PEA and 15%PEA are the same within experimental error. These domain sizes are slightly larger than the 4.2 and 4.0 nm values measured in the 20% poly(ethylene-co-methacrylic acid) sample using a WISE experiment with a variable mix time. A similar analysis was performed for the adsorbed copolymers, 100PEA5% and 450PEA5%. The higher loading had domain sizes comparable to those of the bulk copolymer, ~ 7 and 5 nm for the rigid and mobile components, which is further evidence that the highest loading is bulk-like. In the case of the lower loading, 100PEA5%, it was not possible to fully suppress the component at 33 ppm using the same dipolar filter conditions and this results in the straight line not pasing through zero. The proton lineshape for the transoid component extracted from the 2D WISE experiment (Figure 2.3) shows a triangular proton lineshape. This type of line shape may be due to a superimposition of narrow and broad components. Such lineshapes can arise from a motional gradient along the chain, as observed for long chain fatty acid monolayers bound to ZrO_2,[9] or microheterogeneities within domains, as observed for core-shell polymers.[23]

Table 2.2 ^{1}H Linewidths and Domain Sizes of PEA loadings.

Sample	Proton linewidths at half-height, $\Delta\nu_{1/2}$ (kHz)		Domains sizes (± 1 nm)	
	33 ppm	31 ppm	33 ppm	31 ppm
Bulk PEA 15%	43	21	8	7
100PEA15%	_	21	_	_
Bulk PEA5%	57	20	6	7
100PEA5%	38	17	< 2	< 2
450PEA5%	56	20	7	5

2.5 Discussion

2.5.1 Structure at low coverage

The information derived from solid-state NMR (conformation, mobility and morphology) in combination with FTIR (sticker attachment) provides a detailed view of the adsorbed copolymer structure as a function of loading and sticker density. Polymers which are randomly attached to a surface may adopt train conformations, loop conformations (double tethered chains, or chains between two trains) and tails.[1] At low coverages, adsorbed homopolymers tend to maximize the interaction with the surface by forming train conformations. In the case of a copolymer, the adsorbed structure will depend on the selectivity of the solvent and the relative surface affinities of the two components. Whereas the polyacrylic acid forms strong ionic bonds with the zirconia surface, polyethylene can only interact via van der Waals interactions. The copolymer was adsorbed from a solvent that is selective for polyethylene. During the adsorption process, the acrylic acid groups will bind to the surface while the polyethylene segments will loop out into the favorable solvent environment. Upon drying, the final conformation of the polyethylene segments will depend on the topological constraints created by the strongly bound polyacrylic acid segments. The average distance between adsorption sites will be influenced by the solution conformation of the copolymer. Energetically unfavorable chain conformations may be kinetically trapped by the irreversible (due to formation of strong ionic bonds with zirconia) adsorption of the carboxylic acid sticker groups.

At low loadings, the sticker groups of the copolymer with the higher acrylic acid content, 15% PEA, are all attached to the surface and the polyethylene segments have a gauche/trans population and an apparent mobility similar to the amorphous regions of the bulk polymer, based on the proton linewidths and ^{13}C chemical shifts. This implies the formation of more looped conformations rather than flat, extended train structures which would be expected to have a larger trans content as well as a reduced mobility. Such train conformations have been reported for physisorbed polyethylene on silica.[24] In contrast to polyethylene, the PEA copolymers are strongly chemisorbed to the zirconia surface. The sticker groups attach to the surface with a random distribution, giving rise to a predominance of short looped segments rather than flat trains.

In the case of the adsorbed copolymer with a lower acrylic acid content, 5% PEA, the ^{13}C NMR data shows that certain chain conformations are strongly favored. Even at the lowest loadings, the adsorbed 5% PEA always contains a transoid component. Furthermore, the relative intensities of the transoid and gauchoid components remain constant with increasing coverage until most available surface sites are occupied. The occupation of most of the binding sites is indicated by the appearance of the FTIR band for unbound COOH groups. In a recent study, Wegman and coworkers covalently attached 5%, 10% and 15% PEA to silica gel via glycidoxypropyl and aminoproprуl linkages for use in reverse-phase liquid chromatography.[25] They also observed by solid-state ^{13}C NMR a higher trans content for the 5% PEA as compared to the copolymers with higher acrylic acid contents. The average number of methylene groups between the sticker groups in 5% PEA is much larger than in the 15% PEA. In a crude approximation, assuming an even distribution of acid groups, the 15% PEA and 5% PEA have on average ~ 30 and ~100 methylene groups respectively between sticker groups. In the case of molecular surfactants, 30 methylene units are sufficient for forming looped surface structures with all-trans segments. Allara and coworkers reported the formation of tightly folded, looping structures when the dicarboxylic acid, $HO_2C(CH_2)_{30}CO_2H$ was adsorbed on a silver surface.[26] The IR spectra showed components for all-trans CH_2 segments and a short sequence of conformationally disordered CH_2 groups. The fold was estimated to consist of at least 6 methylene groups and thus the all trans chain segments consisted of 12 methylene groups each. Since polymer chains are much more restricted in regards to surface rearrangements as compared to small molecules and there is a distribution of chain lengths between the sticker groups in a random copolymer, such tightly folded structures are unlikely. In the adsorbed 5% PEA samples, the polyethylene chain segments between sticker groups may be long enough for some folding to occur. Alternatively, a portion of the chain segment between sticker groups could lie flat on the surface, as in the case for physisorbed polyethylene, giving rise to the trans component observed at low coverages. However, the former case is both energetically and entropically more favorable. The selectivity of the solvent and the different surface affinities for the two components should reduce the occurrence of flat polyethylene trains. In either case, the all trans regions would be very small, as supported by the spin diffusion studies. These proposed structures are illustrated schematically in Figure 2.5.

2.5.2 Structure of adsorbed copolymers at high loadings

As the loading is increased, a free acid peak at 1704 cm^{-1} appears in the FTIR-PAS spectra of both adsorbed copolymers, indicating that some sticker groups are not bound to the surface. A transoid component appears in the solid-state ^{13}C NMR spectra of the adsorbed 15% PEA at a loading (150PEA15%) above which a strong signal for unbound sticker groups is first detected in the FTIR-PAS spectra (100PEA15%). In the case of copolymer chains with a higher sticker content, transoid chain segments only occur after occupation of the surface sites by other polymer chains. A related trend is observed for the adsorbed 5% PEA. The relative intensities of the transoid and gauchoid components remain constant with increasing coverage (15PEA5% to 150PEA5%). A large increase in the trans content occurs at 300PEA5%, the same loading at which a large IR band for unbound sticker groups appears. Thus the trans content of the surface-bound copolymer chains appears to be strongly determined by the average length of the segment between the sticker groups. Only when the loading is increased such that the incoming chains are forced to adopt more extended loop and tail conformations, does the trans content increase. At the highest high loadings, the adsorbed copolymers, which consists of extended loops and tails as well as polymer which is not directly adsorbed to the metal oxide surface, appears to be bulk-like in terms of the chain conformation, mobility and morphology. The majority of the polymer chains are no longer subjected to the perturbation caused by the surface.

2.5.3 Mobility of the adsorbed copolymers

Recent experimental work shows that polymer chain mobility may be greatly altered near a surface or interface.[27] If the chain mobility at the polymer surface is different than in the bulk, there are consequences for adhesion, friction, and other properties relevant to the performance of a polymer coating or an adhesive layer. For example, the welding of two glassy polymers would be affected by a lower glass transition temperature at the surface which would lead to more chain entanglements and thus better adhesion than expected for a polymer below its bulk T_g.[27b] The exact meaning of the "surface mobility" must be considered in relation to its effect on the polymer properties. A recent theoretical study of the surface and interior mobility of a polyethylene thin film found an enhanced mobility on a local segmental level at the surface but a diminished diffusivity in the direction normal to the surface.[28] In the case of supported films, the mobility may be enhanced or restricted, depending on the film thickness and the nature of the interaction of the polymer with the solid surface.[4, 27a]

In the case of adsorbed PEA copolymers, the polyethylene segments become more conformationally disordered and apparently more mobile upon adsorption due to the random binding of the sticker groups to the surface which increases the available free volume between chains. However, it is important to note that an increased free volume alone will narrow NMR lines without an increase in mobility. Packing and mobility are often correlated, but when adsorbed on a surface, the polymer chains might be rigid, yet loosely packed. A reduction of the interchain dipolar interactions due to low surface coverages will lead to reduced linewidths. Wideline proton NMR studies of polyethylene inclusion compounds show that the proton linewidth of a rigid isolated polyethylene chain is approximately 30% smaller than that of chains located in the rigid crystalline regions of bulk polyethylene.[29] The transoid component of the adsorbed 5% PEA at low loadings showed a reduced linewidth of 38 kHz as compared to the linewidth of 57 kHz for chains located in the crystalline domains of the bulk copolymer. The proton linewidths of the gauchoid components in both adsorbed copolymers, ~ 20 kHz, is similar to the amorphous regions of the bulk copolymers. If the reduced proton linewidths are primarily due to enhanced mobility, this behavior contrasts sharply with that observed in a solid-state ^{13}C NMR study of physisorbed polyethylene. Inoue and co-workers compared the conformation and dynamic behavior of ^{13}C-labeled polyethylene samples which were solution-crystallized, melt-quenched and adsorbed on silica gel.[23] Although the polyethylene adsorbed on silica gel had the largest mobile component at 30 ppm, the methylene chain motion of this component was found to be much more restricted than the chains in the non-crystalline regions of both the melt-quenched and solution-crystallized bulk polyethylene. The authors suggested that two components with different molecular motions were present. First, there are directly adsorbed chains with mostly trans and some gauche conformations (16:1) which are frozen on the NMR timescale and secondly, there is adsorbed polyethylene not in direct contact with the surface which is undergoing rapid transitions between trans and gauche conformations, similar to the amorphous regions of bulk polyethylene. However, this motion is more restricted than that of the amorphous regions of bulk state. The difference in the motional behavior of the adsorbed polyethylene copolymer versus the homopolymer, as described above, is due to the disordering effect of the sticker binding. ^{13}C NMR relaxation studies of the adsorbed PEA copolymers are currently underway for a more definitive characterization of the relative mobilities.

2.5.4 Chain conformation of adsorbed copolymers

There has been relatively little work, either theoretically or experimentally, concerning the role of the chain conformation on the fracture energy of polymer films on solid surfaces. Experimental work shows the existence of an optimal sticker concentration which gives a maximum in the fracture energy. Below this optimal sticker concentration, the fracture energy increases with sticker concentration. Above this maximum, an increasing sticker concentration decreases the fracture energy due to cohesive failure.[6] In regards to the relation of chain conformation to this behavior, Gutman and Chakraborty argued that a sticker concentration higher than optimal leads to the formation of a flat polymer layer, giving rise to a second diffuse interface between the near-surface chains and those further away from the solid surface.[7a] They propose that the locus of failure is at this second interface. Based on experimental work, Brogly and co-workers have recently proposed a model for the adhesion of ethylene vinylacetate copolymers to alumina in which the chain conformation plays a role.[30] Vibrational studies to determine the orientation of the functional groups were combined with molecular dynamics simulations to obtain the polymer conformation in the adsorbed state. The proposed adsorption mechanism consists in a balance between a high probability to establish interfacial interaction (at low sticker group content) and a low probability for the chain to change in conformation in order to interact (at high sticker group content).[30d] This picture also leads to an optimal sticker concentration for maximum adhesion.

Poly(ethylene-co-acrylic acid) is commonly used as an adhesion promoter for polyethylene coatings on metal and paper surfaces. Simmons and Chakraborty have theoretically investigated the use of random heteropolymers as adhesion promoters between a homopolymer melt and a solid surface.[7b] The conformation of the random heteropolymer as a function of coverage and fraction of adsorbed segments was examined. At low coverages of the heteropolymer, the optimal parameters for adhesion combine a relatively high adsorbed fraction with long loops extending away from the surface to promote entanglements with the bulk homopolymer. At higher coverages, a separate random heteropolymer phase may develop depending on the segment-surface and segment-segment interaction strengths, creating the potential to fail at either the solid-polymer (adhesive failure) or polymer-polymer interface (cohesive failure).

2.6 Conclusions

Since adhesion studies of PEA laminates as a function of acrylic acid content have been reported mostly for alumina surfaces,[5] we cannot directly compare our results with these studies or the theoretical studies described above. The stronger binding of carboxylic acids on zirconia or zirconium alkoxide treated surfaces as compared to alumina[8] may influence the average chain conformation. The adhesion of PEA films to alumina increases both with acrylic acid content and crystallinity. Our spin diffusion and WISE NMR measurements show that for thick layers of PEA on ZrO_2, the morphology and crystallinity is similar to the bulk copolymers. The maximum adhesion of high density polyethylene (HDPE) to alumina/PEA laminates was found when high molecular weight PEA with a medium acrylic acid content (~ 13% wt) was used for the adhesion layer. However, for low density polyethylene (LDPE), high molecular weight, low acrylic acid content PEA layers (~ 3% wt) performed better.[5a] Whether there is any correlation between these adhesion measurements and the chain conformation and sticker attachment as measured by NMR and FTIR respectively would require a similar study of PEA adsorbed on alumina. Previous FTIR studies of the interaction of PEA with alumina have employed solution cast films.[5b,c] However, direct comparisons between hot pressed laminates versus solution cast films may not be valid.[5b]

In summary, the influence of the acrylic acid content on the conformation and mobility of chemisorbed ethylene-acrylic acid random copolymers was studied by solid-state NMR and FTIR photoacoustic spectroscopies. The chain conformation of the adsorbed random copolymer is most strongly influenced by the acrylic acid content rather than the coverage. These studies will be extended to alumina to determine the influence of the metal oxide substrate on the chain conformation and to examine whether correlations with adhesive properties exist. Relaxation measurements and variable temperature experiments are currently underway to further explore the dynamic properties of these adsorbed copolymers.

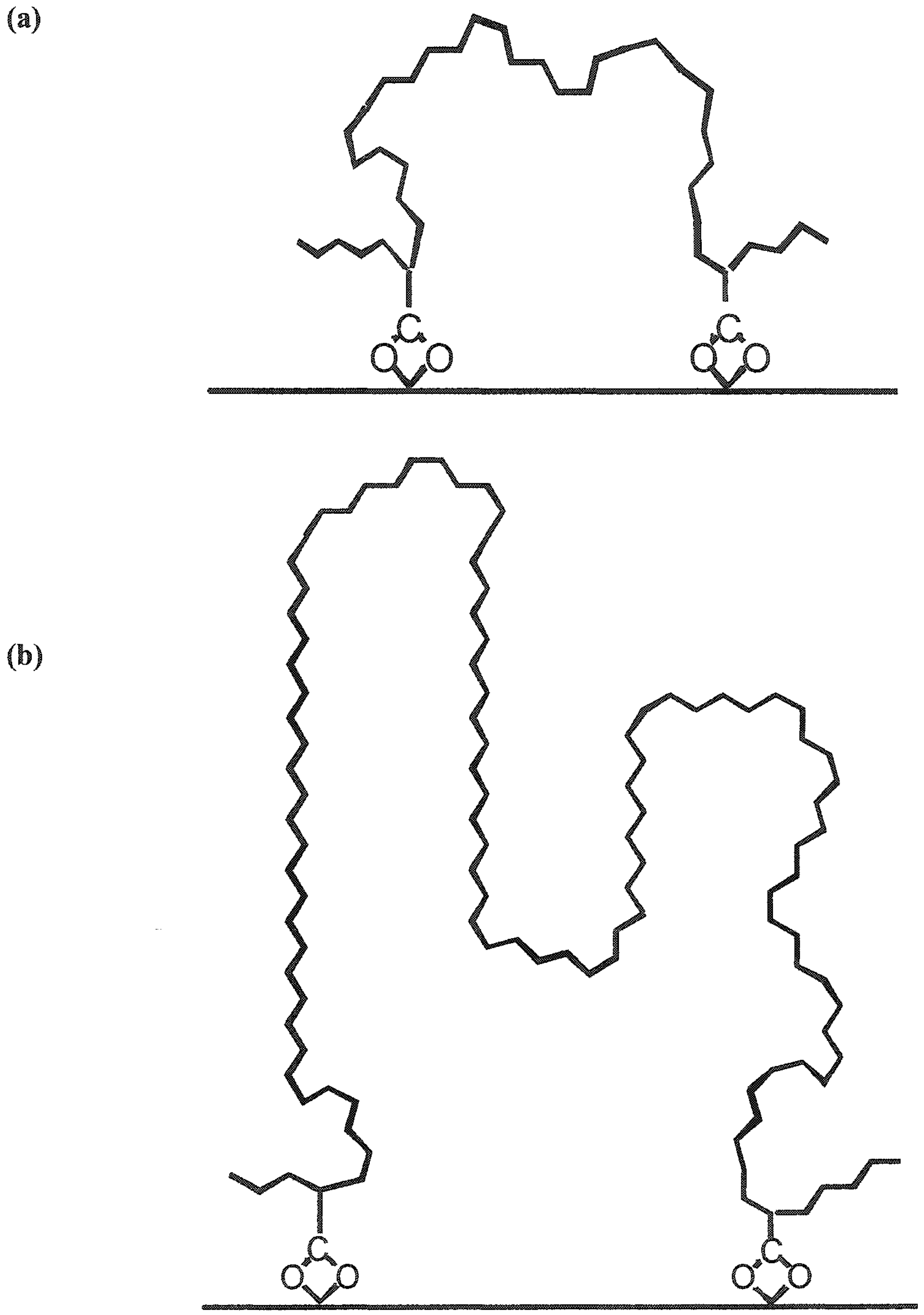

Figure 2.5 A schematic diagram showing the conformations adopted by low loadings of (a) 15% PEA and (b) 5% PEA.

2.7 References

(1) (a) Fleer, G.J.; Stuart, M.A.; Scheutjens, J.M.H.M.; Cosgrove, T.; Vincent, B. *Polymers at Interfaces*; Chapman & Hall: London, 1993. (b) Wool; R.P. *Polymer Interfaces: Structure and Strength* ; Hanser/Gardner: New York, 1995. (c) Jones, R. A. L.; Richards, R.W. *Polymers at Surfaces and Interfaces*; Cambridge University Press: Cambridge, 1999.

(2) (a) Cosgrove, T.; Barnett, K.G. *J. Mag. Res.* **1981**, *43*, 15. (b) Cosgrove, T.; Griffiths, P.C. *Advances in Colloid and Interfaces* **1992**, *42*, 175.

(3) Schimdt-Rohr, K.; Spiess, H.W. *Multidimensional Solid-State NMR and Polymers*, Academic Press, New York, 1994.

(4) (a) Lin, W.Y.; Blum, F.D. *Macromolecules* **1998** *31* 4135. (b) Blum, F. *Ann. Rep. NMR Spectroscopy* **1994**, *28*, 277. (c) Blum, F.D. *Colloids and Surfaces* **1990**, *45*, 361.

(5) (a) Smarook, W. H.; Bonotto, S. *Polym. Eng. Sci.* **1968**, *8*, 41. (b) Ulren, L.; Hjertberg, T.; Ishida, H. *J. Adhesion* **1990**, *31*, 117. (c) Stralin, A.; Hjertberg, T. *Surf. Interface Anal.* **1993**, *20*, 337. (d) Guezenoc, H.; Segui, Y.; Thery, S.; Asfardjani, K. *J. Adhesion Sci. Technol.* **1993**, *7*, 953. (e) Lee, J. H.; Kim, H. W.; Pak, P. K.; Lee, H. B. *J. Polm. Sci. A* **1994**, *32*, 1569. (f) Brack, H. P.; Risen, W. M. *J. Mater. Chem.* **1997**, *7*, 2355. (g) Cho, C. K.; Cho, K.; Park, C. E. *J. Adhesion Sci. Technol.* **1997**, *11*, 433. (h) McEnvoy, R. L.; Krause, S.; Wu, P. *Polymer* **1998**, *39*, 5223.

(6) (a) Gong, L.; Friend, A. D.; Wool, R. P. *Macromolecules* **1998**, *31*, 3709. (b) Lee, I.; Wool, R. P. *Macromolecules* **2000**, *33*, 2680.

(7) (a) Gutman, L.; Chakraborty, A. K. *J. Chem. Phys.* **1994**, *101*, 10074. (b) Simmons, E.R.; Chakraborty, A. K. J. Chem. Phys. 1998, 109, 8667.

(8) (a) Aronoff, Y. G.; Chen, B.; Lu, G.; Seto, C.; Schwartz, J.; Bernasek, S. L. *J. Am. Chem. Soc.* **1997**, *119*, 259. (b) VanderKam, S. K.; Bocarsly, A. B.; Schwartz, J. *Chem. Mater.* **1998**, *10*, 685.

(9) Pawsey, S.; Yach, K.; Halla, J.; Reven, L. *Langmuir* **2000**, *16*, 3294.

(10) (a) Zumbulyadis, N. *Phys. Rev. B* **1986**, *33*, 6495. (b) Tekely, P. *Macromolecules* **1993**, *26*, 7363. (c) Claus, J.; Schmidt-Rohr, K.; Adam, A; Boeffel, C.; Spiess, H.W. *Macromolecules* **1992**, *25*, 5208. (d) Schmidt-Rohr, K.; Clauss, J.; Spiess, H.W. *Macromolecules* **1992**, *25*, 3273.

(11) Egger, N.; Schmidt-Rohr, K.; Blümich, B.; Domke, W.D.; Stapp, B. *J. App. Polym. Sci.* **1992**, *44*, 289.

(12) Goldman, M.; Shen, L. *Phys. Rev.* **1966**, *144*, 321.

(13) Tonelli, E. *NMR Spectroscopy and Polymer Microstructure*. VCH publ., New York, 1989.

(14) (a) Otocka, E. P.; Kwei, T. K. *Macromolecules* **1968**, *1*, 244. (b) MacKnight, W. J.; Taggart, W. P.; McKenna, L. *J. Polymer Sci.: Symp. No. 46* **1974**, 83.

(15) Blümich, B. *Adv. Mat.* **1991**, *3*, 237.

(16) Claus, J.; Schimdt-Rohr, K.; Spiess, H.W. *Acta Polym.* **1993**, *44*, 1.

(17) Cai, W.Z.; Schimdt-Rohr, K.; Egger, N.; Gerharz, B.; Spiess; H.W. *Polymer* **1993**, *34*, 267.

(18) Landfester, K.; Boeffel, C.; Lambla, M.; Spiess, H.W. *Macromolecules* **1996**, *29*, 5972.

(19) (a) Mellinger, F.; Wilhelm, M.; Spiess, H.W. *Macromolecules* **1999**, *32*, 4686. (b) Demco, D. E. Johansson, A.; Tegenfeldt, J. *Solid State NMR* **1995**, *4*, 13.

(20) Hu, W.G.; Schmidt-Rohr, K. *Polymer* **2000**, *41*, 2979.

(21) De Paul, S.M.; Zwanziger, J.W.; Ulrich, R.; Wiesner, U.; Spiess, H.W. *J. Am. Chem. Soc.* **1999**, *121*, 5727.

(22) (a) Mandelkern, L. *Crystallization of Polymers*, Cambridge University Press, Cambridge, 2002. (b) Chin, Y.H.; Kaplan, S. *Mag. Res. Chem.* **1994** *32*, S53.

(23) Landfester, K.; Boeffel, C.; Lambla, M.; Spiess, H. W. *Macromolecules* **1996**, *29*, 5972.

(24) (a) Inoue, D.; Kurosu, H.; Chen, Q.; Ando, I. *Acta Polymer.* **1995**, *46*, 420. (b) Yamanobe, T. in *Solid State NMR of Polymers* eds. Ando, I.; Asakura, T. Elsevier, Amsterdam, 1998.

(25) Wegmann, J.; Albert, K.; Pursch, M.; Sander, L. C. *Anal. Chem.* **2001**, *73*, 1814.

(26) Allara, D.L.; Atre, S.V.; Elliger, C.A.; Snyder, R.G. *J. Am. Chem. Soc.* **1991**, *113*, 1852.

(27) (a) Jones, R. A. L. *Curr. Opin. Colloid Inter.* **1999**, *4*, 153. (b) Jones, R. A. L.; Richards, R. W. *Polymers at Surfaces and Interfaces*, Cambridge University Press: Cambridge, 1999, pp.50-4.

(28) Doruker, P.; Mattice, W. L. *Macromolecules* **1999**, *32*, 194.

(29) Hori, Y.; Tanigawa, T.; Shimada, S.; Kashiwabara, H. *Polymer J.* **1981**, 293.

(30) (a) Brogly, M.; Nardin, M.; Schultz, J. *J. Adhesion* **1996**, *58*, 263. (b) Brogly, M.; Bistac, S.; Schultz, J. *Macromolecules* **1998**, *31*, 3967. (c) Brogly, M.; Bistac, S.; Schultz, J. *Macromol. Symp.* **1999**, *141*, 129. (d) Broglie, M. *Rev. Metall./Cah. Inf. Tech.* **2001**, *98*, 75.

Chapter Three

Dynamics of Adsorbed Polyethylene-Acrylic Acid Copolymers: A Solid-State NMR Study

---

3.1 Preface

Variable temperature ^{13}C CP-MAS, ^{13}C spin-lattice relaxation, and two-dimensional exchange solid-state NMR experiments are used to probe the dynamics of bulk and zirconia-adsorbed polyethylene-co-acrylic acid (PEA) random copolymers. The dependence of chain mobility on copolymer loading and sticker concentration is investigated. These experiments were carried out to distinguish between the two chain conformations proposed for the trans component of the low loadings of 5%PEA in Chapter 2.

3.2 Introduction

Polymer/solid interfaces play a central role in industrial applications of polymers. The microscopic picture, that is, the conformation, dynamics, and morphology of polymers at interfaces, ultimately determines the performance of polymer-based composites, protective coatings and adhesives.[1] However, the extent to which these properties differ from the bulk state is neither theoretically fully understood nor experimentally well characterized. In particular, the relationship between the dynamic features of adsorbed polymers to surface properties has not been explored. In the case of supported films, the mobility maybe enhanced or restricted, depending on the film thickness and the nature of the interaction of the polymer with the solid surface. With decreasing film thickness, confinement eventually perturbs the average conformation of the polymer chains as well as the density, which in turn can affect the glass transition, thermal expansion, and mechanical properties.[1] For example, dewetting experiments on polystyrene films indicate that the polymer density decreased at the surface leading to enhanced mobility and a glass transition temperature in the film lower than that in the bulk state.[2]

The mobility of adsorbed polymers can be probed with different techniques on a wide variety of length scales. For example, X-ray reflectometry[2,3] and ellipsometry probe the behavior of the polymer through its entire thickness. Fluorescence recovery[4] has been used to probe the diffusion of polymer chains, showing that the translational motions of the entire chains appeared to be retarded with decreasing film thickness. Positron annihilation[5] and optical probe reorientation[6] have been applied to detect the free volume and molecular reorientation in polymer thin films. For characterizing the dynamic behavior on a molecular length scale, NMR spectroscopy is the method of choice. Solid-state NMR is routinely used to characterize the local segmental motions in bulk solid polymers but is far less commonly applied to adsorbed polymers due to sensitivity problems.[7]

Copolymers containing polar groups, such as hydroxyl or carboxylic acid groups, are commonly used to increase the adhesion of polymer films to metal surfaces. Previous studies of these films have focused on the mechanical properties rather than the microscopic structure or dynamic properties. These studies have indicated that a critical concentration of polar sticker groups is required for an optimal chain connectivity to the surface and a maximum fracture energy.[8] Theoretical studies of adsorbed random copolymers predict that this fracture energy is also associated with the chain conformation at the surface. Simmons and Chakraborty theoretically investigated the use of random heteropolymers as adhesion promoters between a homopolymer melt and a solid surface. At low coverages of the heteropolymer, the optimal parameters for adhesion combine a relatively high adsorbed fraction with long loops extending away from the surface to promote entanglements with the bulk homopolymer.[9] However, little work has been carried out to corroborate these and other theoretical results concerning the relation between polymer conformation and adhesion.

Our previous study of bulk and adsorbed polyethylene-co-acrylic acid (PEA) random copolymers revealed a key finding: the existence of a preferred chain conformation at the surface dictated by the sticker group density rather than the surface coverage.[10] The adsorbed copolymer structure will depend on the selectivity of the solvent and the relative surface affinities of the two components. PEA was adsorbed from a solvent that is selective for polyethylene. During the adsorption process, the acrylic acid groups will bind to the surface while the polyethylene segments will loop out into a favorable solvent environment. Upon drying, the final conformation of the polyethylene segments will depend on the topological constraints created by the irreversible adsorption of the carboxylic acid sticker groups. Energetically unfavorable chain conformations may be kinetically trapped.

In the case of adsorbed PEA with a low acrylic acid content, a trans conformation of a significant fraction of the polyethylene chain segments was observed which persisted down to the lowest coverages. This trans component may arise from the formation of trains where the chain segments lie flat on the surface. Alternatively, a low density of sticker groups may allow for the formation of loops long enough for some chain folding. This folded looped structure of the adsorbed copolymer would differ greatly from the usual conformation of physisorbed homopolymers, which typically maximize the interaction with the surface by forming trains. A study of the chain dynamics may help distinguish between the two possible structures since the mobility of the trans component arising from partially folded long loops is expected to be higher than either a flat train conformation or chains located in the crystalline regions of the bulk copolymer. In this paper, the dynamics of bulk and adsorbed PEA samples is studied by variable temperature ^{13}C CP-MAS, ^{13}C spin-lattice relaxation, and two-dimensional exchange solid-state NMR experiments to provide further insight into the surface structures of adsorbed polyethylene-acrylic acid copolymers.

3.3 Experimental section

Sample preparation. Random polyethylene-co-acrylic acid (PEA) copolymers were used as received (Scientific Polymer Products, Inc.). The copolymer used, 5% PEA, contains 5% acrylic acid by weight. Nonporous zirconia (ZrO_2) powder (monoclinic, VP zirconium dioxide, Degussa Corp.) was calcinated at 400°C to eliminate any residual organic impurities. The reported average primary particle size of this ZrO_2 is 30 nm, and the BET surface area is 40 m^2/g. Zirconia powder (2 grams) was dispersed in 250 ml xylene by sonication for 15 minutes. The copolymer solutions were prepared by dissolving the appropriate amount of polymer in 50 ml of warm xylene. Samples were prepared using 15, 60, 100 and 450 mg of polymer per gram of zirconia powder. These samples are designated as 15PEA5%, 60PEA5%, 100PEA5% and 450PEA5%. The copolymer solutions were added to the dispersed zirconia powder under stirring. The resulting mixture was refluxed with stirring for one day. The samples were washed a total of six times each by redispersing the powder in 40 ml xylene with gentle heating, filtering, and then drying under vacuum after the final washing step. The carbon content in percent weight (%C) determined from elemental analyses for selected samples are reproduced from reference 10 in Table 3.1.

Table 3.1 Samples, preparation loadings and adsorbed amounts of selected PEA5% loadings.

Sample Name	Preparation loadings (mg polymer/g ZrO_2)	Adsorbed amount (% C)
5%PEA bulk	-	-
100PEA5%	100	6.4
450PEA5%	450	18.9

%C : is the percentage of carbon in an adsorbed polymer sample = [(wt C)/(wt polymer + wt zirconia)] x 100%.

Solid-State NMR. Solid-state ^{13}C NMR spectra (67.92 MHz) were recorded on a Chemagnetics CMX-270 NMR spectrometer with a 7 mm double-tuned fast magic angle spinning (MAS) Doty probe. Samples were spun at a rate of 3 kHz. A pulse delay of 3 s for both bulk (100 scans) and loadings (8000 scans) was used to acquire the ^{13}C CP-MAS spectra. For the ^{1}H-^{13}C cross polarization (CP) experiments, ^{1}H 90° pulse widths between

3 and 4 μs and a contact time of 3 ms were used. Fully relaxed dipolar decoupled magic angle spinning (DD-MAS) ^{13}C NMR spectra were also acquired for the bulk polymers using a pulse delay of 600 s. For the variable-temperature CP-MAS experiments, the sample temperature was controlled to within ± 2° by a Chemagnetics temperature controller.

^{13}C two-dimensional (2D) exchange experiments[11] are used to probe ultraslow motions on bulk and adsorbed samples. The pulse sequence consists of a preparation period where cross polarization is used to create ^{13}C transverse magnetization which is allowed to precess during the subsequent evolution period and then stored along the z axis by applying a 90° pulse to the ^{13}C spins. During the ensuing mix time, if any molecular reorientations occur, ^{13}C precessional frequencies will be altered when a second 90° pulse restores the magnetization to the transverse plane. The ^{13}C signal is acquired during the second evolution period. If no molecular reorientations occur the frequencies during the two evolution times will be identical and the 2D spectrum will contain intensity only the main diagonal where $f_1 = f_2$. By varying the mix times, motions with correlation times in the range of 10^{-5}s < τ_c < 10^2s can be detected where the upper limit is determined by the ^{13}C spin-lattice relaxation time. 2D exchange spectra are acquired on a Chemagnetics CMX-300 NMR spectrometer using a Chemagnetics PENCIL probe with 7.5 mm zirconia rotors. Pulse widths between 3.5 and 4.5 μs, a contact time of 2 ms, a MAS rate of 3kHz, and a pulse delay of 2 s were used for both bulk (300 scans) and adsorbed (1000 scans) samples. The spectra were taken with 64-128 t_1 increments of 333 μs. ^{13}C spin-lattice relaxation times were measured using the Torchia pulse sequence.[12] Two runs were done with sets of short and long relaxation delays to measure relaxation times of disordered and ordered components of bulk and adsorbed samples. A pulse delay of 5 s was used.

FTIR-PAS. All spectra were run on powder samples of bulk and adsorbed polymers using a Fourier transform Mattson Research series 1 spectrometer equipped with a photoacoustic spectroscopy cell (MTEC model 300) at 1.0 cm^{-1} nominal resolution.

3.4 Results

3.4.1 ^{13}C CP-MAS NMR and FTIR-PAS

The ^{13}C CP-MAS NMR and FTIR-PAS spectra of bulk 5%PEA, and of the loadings 100PEA5% and 450PEA5% are shown in Figure 3.1. The ^{13}C CP-MAS NMR spectrum of 5%PEA at 25°C is similar to that of polyethylene (PE) which consists of a sharp peak at 33 ppm arising from all-trans polymer chains within the crystalline regions and a broader peak at 31 ppm due to more mobile chains within the amorphous regions which contain gauche defects. The methylene carbon in this conformation is shielded relative to the all-trans one due to the γ-gauche effect.[13] The FTIR-PAS spectrum of 5%PEA contains a peak at ~ 1700 cm^{-1} corresponding to dimerized acid groups. The ^{13}C CP-MAS NMR spectrum of the adsorbed copolymer sample, 100PEA5%, displays resonances at 33 and 31 ppm, which are of comparable relative intensities. Fully relaxed ^{13}C DD-MAS NMR spectra of the adsorbed samples showed similar relative intensities to the ^{13}C CP-MAS NMR spectra. Although these two peaks are normally assigned to chains in the crystalline and amorphous regions in the case of bulk polyethylene, in the case of adsorbed polymers these resonances are more properly described as arising from chain segments with a high trans content and disordered chain segments containing a higher population of gauche defects. The absence of a free acid C=O band at ~1700 cm^{-1} in the FTIR-PAS spectrum of 100PEA5% and the simultaneous appearance of new bands in the carboxylate region indicates that all the carboxylic acid groups are bound to the surface in this particular loading. The ^{13}C CP-MAS NMR spectrum of the higher loading, 450PEA5%, is bulk-like in terms of the relative intensities of the 33 and 31 ppm peaks. Its FTIR-PAS spectrum shows a strong free acid peak at 1700 cm^{-1} corresponding to unbound acid groups as well as peaks at ~1540 and ~1460 cm^{-1} for surface-bound carboxylate groups.

3.4.2 Variable Temperature ^{13}C CP-MAS NMR

The variable temperature ^{13}C CP-MAS NMR spectra of bulk 5%PEA, and for the adsorbed copolymer samples, 100PEA5% and 450PEA5%, are given in Figure 3.2. The spectra indicate how the relative trans/gauche populations vary with temperature, but the estimate is approximate since cross polarization experiments are not strictly quantitative due to differences in the cross polarization efficiency with varying molecular mobility. However direct ^{13}C polarization experiments using long acquisition delay times showed that variation in the cross polarization efficiency was not a large factor. For bulk 5%PEA at –50°C, Figure 3.2a, the transoid component at 33 ppm dominates the spectrum and 31 ppm gauchoid component is no longer visible. Variable temperature ^{13}C NMR studies of polyethylene have shown that the resonance of the amorphous component typically broadens into the baseline in this temperature range where the motional frequency matches the decoupling frequency. The broad amorphous peak also shifts slightly upfield due to a change in the gauche and trans conformers.[14] A similar process occurs in

5%PEA in both the bulk and adsorbed states. As the temperature is raised to 70°C, the 31 ppm peak of the bulk 5%PEA narrows and increases in intensity while the trans component diminishes. The relative intensities of the 31 and 33 ppm peaks at 70°C are similar to those observed in the variable temperature ^{13}C CP-MAS spectra of PE.[14]

The spectrum of the adsorbed copolymer sample with the lower loading, 100PEA5% (Figure 3.2b), displays resonances at 33 and 31 ppm, which are of comparable relative intensities at room temperature. The trans component dominates the spectrum at –50°C and gradually decreases with increasing temperature until 70°C where it is completely gone. The adsorbed copolymer sample with the highest loading, 450PEA5% (Figure 3.2c), displayed a thermal behavior closer to that of the bulk copolymer. The trans component again dominates the spectrum at –50°C with the 31 ppm peak broadened into the baseline but at 70°C the trans component is still present. However, the relative intensities of the 33 and 31 ppm peaks show that the 450PEA5% is more disordered than the bulk copolymer at 70 °C. This is due to the fact that the 450PEA5% sample, although bulk-like in regards to the appearance of the room temperature ^{13}C NMR spectrum, still contains a significant fraction of surface-bound segments. These chemisorbed chains disorder at lower temperatures than those in the bulk-like environment of the chains not in direct contact with the surface, as evident from the thermal behavior of the 100PEA5% sample which is completely surface-bound. Upon cooling, the spectra of both the bulk and adsorbed copolymers return to their original states, showing that this thermal disordering process is completely reversible.

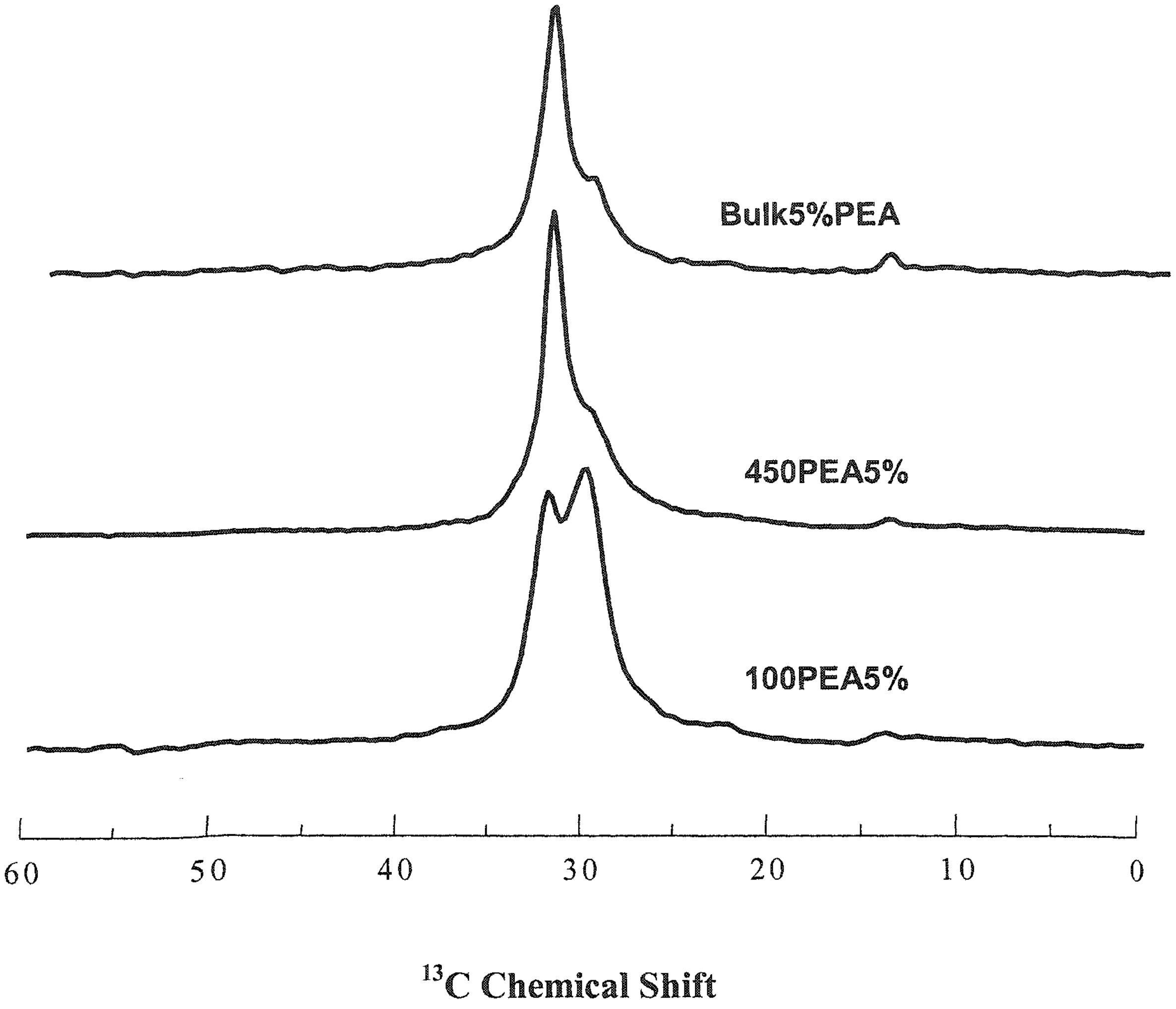
Bulk5%PEA
450PEA5%
100PEA5%
60
50
40
30
20
10
0
^{13}C Chemical Shift

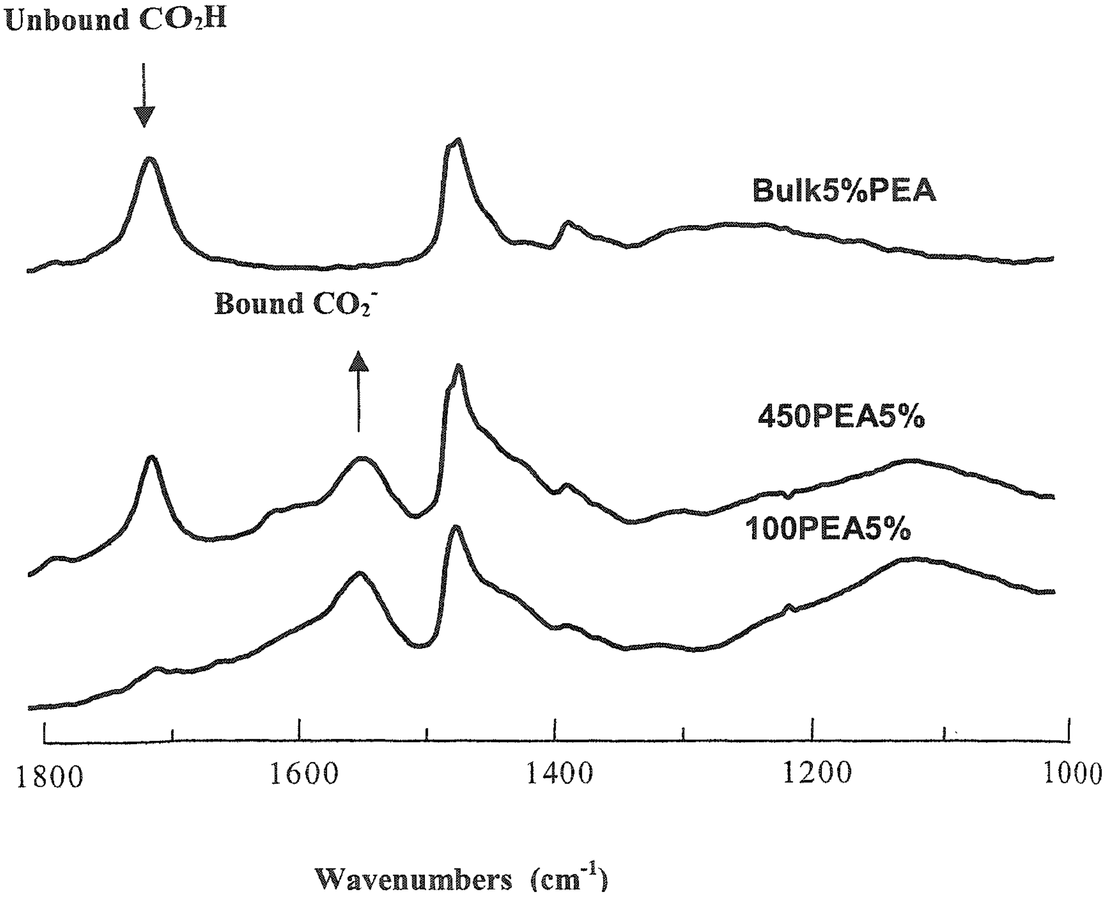

Figure 3.1. FTIR-PAS and ^{13}C CP-MAS spectra of 5%PEA, 450PEA5%, and 100PEA5% at 25°C.

(a)

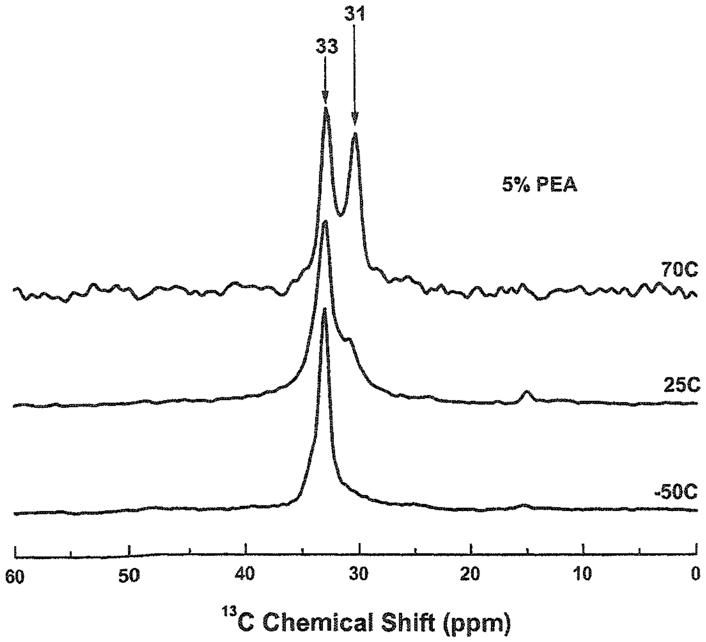
31
33
5% PEA
70C
25C
-50C
60
50
40
30
20
10
0
^{13}C Chemical Shift (ppm)

(b)

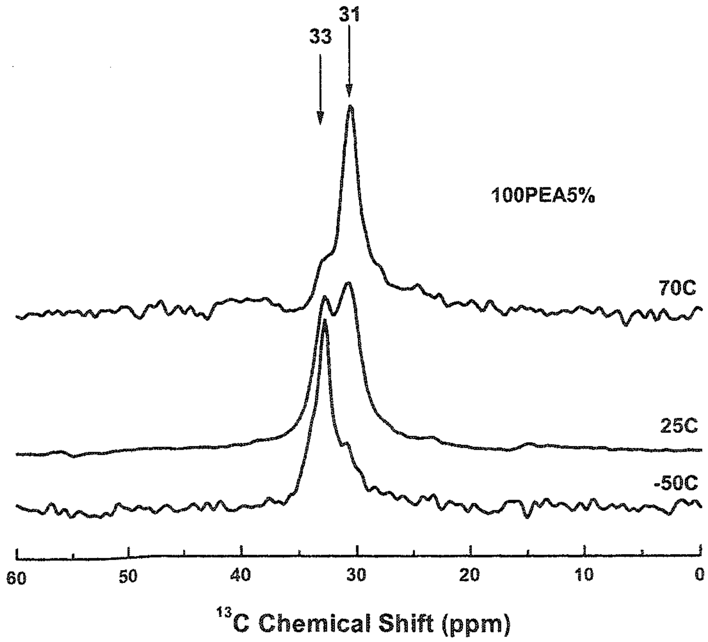
31
33
100PEA5%
70C
25C
-50C
60
50
40
30
20
10
0
^{13}C Chemical Shift (ppm)

(c)

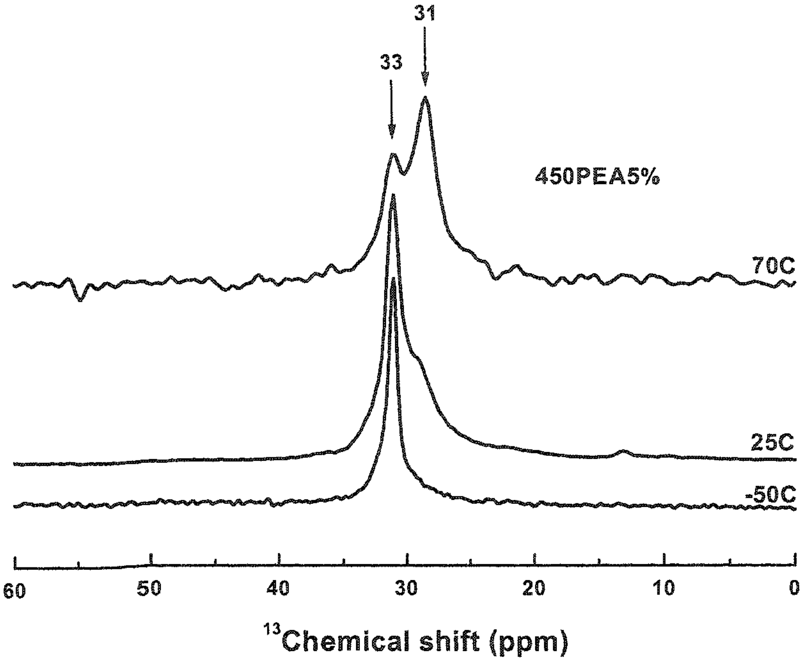

Figure 3.2. Variable temperature ^{13}C CP-MAS of (a) 5%PEA, (b) 100PEA5%, and (c) 450PEA5%.

3.4.3 Spin-lattice Relaxation

Variable temperature ^{13}C spin-lattice relaxation times were measured to gain insight into the local dynamics of these systems. The T_{1C} of the amorphous component of 5%PEA bulk copolymer was measured as a function of temperature and a minimum T_{1C} value was detected at ~ 25°C. The T_{1C} minimum for the amorphous regions of polyethylene is found at 13°C.[15] The T_1 minimum occurs when the local motional frequencies are on the order of the Larmor frequency of the nucleus under observation, which in our case is at ~ 75 MHz for ^{13}C. The higher temperature of the T_{1C} minima of the copolymer indicates that the amorphous component of 5%PEA is less mobile than that of polyethylene. Likewise, the ^{1}H linewidth of the amorphous component of 5%PEA is broader than typical values for polyethylene.[10] The more restricted mobility of the amorphous regions of the copolymer is presumably due to the presence of dimerized acid groups, which lie in the amorphous phase and act as cross-links. The relaxation behavior of a copolymer with a higher acrylic acid content, 15%PEA, was also studied. The amorphous T_{1C} values are similar but the crystalline T_{1C} of 5%PEA (115 s) is significantly higher than 15%PEA (31 s).

Unlike the 5%PEA, low loadings of 15%PEA display only a single peak at 31 ppm, assigned to chain segments with a high fraction of gauche conformers. The disordered components of the 5%PEA and 15%PEA adsorbed copolymers had ^{13}C spin-lattice relaxation times (~ 0.40 s) similar to the amorphous regions of the bulk copolymers revealing comparable chain dynamics. The proton linewidth of 38 kHz[10] and T_{1C} of 65 s of the trans component at 33 ppm of 5PEA5%, the lowest loading of the 5%PEA adsorbed copolymer, are significantly reduced as compared to the corresponding values for the crystalline component at 33 ppm of the bulk copolymer (57 kHz,[10] 115 s). As seen in Table 3.2, the T_{1C} of the trans component of the adsorbed 5%PEA copolymer samples increases as a function of loading reaching that of the bulk copolymer for the highest loading. A larger T_{1C} value indicates a more restricted mobility if the systems fall on the slow side of the T_1 versus correlation times or T_1 versus 1/T curves, the so-called slow motional regime. Since the T_{1C} values of the 33 ppm peaks of the adsorbed 5% PEA samples were found to decrease with increasing temperature, the chain segments of the trans components of the adsorbed copolymers are all in slow motional regime. Thus the lower T_{1C} values of the trans components of the adsorbed PEA5% samples indicates an enhanced mobility as compared to the all trans chains residing in the crystalline regions of the bulk 5%PEA copolymer.

Table 3.2. ^{13}C Spin-lattice relaxation times of amorphous/crystalline components of PEA and disordered/ordered components of loadings.

Sample Name	**T_{1C}(sec)***		
	31 ppm	**33 ppm**	
		25°C	**40°C**
5%PEA	0.5	115	70
450PEA5%	0.4	130	110
100PEA5%	0.5	103	-
60PEA5%	0.5	82	66
15PEA5%	0.5	65	-

* The uncertainties for all values of the 31 ppm peak were ~ 0.1 sec and those of the 33 ppm peak were ~ 5-10 % of the T_{1C}.

3.4.4 2D Exchange NMR

2D ^{13}C exchange experiments were carried out on the bulk and adsorbed copolymers as well as on a model system, an adsorbed fatty acid, to determine whether the ordered and disordered components of the adsorbed copolymers are undergoing a dynamic exchange process. Figure 3.3 shows the 2D exchange NMR spectrum of bulk 5%PEA at 55°C. At a mix time of 1 ms, no exchange is observed. For a long mixing time of 200 ms, the presence of weak broad off-diagonal intensities indicates that there is some exchange between chains in the amorphous (31 ppm) and crystalline (33 ppm) domains. The 2D exchange spectrum for the bulk copolymer is similar in appearance to those observed for low density polyethylene.[16] Off-diagonal intensities were not observed for 100PEA5% at a mixing time of 200 ms indicating that no exchange is occurring in the system. A model system of a long chain carboxylic acid, docosanoic acid $\{CH_3(CH_2)_{20}CO_2H\}$, adsorbed on ZrO_2 was prepared.[17] Only enough surfactant for a 50% coverage was used in order to create a partially ordered system to mimic the spectrum of the low loading adsorbed 5% PEA copolymer. The room temperature ^{13}C NMR spectrum of this submonolayer sample displayed peaks at 33 and 31 ppm whereas the spectrum of a complete monolayer contains only a 33 ppm peak for all trans chains. No off-diagonal intensity for a 200 ms mix time was observed in the 2D exchange NMR spectrum of the sub-monolayer sample of adsorbed docosanoic acid. This result indicates that separate domains of all trans chains and disordered chains are present rather than domains of partially ordered chains. This is due to the fact that the surfactant molecules are only attached at one end and have relatively short chains so that the formation of such structures is kinetically feasible.

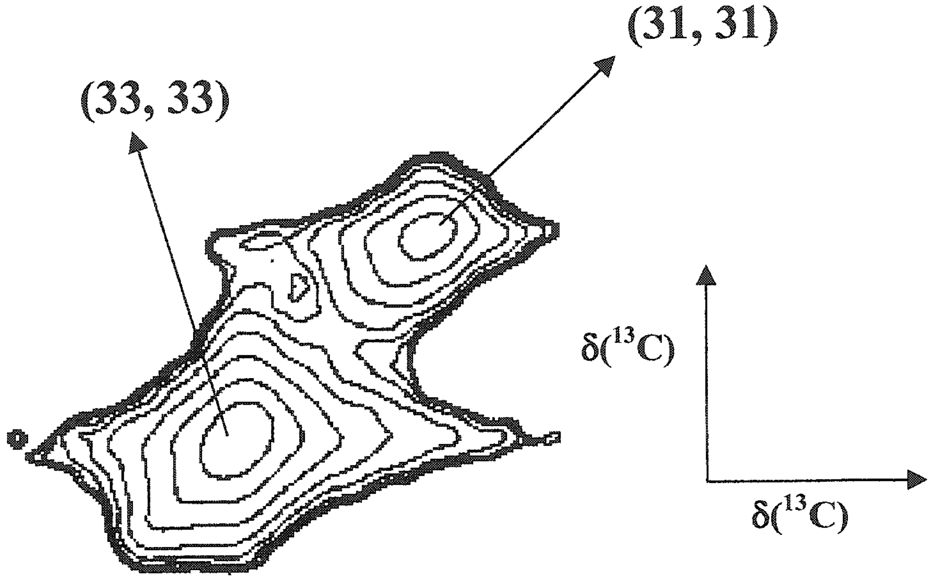

Figure 3.3 ^{13}C CP-MAS 2D Exchange NMR contour plot of 5%PEA at 55°C for mixing time 200 ms.

3.5 Discussion

Our previous study of bulk and adsorbed poly(ethylene-co-acrylic acid) (PEA) showed that the surface chain conformation depends strongly on the sticker group density.[10] Adsorbed PEA with a 5% w/w acrylic acid content, 5%PEA, contains transoid chain segments at all loadings, as indicated by the 33 ppm peak in the ^{13}C NMR spectra. When PEA with a higher acrylic acid content of 15% w/w is adsorbed, the spectra contain a single peak at 31 ppm for gauchoid chain segments and a 33 ppm trans component only appears at higher loadings where unbound acid groups are present. For both adsorbed copolymers, a change in the relative intensities of the 33 and 31 ppm peaks in the ^{13}C NMR spectra coincides with the appearance of a peak for unbound acid groups in the FTIR-PAS spectra.[10] This indicates that the average chain conformation of both adsorbed copolymers remains constant with increasing coverage until most available surface sites are occupied. The adsorbed copolymers with the highest loadings, where the majority of the polymer chains are no longer subjected to the perturbation caused by the surface appear to be bulk-like in terms of the chain conformation, mobility and morphology.

The trans component of the low loadings of the 5%PEA may arise from extended chains, lying flat on the surface (trains) or loops which are long enough for some chain folding to occur. In the case of the adsorbed 15% PEA samples, the average length of ~ 30 methylene units between sticker groups is presumably too short to form such a folded structure as compared to the adsorbed 5% PEA which has an average of ~ 100 methylene carbons between acid groups. The proposed folded looped structure is expected to have an enhanced mobility as compared to adsorbed chains lying flat on the surface. The trans component of the surface-bound polymer was found to have a reduced ^{1}H linewidth[10] relative to the bulk 5%PEA. However, this is not enough evidence to compare relative mobilities, since for adsorbed polymers a smaller proton linewidth, due to weaker dipolar interactions, does not necessarily imply enhanced mobility but can also result from a less dense chain packing as compared to the bulk state. The ^{13}C relaxation measurements reported here show that the reduction in the proton linewidth does arise at least in part from an enhanced mobility of the trans component of the adsorbed copolymer. As the copolymer loading is increased, the mobility of this component becomes more restricted and comparable to the crystalline regions of the bulk copolymer for the highest loading. So although the average chain conformation does not appear to change significantly until all binding sites are occupied, the mobility of the trans component does depend on coverage. However the mobility of the disordered component at 31 ppm does not show any coverage dependence, instead the ^{13}C spin-lattice relaxation times of all loadings are similar to the amorphous regions of the bulk copolymer. The dynamic state of adsorbed PEA differs greatly from that of the physisorbed homopolymer. In a solid-state ^{13}C NMR study of polyethylene adsorbed on silica[15], a trans component was also detected but was assigned to chain segments directly adsorbed onto the silica surface. In this case, the trans component was described as being essentially frozen on the NMR time-scale but the relaxation times were only measured for the amorphous component. Unlike the adsorbed PEA, the methylene chain motion of the disordered component of PE/silica is much more restricted than the chains in the amorphous regions of bulk polyethylene. This behavior conforms to the usual observation that the mobility of adsorbed amorphous homopolymers generally is reduced as compared to the bulk state. The difference in the motional behavior of the disordered component of the adsorbed polyethylene copolymer versus the homopolymer, as described above, is due to the disordering effect caused by sticker binding. Instead of a more restricted motion due to polymer/surface interactions, the random pinning of the chains increases the free volume available for chain motion relative to the bulk state.

The comparison of the relaxation rates of the bulk versus the adsorbed copolymer lends some support to the looping versus trains structure. However, the mobility of flat adsorbed polyethylene segments could also be enhanced relative to the crystalline regions of the bulk state. 2D ^{13}C exchange NMR experiments were carried out in an effort to determine whether there is any dynamic exchange between the ordered and disordered components of the adsorbed copolymer. Exchange between these two components would be impossible or greatly restricted in the case of the train structure consisting of flat chains extended between completely immobilized sticker groups. 2D exchange NMR experiments of ^{13}C labeled long chain fatty acids adsorbed on zirconia show that no reorientation of the carboxylate group occurs on the NMR time scale even when heated above the chain melting temperature.[17] Since the chains remain pinned to the surface in the case of small molecules, the sticker groups of the adsorbed copolymers must also be completely immobilized. In the case of a folded loop structure for the adsorbed copolymer, exchange between the 33 and 31 ppm components could conceivably occur via unfolding and refolding of the loops.

The very weak off-diagonal peaks observed in the 2D exchange NMR experiment shown in Figure 3.3 of the bulk PEA indicate that there is only a minor amount of exchange between segments in amorphous and crystalline domains. The poor resolution due to the small difference in the isotropic shifts of the amorphous and crystalline regions and the peak broadness make detection of such cross peaks difficult. Even in highly oriented drawn polyethylene samples which have much better resolution between the two resonances, the intensities of these cross peaks are normally only a small fraction of the diagonal peak intensities.[18] In case of polyethylene, such off-diagonal intensities are attributed to chain diffusion between the amorphous and crystalline regions due to 180° rotation and translation of the chains. The exchange in PEA is expected to be absent or greatly hindered compared to PE due to the presence of the dimerized acid groups, which act as cross-links. Klein and coworkers observed that chain diffusion is more enhanced in a model system of monodisperse n-alkane $\{C_{294}H_{590}\}$ than in slow-cooled and pressure-annealed PE, because of the presence of cross-links in the latter, which diminish the chain diffusion.[19] No evidence for even weak exchange was observed for 100PEA5% at a mixing time of 200 ms. Unlike the bulk copolymers, a diffusion mechanism is not possible since the chains are pinned to the surface. Exchange via unfolding and refolding of the loops could still be occurring at longer mixing times but the experiment is limited by the short relaxation time of the amorphous component ($T_{1C} \sim 0.5$ s).

The variable temperature ^{13}C CP-MAS experiments provide the strongest support for the folded loop structure, given the known thermal stability of the carboxylate surface bonds. The variable temperature spectra show that average chain conformation of the adsorbed copolymers is not thermally stable. At low temperatures, the trans component dominates the spectra of both the bulk and adsorbed 5% PEA copolymers due to the broadening of the amorphous peak. While the trans component diminishes relative to the disordered component at high temperatures for the bulk copolymer and the 450PEA5%, it completely disappeared for the 100PEA5% adsorbed copolymer sample, which has only chains directly attached to the surface. The very low intensity of the ordered peak at 70°C is likely due to unfolding of the folded/looped structure. Upon cooling, the room temperature spectra were recovered for both the bulk and adsorbed samples, demonstrating that this thermal chain disordering process is reversible.

Although the self-assembled monolayers more closely resemble polymer tails or brushes rather than the folded looped structures proposed here, the thermal behavior of the average chain conformation as measured by ^{13}C NMR is similar to the adsorbed PEA. The average conformation and the temperatures of the reversible order/disorder transitions of self-assembled monolayers depend more strongly on the chain length rather than the exact nature of the surface bond[20], just as the average conformation of the adsorbed copolymer is strongly determined by the average number of methylene units between the acid groups. However, unlike the adsorbed PEA, the conformational order of the adsorbed fatty acids depends strongly on the surface coverage.[17] The gradual chain melting process in self-assembled monolayers has been shown to start at the methyl terminated chain ends and work down to the chemisorbed headgroups which remain immobilized.[20] The disordering process of the adsorbed PEA copolymers is also gradual but would have to occur via some sort of chain unfolding/refolding process of the looped structures. Given that the sticker groups do not detach from the surface, a structure consisting of flat extended chains between the sticker groups is probably too constrained for complete conformational disordering of the polyethylene chain segments. The fact that topological constraints of the adsorbed copolymer created by the sticker groups remain unchanged during heating facilitates the return to the previous average chain conformation upon cooling.

As noted previously, the mobility of the ordered component, unlike the average chain conformation, is coverage dependent. The decreasing mobility in a folded loop structure with increasing coverage may be explained by the decrease in the available free volume for chain motion as the remaining surface sites are occupied. As more polymer chains are adsorbed, intermolecular interactions between neighboring looped chains develop, leading to denser chain packing and more restricted motion. However, the extent of folding of the individual adsorbed chains, and hence the trans/gauche population, is not determined by these interactions between neighboring chains but rather by the average number of methylene groups between the sticker groups. Thus the increasing intermolecular interactions with increasing coverage lead to more restricted motion without changes in the average conformation of the individual adsorbed copolymer chains.

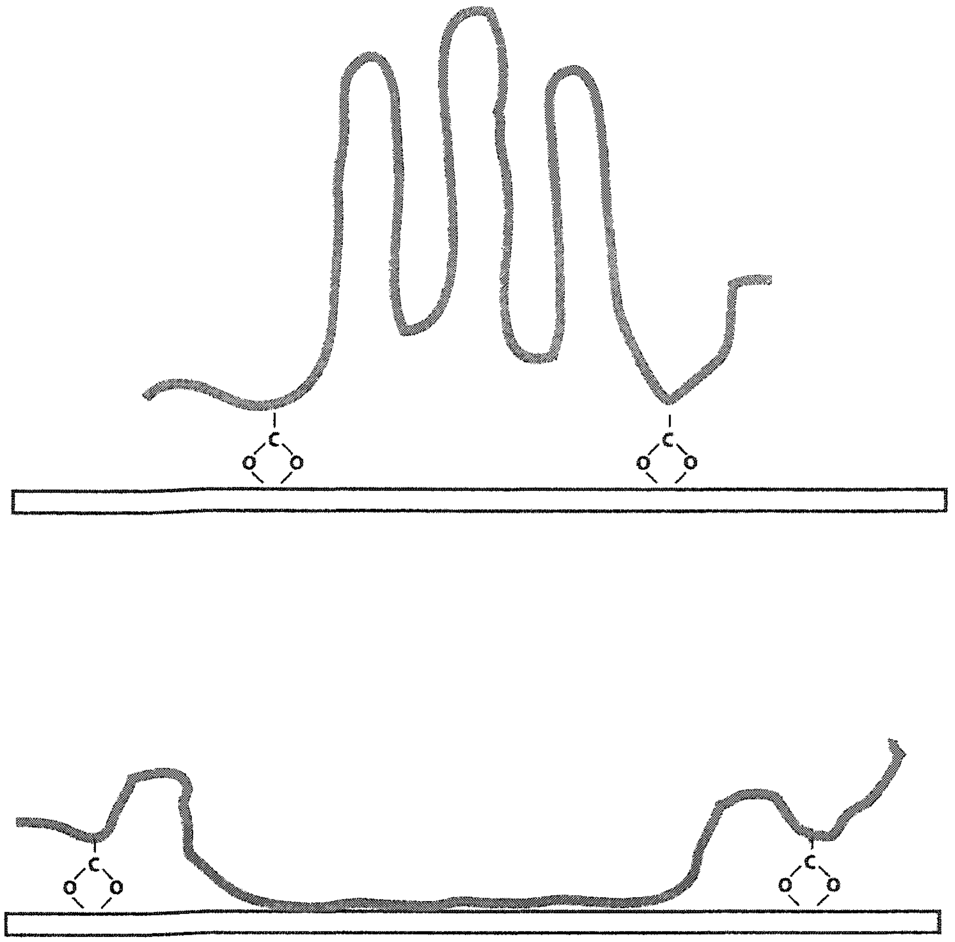

Figure 3.4. A schematic diagram showing the possible conformations adopted by low loadings of 5% PEA (a) PE segments folding between sticker groups and (b) PE segments lying flat on the surface in an all-trans zig-zag conformation.

3.6 Conclusions

The chain dynamics of a chemisorbed ethylene-acrylic acid random copolymer, (PEA), was studied by ^{13}C solid-state NMR. For a copolymer with a low density of sticker groups, there is a preferred conformation at low coverage which contains a significant trans component. ^{13}C spin-lattice relaxation measurements show an enhanced mobility of this trans component as compared to the bulk crystalline regions. Complete disordering of the adsorbed copolymer occurs upon heating although the acrylic acid segments remain bound to the surface. The enhanced mobility and the thermal behavior of the ordered component is more consistent with a structure of partially folded loops rather than flat extended chains. Although the average chain conformation does not change until all surface binding sites are occupied, the mobility of the trans component is coverage dependent. This trend may be rationalized by the development of intermolecular interactions with increasing coverage which reduce the available free volume for chain motion, but do not affect the extent of folding which is primarily determined by the sticker group density.

3.7 References

(1) (a) Fleer, G.J.; Stuart, M.A.; Scheutjens, J.M.H.M.; Cosgrove, T.; Vincent, B. *Polymers at Interfaces*; Chapman & Hall: London, 1993. (b) Wool, R.P. *Polymer Interfaces: Structure and Strength* ; Hanser/Gardner: New York, 1995. (c) Jones, R. A.L.; Richards, R.W. *Polymers at Surfaces and Interfaces*; Cambridge University Press: Cambridge, 1999.

(2) Reiter, G. *Macromolecules* **1994**, *27*, 3046.

(3) Orts, W.J.; van Zanten, J.H.; Wu, W.L.; Satiga, S.K. *Phys. Rev. Lett.* **1993**, *71*, 867.

(4) Frank, B.; Gast, A.P.; Russell, T.P.; Brown, H.R.; Hawker, C. *Macromolecules* **1996**, *29*, 6531.

(5) Jean, Y.C.; Zhang, R.W.; Cao, H.; Yuan, J.P.; Huang, C.M.; Nielsen, B.; Asoka-Kumar, P. *Phys. Rev. B: Condens. Matter* **1997**, *56*, R8459-R8462.

(6) Hall, D.B.; Hooker, J.C.; Torkelson, J.M. *Macromolecules* **1997**, *30*, 667-669.

(7) (a) Lin, W.Y.; Blum, F.D. *Macromolecules* **1998**, *31*, 4135. (b) Blum, F. *Ann. Rep. NMR Spectroscopy* **1994**, *28*, 277. (c) Blum, F.D. *Colloids and Surfaces* **1990**, *45*, 361.

(8) (a) Gong, L.; Friend, A. D.; Wool, R. P. *Macromolecules* **1998**, *31*, 3709. (b) Lee, I.; Wool, R. P. *Macromolecules* **2000**, *33*, 2680.

(9) (a) Gutman, L.; Chakraborty, A. K. *J. Chem. Phys.* **1994**, *101*, 10074. (b) Simmons, E.R.; Chakraborty, A. K. *J. Chem. Phys.* **1998**, *109*, 8667.

(10) Nasreddine, V.; Halla, J.; Reven, L. *Macromolecules* **2001**, *34*, 7403.

(11) Solum, M.; Zilm, K.W.; Michl, J.; Grant, D.M. *J. Phys. Chem.* **1983**, *87*, 2940.

(12) Torchia, D.A. *J. Magn. Reson.* **1978**, *36*, 91.

(13) Tonelli, E. *NMR Spectroscopy and Polymer Microstructure.* VCH publ., New York, 1989.

(14) Chen, Q.; Yamada, T.; kuroso, H.; Ando, I.; Shiono, T.; Doi, Y. *J. Mol. Struc.* **1991**, *263*, 319.

(15) Inoue, D.; Kurosu, H.; Chen, Q.; Ando, I. *Acta Polym.* **1995**, *46*, 420.

(16) Kazuhiro, K.; Kaji, H.; Horii, F. *Macromolecules* **2000**, *33*, 4453.

(17) Pawsey, S.; Yach, K.; Halla, J.; Reven, L. *Langmuir* **2000**, *16*, 3294.

(18) Schimdt-Rohr, K.; Spiess, H.W. *Macromolecules* **1991**, *24*, 5288.

(19) Klein, P.G.; Robertson, M.B.; Driver, M.A.N.; Ward, I.M.; Packer, K.J. *Polymer International* **1998**, *47*, 76.

(20) Badia, A.; Lennox, R.B.; Reven, L. *Acc. Chem. Res.* **2000**, *33*, 475.

Chapter Four

A ^{129}Xe NMR study of Adsorbed Polyethylene-co-Acrylic Acid Random Copolymers

4.1 Preface

In Chapters 2 and 3, the chain conformation, dynamics, and morphology of bulk and zirconia-adsorbed PEA were investigated. In this chapter, ^{129}Xe NMR is used to study the dynamics and morphology of bulk and zirconia-adsorbed PEA, a semi-crystalline random copolymer. Although the technique has usually been used to characterize solid amorphous polymers in the bulk, we demonstrate that it can give important morphological information about semi-crystalline polymers and their films. The effect of the copolymer loading on the morphology is investigated, and the uniformity of polymer coatings is probed. Variable temperature ^{129}Xe NMR is used to determine the glass transition temperature of the bulk copolymer.

4.2 Introduction

^{129}Xe NMR has been used as an inert probe of porous, liquid crystalline and polymeric materials.[1] The large polarizability of xenon gives rise to a large chemical shift range that is extremely sensitive to the local environment. ^{129}Xe NMR has been most widely applied to microporous materials, in particular metal oxide powders and zeolites, since the chemical shift is inversely proportional to the void space. To a lesser extent, the morphology of amorphous and semi-crystalline polymers and polymer blends has been studied by ^{129}Xe NMR.[2,3] Xenon dissolves only into the amorphous regions where the motion of the polymer chains create free volume. The ^{129}Xe chemical shift is characteristic of particular polymers with the majority of polymers in the 200-230 ppm region at room temperature. This variation is due to the density dependence of the ^{129}Xe chemical shift. Therefore, breaks in the slope of the ^{129}Xe chemical shift and linewidth versus temperature occur at the glass transition.

In the case of high surface area, nonporous metal oxides like fumed silica, the ^{129}Xe shift will detect microvoids created by particle aggregation. ^{129}Xe NMR has been used previously to study the microporosity of nascent polyethylene over a silica supported catalyst.[4] At low polymer yields, only the signal from the metal oxide support is detected but at high yield, additional signals appear for xenon residing in the amorphous regions of polyethylene and in the micropores within the nascent polyethylene. Whereas the ^{129}Xe signal due to xenon occupying the microvoids formed by the metal oxide powder is rapidly relaxed, ^{129}Xe residing in the organic microporous structure showed relatively long relaxation times. Following on from this precedent, we exploit ^{129}Xe NMR as a probe of both metal oxides powders and polymers to examine the morphology of a random copolymer of polyethylene and acrylic acid chemisorbed onto nonporous zirconia powder. We have also chosen this copolymer because we are interested in applying this technique to a semi-crystalline polymers and see how it differs from amorphous polymers which are more commonly used in ^{129}Xe NMR studies. Our ^{13}C NMR and FTIR study of adsorbed ethylene-acrylic acid copolymers, widely used to enhance the adhesion of polyethylene films, revealed a strong dependence of the surface chain conformation on the acrylic acid content rather than the coverage.[5] Above a certain loading, the copolymer displayed bulk-like behavior. ^{129}Xe NMR was applied to the PEA/ZrO_2 to gain further insight into the effect of the copolymer loading on the dynamics and morphology. The bulk copolymer was also studied by variable temperature ^{129}Xe NMR.

4.3 Experimental section

Sample preparation. The samples used in this chapter are 15PEA5%, 30PEA5%, 60PEA5%, 100PEA5%, and 450PEA5%. 15PEA5% stands for an initial loading of 15 mg PEA5% per 1 g of ZrO_2. Refer to Chapter 2 for preparation method and amounts adsorbed.

Instrumentation. The molecular weight and polydispersity index of PEA5% are $M_w \sim 7900$ and $M_w/M_n \sim 1.8$ as determined by Gel Permeation Chromatography (GPC).

The gas used in these experiments was ^{129}Xe with 26.44% natural abundance from Air Liquide Canada Inc. The samples were placed in a specially designed sample holder, which is connected to a vacuum system. All the samples were heated under vacuum overnight and loaded with xenon gas and left overnight for the xenon to equilibrate before the experiment is started. This corresponds to sample masses around 0.2 g. The xenon pressure in the sample after sealing was 100-120 psi.

74.71 MHz ^{129}Xe single pulse Bloch decay spectra were acquired on a Chemagnetics CMX-270 NMR spectrometer using a variable temperature static probe with a coil diameter of 9 mm internal diameter. A pulse width of 2.70 μs (90° pulse =

7.20 μs) and a pulse delay of 50 s were used. ^{129}Xe spin-lattice relaxation times were measured using a saturation recovery pulse sequence. Variable temperature experiments were acquired at 138.3 MHz with a 16.3 μs 90° pulse, and a pulse delay of 50 s on a Varian Unity 500 NMR spectrometer. A two-channel 10 mm broad-band probe was employed. The experiments were performed in heavy-walled, 10 mm NMR tubes (with a 7 mm internal diameter) and packed to a depth of 4-5 cm. This corresponds to sample masses between 0.6 and 0.8 g, with 100-120 psi xenon pressure.

4.4 Results and Discussion

4.4.1 1D and Variable temperature ^{129}Xe NMR of bulk PEA

The ^{129}Xe NMR spectrum of bulk 5%PEA at 25°C is shown in Figure 4.1. The first peak at 0 ppm is due to unadsorbed or free xenon gas and the second peak at 202 ppm is due to xenon adsorbed within the amorphous region of the semi-crystalline copolymer. This is very similar to the xenon chemical shift observed in low-density polyethylene (LDPE)[6], since 5%PEA is 95% polyethylene by weight. There is a dynamic equilibrium between free unadsorbed xenon and xenon adsorbed at the different sites. The xenon interacts with the polymer chains via dispersive Van der Waals interactions and its chemical shift reflects the extent of the interaction of xenon atoms with different sites and its residence time at these sites. The peak at 202 ppm indicates that there is one region or environment within the amorphous component of 5%PEA. Stengle et al.[6] have observed two peaks for adsorbed xenon for linear low-density polyethylene (LLDPE). This indicates some structure differences from LDPE, corresponding to two sub-regions in the amorphous phase. This is significant, since although LLDPE is above its glass transition temperature, one can still observe different sub-regions in the amorphous phase. At 25°C, 5%PEA is above its glass transition temperature so the polymer chains will have enhanced mobility. The xenon atoms will thus experience an averaged environment due to increased chain mobility giving rise to narrow lines. This is in contrast to broadened xenon lines in glassy polymers due to microscopic heterogeneity. Figures 4.2 and 4.3 show the plots of the linewidth and chemical shift of the 202 ppm peak versus temperature.

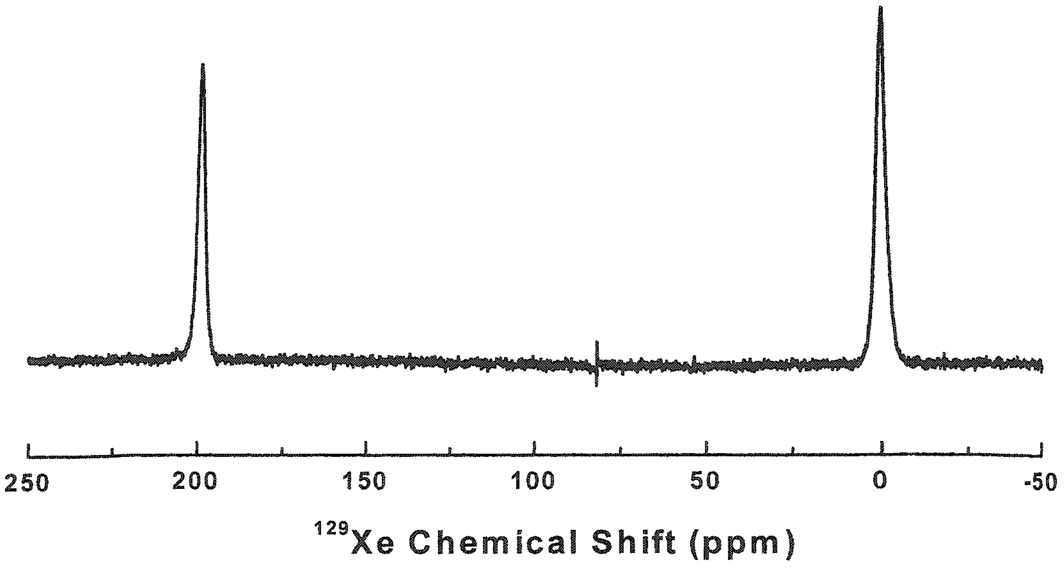

Figure 4.1 ^{129}Xe NMR spectrum of bulk 5%PEA 25°C.

As the temperature increases, the rate of chemical exchange of xenon among the different environments within the amorphous region increases. At low temperatures, the mobility of the xenon diminishes due to densification of the polymer leading to line broadening and to a downfield shift. The resonance corresponding to free xenon gas (@ 0 ppm) broadened at lower temperatures. The xenon linewidth of the 202 ppm resonance at 25°C is 346 Hz compared to 250 Hz for LDPE[7] at the same temperature. The larger xenon linewidth is due to the presence of the acid groups in the amorphous region in 5%PEA. These acid groups dimerize and act as cross-links that restrict the polymer chains' mobility and thus broaden the lines. Plots of the xenon linewidth versus temperature, like that of Figure 4.2, have been used to determine the glass transition temperature (T_g) of amorphous polymers by fitting the set of data to two straight lines that intersect at T_g[6]. This sharp break at T_g occurs because the xenon linewidth is sensitive to the surrounding medium which changes from glassy (rigid) to rubbery (mobile) as temperature is increased. A smaller break usually occurs for the chemical shift, which is less sensitive to changes in mobility. From Figure 4.2, the break is less pronounced since glass transitions in semi-crystalline polymers are not as sharp as those in amorphous polymers. When the data is fitted to two linear regions we obtain a T_g value (~ -10 ± 5°C) comparable to that of PEA polymers[8] with similar composition. Kentgens et al.[7] performed variable temperature ^{129}Xe NMR experiments on LDPE, LLDPE, and HDPE down to - 40°C, which is just below the β transition in PE. The linewidth increased for all samples from -20°C to -40°C, nevertheless the increase was most pronounced for LDPE. The β transition in PE is associated with branching and since

LDPE has the highest fraction of branching, it is most affected by the decrease in temperature and has the largest linewidth at -40°C.

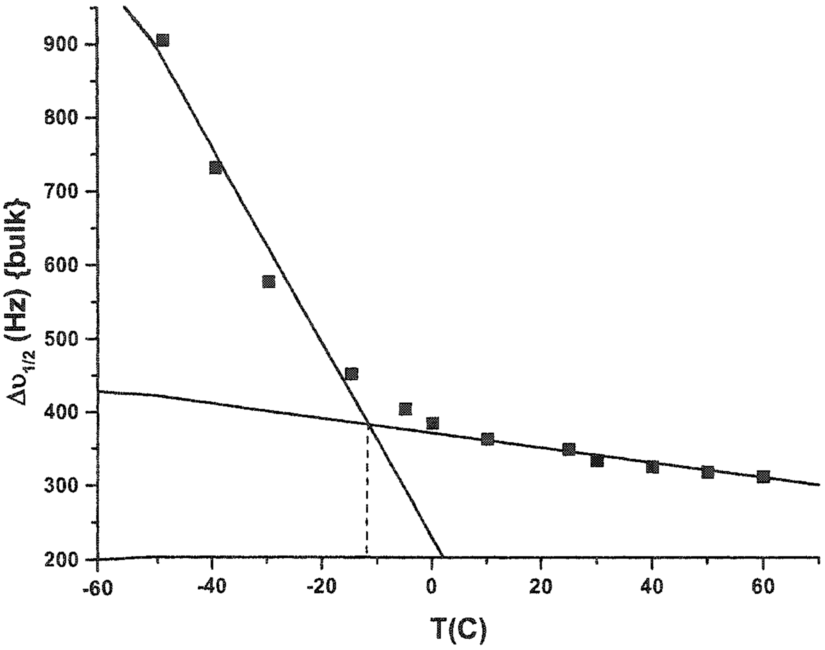

Figure 4.2 Plot of the linewidth of the bulk xenon signal at 202 ppm versus temperature.

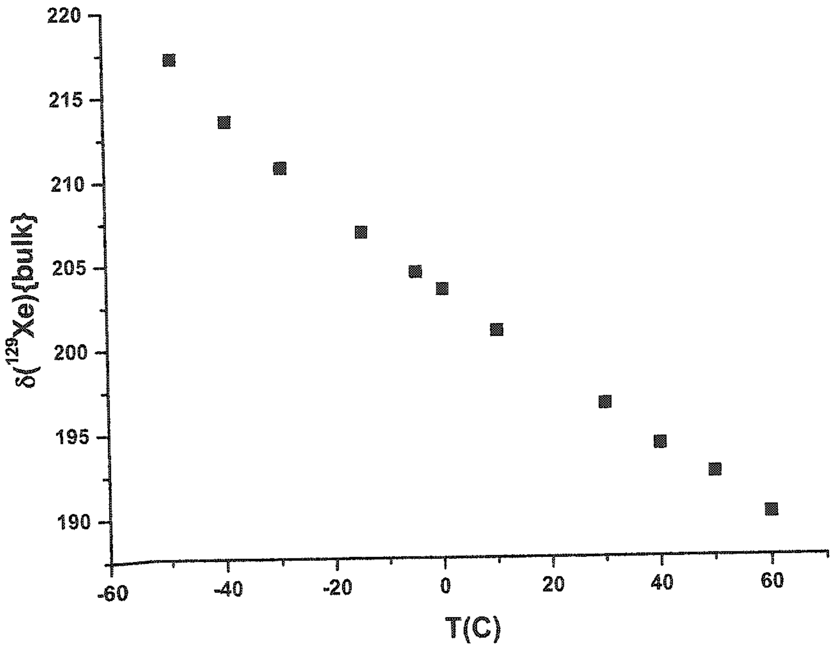

Figure 4.3 Plot of the chemical shift of the bulk xenon signal at 202 ppm versus temperature.

4.4.2 1D and ^{129}Xe NMR Spin-lattice relaxation of PEA loadings

The ^{129}Xe NMR spectra of the PEA loadings are shown in Figure 4.4. The copolymer is chemisorbed onto zirconia via the carboxylic acid (sticker) groups that form a surface carboxylate bond.[5] The spectrum labeled ZrO_2 corresponds to xenon adsorbed on the surface of bare zirconia (5.3 ppm). At low polymer loadings, the xenon is adsorbed into the microvoids created by the aggregation of zirconia. The copolymer loadings are 15PEA5%, 30PEA5%, 60PEA5%, 100PEA5%, and 450PEA5%. The 15PEA5% corresponds to an initial loading of 15 mg polymer/1 g ZrO_2 and the amount adsorbed is determined from elemental analysis. Two peaks are observed for all loadings, one at 0 ppm for free unadsorbed xenon gas and the second downfield for adsorbed xenon gas. For 15PEA5%, a peak at 19.8 ppm is observed for adsorbed xenon as well as a broad resonance. This is due to heterogeneity of the loadings where xenon is exposed to different environments. Similarly, 30PEA5% has a peak at 24.0 ppm with shoulders at 16 ppm and 34 ppm. Figure 4.5 shows the plot of the chemical shift of adsorbed xenon as a function of copolymer loading. We observe that the xenon chemical shift increases as a function of polymer loading. This is an indication that xenon becomes more restricted as more polymer is adsorbed due to a diminishing microvoid size. In the limit of the high loading, 450PEA5%, bulk-like behavior is observed, with the appearance of a new small peak at ~ 200 ppm ($\Delta\upsilon_{1/2}$ = 505 Hz). This peak corresponds to xenon absorbed in a bulk-like environment (202 ppm for bulk 5%PEA) with the peak being broader than the bulk signal in 5%PEA due to a larger chemical shift heterogeneity. The chemical shift and linewidth of this peak also increased with decreasing temperature. This loading also has a peak at 35 ppm for xenon in microvoids, which is similar to that of the 100PEA5%

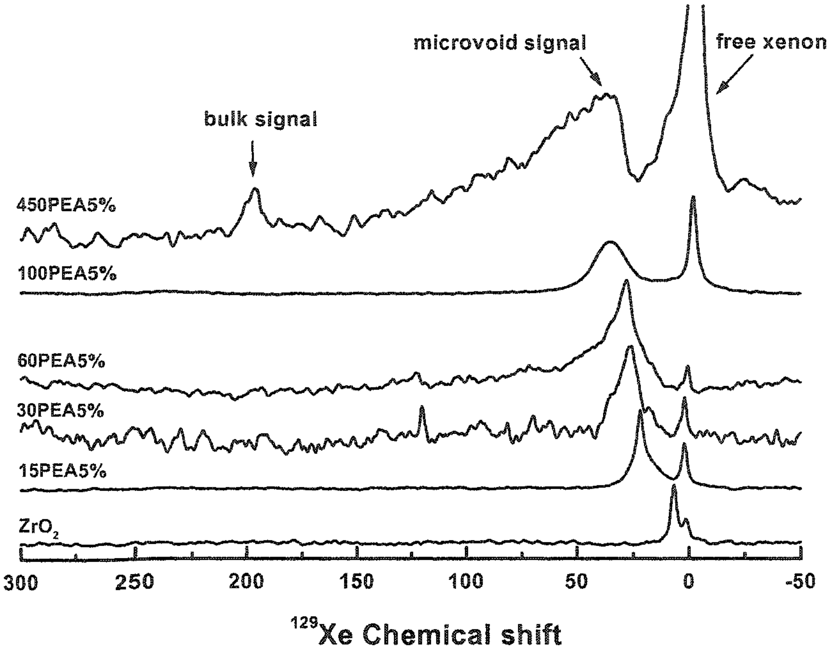

Figure 4.4 ^{129}Xe NMR spectra of copolymer loadings 25°C.

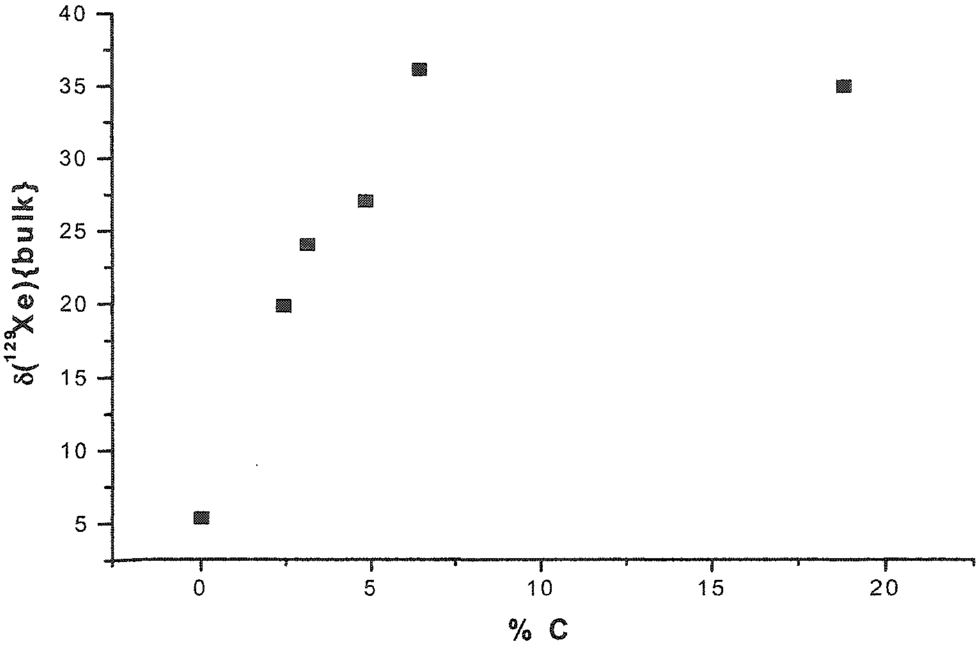

Figure 4.5 Plot of the chemical shift of adsorbed xenon versus copolymer loading.

loading. This shows that as the copolymer loading increases the size of microvoids diminish and in the limit of high loadings the microvoids sizes reaches a limit where it ceases to change dramatically. Thus from our data, we observe that xenon experiences two different environments: microvoids in low loadings and a bulk-like medium in high loadings. This is in agreement with our previous solid-state NMR results[5], where these low loadings showed comparable morphologies and structure and the high loadings were bulk-like. A similar behavior was observed by Ferrero et al.[4] when xenon was adsorbed on silica/PE samples tested for microporosity. At low PE loadings, a broad peak at 50 ppm was observed. This was due to adsorption of xenon in PE micropores. In the limit of high loadings of PE, a bulk xenon signal was observed at 205 ppm. This was attributed to xenon gas dissolved (absorbed) within the amorphous region of the polymer.

^{129}Xe spin-lattice relaxation, T_1(Xe), also increased slightly with copolymer loading. The measured values for 15PEA5% and 100PEA5% polymer loadings were 3.7 and 5.3 s respectively. The relaxation time of the highest loading was similar to xenon in the bulk copolymer (> 10 s), showing that Xe gas can no longer access zirconia surface sites. Xenon relaxes more rapidly on bare zirconia [T_1(Xe) ~ 3 sec] due to surface interactions with surface hydroxyls or paramagnetic centers. For low loadings, the xenon will fill microvoids created by polymer-coated zirconia and thus interact with the hydrophobic polymer chains via weak van der Waals interactions resulting in slower relaxation and longer T_1(Xe) values. In the limit of high loadings, xenon is in a bulk-like environment and T_1(Xe) approaches that of 5%PEA

4.5 Conclusions

We report a ^{129}Xe NMR study of a random copolymer of polyethylene-co-acrylic acid (PEA). The xenon chemical shift and linewidth increased with decreasing temperature, due to densification of the copolymer at lower temperatures. The xenon chemical shift of chemisorbed samples increased as a function of copolymer loading, with a new peak appearing around 200 ppm for high loadings. Xenon experiences two different environments: microvoids in low loadings and a bulk-like medium in high loadings We have also observed an increase in T_1(Xe) as a function of loading due to blocking of xenon from the zirconia surface by polymer chains. In addition to the well-known use of xenon as a probe of the amorphous component of solid polymers, xenon relaxation measurements provide a method for probing the uniformity of polymer coatings on surfaces. We have also demonstrated that the calorimetric glass transition temperature of 5%PEA can be detected using variable temperature ^{129}Xe NMR. Since the glass transitions in semi-crystalline polymers are not as sharp as those in amorphous polymers, future experiments will be performed on amorphous polymer films to determine whether ^{129}Xe NMR can be used to measure the surface effect on the polymer glass transition temperature.

4.6 References

(1) Raftery, D; Chmelka, B.F. *NMR Basic Principles and Progress*, **1994**, *30*, 111.

(2) Walton, J.H. *Polym. Polym. Compos.* **1994**, *2*, 35.

(3) Walton, J.H.; Miller, J.B.; Roland, C.M. *J. Polym. Sci., Part B*, **1992**, *30*, 527.

(4) Ferrero, M.A.; Webb, S.W.; Corner, Wm. C.; Bonardet, J.L.; Fraissard, J. *Langmuir* **1992**, *8(9)*, 2269.

(5) Nasreddine, V.; Halla, J.; Reven, L. *Macromolecules* **2001**, *34*, 7403.

(6) Stengle, T.R.; Williamson, K.L. *Macromolecules* **1987**, *20*, 1430.

(7) Kentgens, A.P.M.; van Boxtel, H.A.; Verweel, R.J.; Veeman, W.S. *Macromolecules* **1991**, *24*, 3712.

(8) Otocka, E. P.; Kwei, T. K. *Macromolecules* **1968**, *1*, 244.

Chapter Five

^{13}C Solid-State NMR of Adsorbed Polypropylene-Acrylic acid Copolymers

5.1 Preface

In this chapter we investigate the chain conformation and dynamics of another random copolymer poly(propylene-co-acrylic acid) (PPA) in the bulk and adsorbed states. Like the PEA/zirconia system, the PPA/zirconia system is an example of an adsorbed polymer strongly interacting with the surface. The hydrophobic component of this copolymer, polypropylene (PP) is also another important semi-crystalline polymer whose bulk structure and dynamics has been extensively studied by ^{13}C solid-state NMR. The different adsorption behavior of PPA and PEA on zirconia are compared.

5.2 Introduction

Polypropylene (PP) is one of the main polyolefins used in industry. It is widely employed because it is inexpensive, has excellent physical and mechanical properties, and PP-based materials can be easily recycled. However, PP is limited by its low surface energy and a lack of reactive sites, resulting in poor adhesion of PP to polar materials. To overcome this drawback, there have been many techniques used for the chemical modification of polypropylene to improve its adhesion. Solution-state oxidative etching, plasma oxidation, physical blending and various grafting methodologies are among the different methods used to introduce polar groups into PP.[1] The incorporation of different monomers such as maleic anhydride, maleic acid, and acrylic acid produces functionalized polypropylenes which can be used as in situ compatibilizers of polymer alloys such as polyolefin polyamides and polyesters because these functionalities are able to react with –OH, –COOH, and $-NH_2$. Moreover, introducing small amounts of comonomers into PP lowers the melting and welding temperatures, thus producing better films.[2] Improving the adhesion of polypropylene to surfaces has been the focus of research on PP-based composites. The adhesion between PP and inorganic fillers/clays has been shown to be the single largest factor controlling the physical and mechanical properties of these materials.[3]

Most experimental studies of these systems have focused on mechanical properties, such as peeling tests, and little is known about the microscopic structure at the polymer/substrate interface or the role it plays in determining the adhesive properties. In addition to the presence of a sufficient number of polar "sticker groups", the adhesion of functionalized polyolefins may depend on the chain conformation at the interface. Maximum adhesion is achieved at a critical sticker group density but theoretical studies predict that a very high density will lead to a flat chain conformation at the polymer/substrate interface. Such a structure can create a second more diffuse interface, which will become the locus of cohesive failure. Knowledge of the surface chain configuration of polymers, which have been functionalized to promote adhesion, will help determine whether this is an important factor.[4]

In general, most fundamental studies of polymers at surfaces and interfaces have concerned amorphous rather than semi-crystalline polymers such as PP since the tendency to crystallize adds another level of complexity. However, the surface properties of semi-crystalline polymers as well as the effect of reduced dimensionality on the crystallization of polymers are of great fundamental interest. The structure, morphology and dynamics of bulk semi-crystalline polymers, polyethylene and polypropylene in particular, have been studied in great detail by solid-state NMR techniques.[5] Given that the relation between the chain conformation and the ^{13}C chemical shift is well understood, NMR can be directly used to determine the chain conformation of adsorbed polymers. Solid-state NMR has not been widely applied to adsorbed polymers due to the intrinsic low sensitivity of this technique. Moreover, the majority of the existing NMR studies on adsorbed polymers concern amorphous polymers.[6] However, a detailed NMR and FTIR-PAS study of the adsorption behavior of a semi-crystalline copolymer, poly(ethylene-co-acrylic acid) (PEA), revealed a preferred chain conformation which depended on the acrylic acid content rather than the surface coverage. Additional dynamic studies support the proposal that this copolymer forms folded looping structures rather than flat extended trains. In this paper, we extend these studies to a closely related semi-crystalline polymer, polypropylene, to explore the generality of these results. The chain conformation and dynamics of bulk and adsorbed polypropylene-co-acrylic acid (PPA) random copolymers are studied by FTIR and solid-state NMR spectroscopy. Carboxylic acid groups have been incorporated into the PP backbone by free radical polymerization and act as anchor groups that pin the polymer to the surface of zirconia. The same metal oxide substrate used for the PEA study, a nonporous zirconia powder, is used here since the nature of the binding of carboxylic acid groups to zirconium oxide is well understood.[7] We compare the results for the bulk and adsorbed copolymer, and investigate how the polymer configuration and mobility are altered upon adsorption.

5.3 Experimental section

Sample preparation. A polypropylene-co-acrylic acid (PPA) random copolymer was used as-received (M_n = 50,000, T_m = 168°C) (Scientific Polymer Products, Inc.). The copolymer used (PPAC6%) contains 6% acrylic acid by weight and the PP part is mainly isotactic. Overall, the material is 50% crystalline as measured by DSC. Nonporous zirconia (ZrO_2) powder (monoclinic, VP zirconium dioxide, Degussa Corp.) was calcinated at 400°C to eliminate any residual organic impurities. The reported average primary particle size of this ZrO_2 is 30 nm, and the BET surface area is 40 m^2/g. Zirconia powder (2 grams) was dispersed in 250 ml of hot toluene by sonication for 15 minutes. The copolymer solutions were prepared by dissolving the appropriate amount of polymer in 50 ml of hot toluene. A total of 5 samples were prepared for each copolymer using 60, 120, 200, 300, and 900 mg of polymer. These samples will be referred to as 30PPA6%, 60PPA6%, 100PPA6%, 150PPA6%, and 450PPA6% respectively. The copolymer solution was added to the dispersed zirconia powder under stirring. The resulting mixture was refluxed with stirring for one day. The sample was washed a total of six times each by redispersing the powder in 40 ml toluene with gentle heating, filtering, and then drying under vacuum after the final washing step. The samples studied along with the carbon content in percent weight (%C) determined from elemental analysis are summarized in Table 5.1.

Instrumentation. Solid-state ^{13}C NMR spectra (75.3 MHz) were recorded on a Chemagnetics CMX-300 NMR spectrometer with a 7.5 mm double-tuned fast magic angle spinning (MAS) Pencil probe. Proton pulse widths of 4.25 μs, a contact time of 3 ms, a pulse delay of 5 s, and a MAS rate of 3 kHz were used in all experiments for both bulk and adsorbed polymers. ^{13}C spin-lattice relaxation times were measured using the Torchia pulse sequence.[8] Two runs, one consisting of short relaxation delays and one of long delays were used to measure relaxation times of amorphous and crystalline components. The inversion recovery method was also used to measure the T_{1C} of the amorphous phase. ^{1}H spin-lattice relaxation in the rotating frame ($T_{1\rho H}$) were measured by varying an interval, τ, before cross polarization and a spin-locking field of 50 kHz was used. For the variable temperature CP-MAS experiments, the sample temperature was controlled to within ± 1° by a Chemagnetics temperature controller.

Table 5.1 Samples, preparation loadings and adsorbed amounts of PPA6%.

Sample name	Preparation loadings (mg polymer/g ZrO_2)	Adsorbed amount (% C)
30PPA6%	30	1.3
60PPA6%	60	4.5
100PPA6%	100	3.0
150PPA6%	150	4.0
450PPA6%	450	16.7

5.4 Results

5.4.1 ^{13}C CP-MAS and FTIR-PAS

The ^{13}C CP-MAS NMR and FTIR-PAS spectra of bulk PPA6% and the two copolymer loadings 60PPA6% and 450PPA6% are shown in Figure 5.1. The bulk copolymer investigated is mainly isotactic. Its FTIR spectrum has all the peaks characteristic of the stereoregular sequence of iPP (808, 840, 898, 972, 995, 1100 cm^{-1}) with a peak at ~ 1710 cm^{-1} corresponding to hydrogen bonded carboxylic acid groups. The various isomorphs of iPP can only be distinguished in the far-infrared region.[9] The ^{13}C CP-MAS NMR spectrum of PPA6% consists of a peak at 22.0 ppm for the methyl resonance with a small shoulder at 22.8 ppm, a second peak at 26.7 ppm for the methine resonance, and a third peak for the methylene resonance split into 44.0 and 44.8 ppm. The observed chemical shifts correspond only to the crystalline regions, the amorphous resonances of PP are generally broadened into the baseline. Saito et al. observed the amorphous resonances only at elevated temperatures when performing ^{13}C NMR with no cross-polarization. The poor resolution of the splittings of the crystalline regions of PPA is typical of poorly annealed i-PP or i-PP quenched from the melt and is attributed to imperfect chain packing.[10] The presence of the acid groups may also reduce the efficiency of chain packing.

The chemisorption of the acid groups in the adsorbed copolymer samples is indicated by the appearance of two new broad intense bands in the C-O stretching region of the FTIR-PAS spectra at 1460 and 1558 cm^{-1}, which are assigned[11] to the asymmetric and symmetric C-O stretches of a chelating bidentate zirconium carboxylate surface bond. The ^{13}C CP-MAS NMR spectrum of the adsorbed copolymer sample, 60PPA6%, shows that the down field resonances of the methyl and methylene carbon splittings are more intense than the downfield resonances compared to bulk PPA6%. The ratio of downfield to upfield resonances of the methyl and methylene splittings are 1:1 and 1:0.8 respectively. In addition to the two peaks at 22.0 ppm and 22.6 ppm for the –CH_3 group,

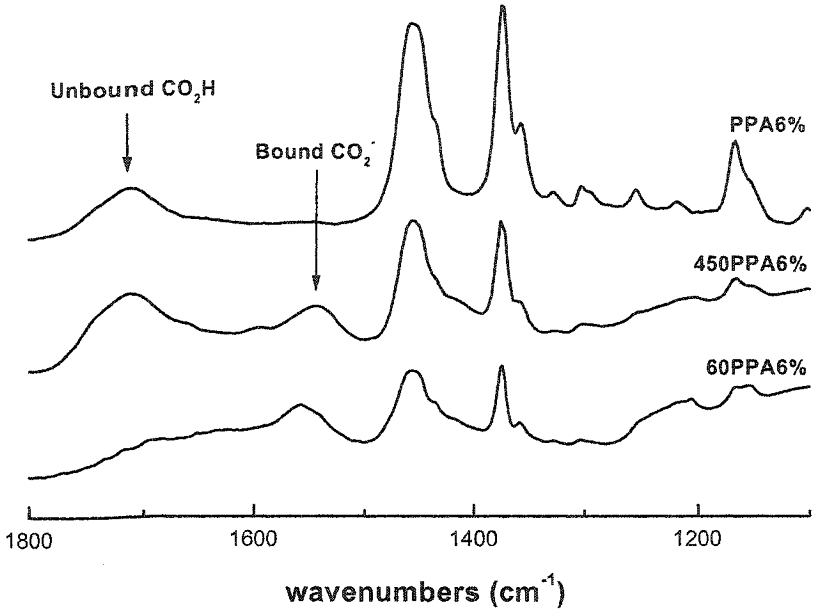

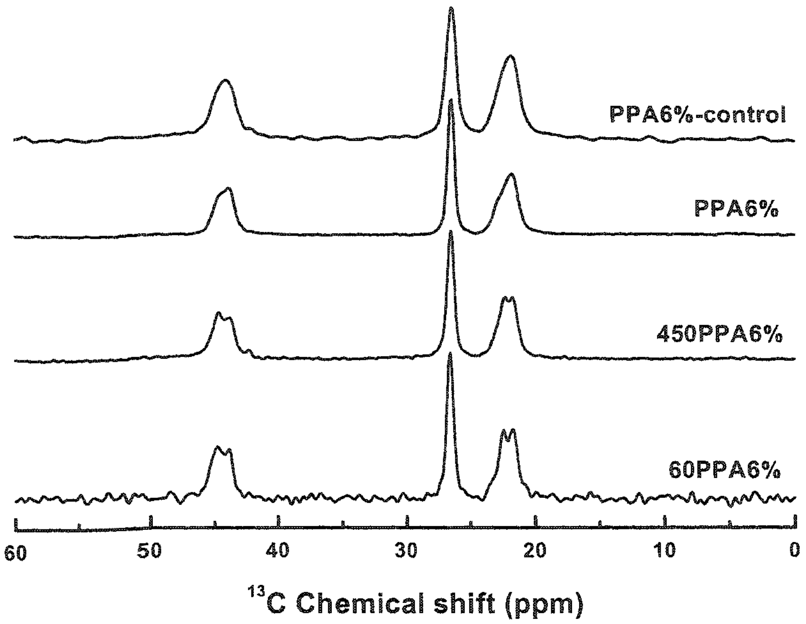

Figure 5.1 FTIR and ^{13}C CP-MAS spectra of 60PPA6%, 450PPA6%, and PPA6% at 25°C.

a shoulder around 23.0 ppm is also observed showing that there are three different local environments for the methyl groups. The resolved splittings are observed for all the adsorbed copolymer samples, listed in Table 5.1, including the highest loading 450PPA6%. No changes in the ^{13}C CP-MAS NMR spectra were observed when bulk and adsorbed samples were annealed at 100°C for one hour.

A sample was also prepared with the same temperature and solvent conditions as the 60PPA6% sample, but without adding any zirconia, to check if the splittings in the NMR spectra of the adsorbed copolymer samples are due to recrystallization of unbound polymer rather than a surface effect. All lines in the ^{13}C CP-MAS spectrum of this sample were broad and featureless as shown in Figure 5.1 (PPA6%-control), evidence that the splittings observed for the adsorbed polymer are somehow associated with the interaction of PPA with zirconia.

5.4.2 Variable temperature ^{13}C CP-MAS

Figure 5.2 shows the variable temperature ^{13}C CP-MAS of the bulk copolymer, PPA6%. As the temperature increased, the splittings diminished as a result of the down field shift of the upfield lines. This is due to the onset of molecular motion in the crystalline domains[10], which averages each crystalline carbon resonance over the two sites. At 120°C, two downfield lines appear at 29 ppm and 47 ppm. At 170°C, above the melting temperature (168°C) of PPA6%, the signal to noise ratio drastically decreases since the efficiency of cross polarization diminishes due to enhanced mobility. Since these downfield chemical shifts are very close to those of the isotactic sequence in solution, they can be assigned to the molten polymer.[10] Upon cooling back to room temperature, the splittings in the ^{13}C NMR spectrum of the bulk

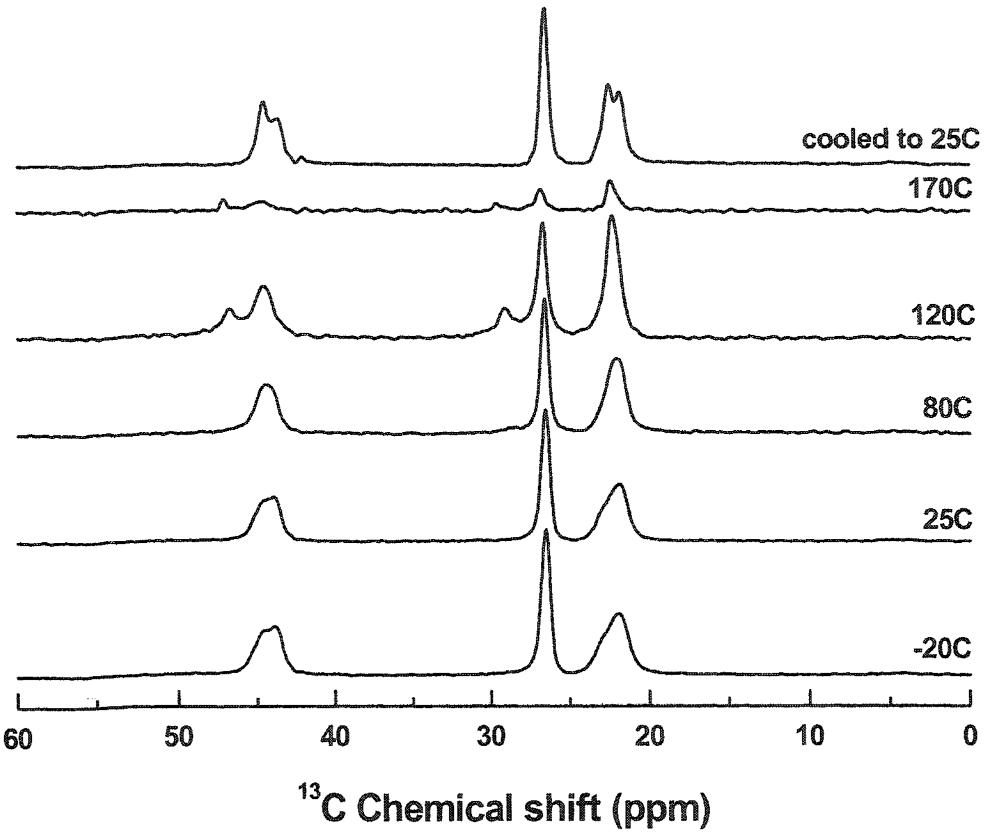

Figure 5.2 Variable temperature ^{13}C CP-MAS of PPA6%.

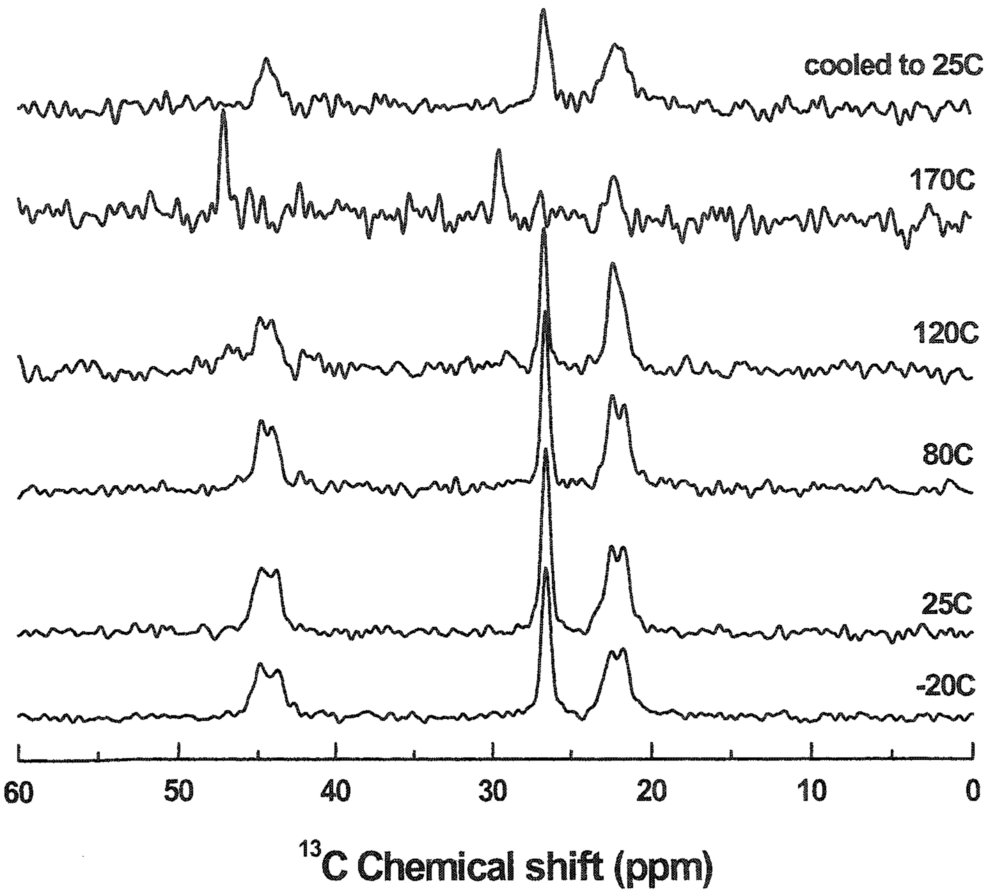

Figure 5.3 Variable temperature ^{13}C CP-MAS of 60PPA6%.

PPA6% are very similar to that of the α–form of isotactic PP. Before the copolymer was heated, the splittings are poorly resolved due to imperfect chain packing. After cooling from the melt the ratios were 1.2:1 for both carbons. When the temperature was decreased to -20°C, which is below the T_g of PPA6% (5°C), no changes were observed compared to the bulk spectrum at 25°C.

The variable temperature ^{13}C CP-MAS NMR spectra of the adsorbed copolymer sample, 60PPA6%, are shown in Figure 5.3. At 80°C, the splittings of the methyl and methylene resonances are still resolved, in contrast to the bulk copolymer where all lines become broad singlets. At 120°C the amorphous-like peaks of the methine and methylene peaks start appearing and the splittings of the methyl resonance diminish. Upon heating to 170 °C, a similar behavior to the bulk is observed (substantial loss of intensity). Upon cooling to 25°C, the spectra of the surface-bound copolymer became broad and featureless. Similar to the bulk copolymer, no changes where observed in the ^{13}C CP-MAS spectrum when the temperature was decreased to -20°C.

5.4.3 ^{13}C spin-lattice relaxation

^{13}C spin-lattice relaxation times of PPA6% and loadings for all resonances are measured to investigate the local dynamics of bulk and adsorbed samples. For PPA6%, the T_{1C} value for CH_3 is 0.6 s. For the adsorbed copolymer samples, $T_{1C}(CH_3)$ was around 0.4-0.5 s. The spin-lattice relaxation times of methyl carbons are in the fast motional regime (increase with increasing temperature) and are dominated by their internal motions and not by the segmental motions of the i-PP. Gomez et al.[12b] showed that the two methyl resonances in the ^{13}C CP-MAS spectrum of α-iPP relax at different rates with T_{1C} = 0.43 and 0.80 s for the downfield and upfield

Table 5.2 ^{13}C Spin-lattice (T_{1C}) data for Bulk and Adsorbed PPA6%.

Sample name	T_{1C} (s)*			
	CH	CH$_2$		CH$_3$
	27 ppm	44.2 ppm	44.8 ppm	22.0/ 22.8 ppm
60PPA6%	20	33	34	0.4
100PPA6%	16	38	38	0.5
150PPA6%	27	44	42	0.5
450PPA6%	26	43	47	0.5
PPA6%	31	44	44	0.6

* The uncertainties were ~ 0.1 sec for CH_3 and ~ 1 sec for CH and CH_2 carbons.

peaks, respectively. They attributed the higher mobility of the upfield methyl resonance to the fact that it corresponds to packing of more distantly spaced helices. The T_{1C} of the methine and methylene carbons is 31 and 44 s. For the adsorbed copolymer, 60PPA6%, these values decreased to 20 and 34 s, indicating enhanced backbone mobility since variable temperature measurements indicate that these carbons are in the slow motional regime. As the copolymer loading increased those values increased and became comparable to those of the bulk for high loadings (Table 5.2). Proton spin-lattice relaxation times ($T_{1\rho H}$) in the rotating frame, which probe low frequency motions in the kHz range, were measured for PPA6% and 60PPA6%. A value of ~ 25 ± 2 ms was obtained for all resonances for the bulk copolymer due to the effects of proton spin diffusion. For the adsorbed copolymer sample, 60PPA6%, $T_{1\rho H}$ was ~ 32 ± 2 ms. $T_{1\rho H}$ increased with temperature so the observed increase in $T_{1\rho H}$ upon adsorption indicates enhanced mobility of polymer chains. No appreciable changes in the relaxation times were observed when samples were annealed at 100°C for one hour.

5.5 Discussion

Polypropylene is a stereoregular vinyl polymer that has different polymorphs in the crystalline form such as monoclinic (α), hexagonal (β), orthorhombic (γ), and smectic.[13] The thermodynamically stable α–form consists of i-PP chains in a 3_1 helical conformation packed in a monoclinic unit cell. Its ^{13}C CP-MAS spectrum[12] displays a methyl peak split into two resonances at 22.1 and 22.6 ppm, a methine peak at 26.8 ppm, and a methylene peak split into two resonances at 44.2 and 45.2 ppm. The ratio of downfield to upfield resonances for the methyl and methylene carbon splittings is 2:1. These splittings are attributed to the presence of inequivalent sites, A and B, produced by pairing of helices of opposite handedness, which are also present in the ratio 2:1. The A sites correspond to a separation of 5.28 Å between helical axes, while for the B sites the helices are 6.14 Å apart. The metastable β-form crystal contains hexagonally packed 3_1 helical chains, which are arranged in groups of the same helical handedness, resulting in distant packing of left- and right-handed chains. Its ^{13}C CP-MAS spectrum[12] consists of three unsplit peaks for methyl, methine, and methylene carbons at 22.9, 27.1, and 45.0 ppm respectively. The γ–form is preferentially formed at high pressures and has an orthorhombic unit cell formed by bilayers composed of two parallel helices. The ^{13}C CP-

MAS spectrum[12] of the γ–form has the same chemical shifts as the α–form but the ratio of downfield to upfield resonances of methyl and methyelene carbon splittings have a ratio 1:2. If i-PP is quenched from the melt to low temperatures, a combination of a glass and a disordered (mesomorphic) phase is formed, which still has a helix conformation. The ^{13}C CP-MAS of this isomorph has a methyl peak at 22.9 ppm, a methine at 27.1 ppm, and a methylene peak at 45.0 ppm. Random copolymers of propylene with 2.5-20 % by weight of other olefins have been found to crystallize in the γ–form.[14] In general, the amorphous signals of semicrystalline forms of polypropylene are not visible due to the broadness of the resonances. Saito and coworkers detected by NMR the broad amorphous component at 23°C for a PP sample crystallized at 140°C.[10]

The ^{13}C CP-MAS spectrum of the as received bulk PPA6% copolymer corresponds most closely to that of α-iPP crystallized at 100°C for one hour.[10] The poorly resolved splittings are typical of insufficiently annealed iPP samples. The spectra of the smectic and β forms do not resemble that of the PPA6% copolymer since the former has no splittings and the chemical shifts of $-CH_3$ and $-CH_2$ of the latter differ by 1 ppm from those of PPA6%.[12]

The ^{13}C CP-MAS of the adsorbed polymer sample, 60PPA6%, has narrower lines and more resolved splittings than the bulk copolymer. Line narrowing is observed for all the copolymer loadings listed in Table 5.1, including the highest loading 450PPA6%. The splittings become more pronounced with decreasing coverage. It is unexpected to have such narrow ^{13}C NMR lines for an adsorbed polymer, since the well-defined positions and high degree of long range order of the polymer chains in the crystalline regions are normally lost upon adsorption.

Differences in the ^{13}C CP-MAS NMR linewidths of the adsorbed versus the bulk copolymer could conceivably be due to changes in the efficiency of proton decoupling as related to changes in the motional frequencies. The proton decoupling efficiency is sensitive to the motional frequencies when they become similar in magnitude to the decoupling frequency. This possibility was ruled out by acquiring the ^{13}C CP-MAS spectra of PPA6% and 60PPA6% at different proton decoupling frequencies and MAS speeds. ^{13}C spin-lattice relaxation experiments showed that the mobility of the adsorbed copolymer is slightly enhanced as compared to the bulk copolymer. The T_{1C} values decreased from ~ 40 s for the bulk copolymer to ~ 30 s for the adsorbed copolymer sample with the lowest loading. However, motional averaging cannot be responsible for the observed line narrowing of the adsorbed copolymers. The mobility of the adsorbed copolymers remains in the slow motional regime and the increase in mobility is insufficient to cause motional narrowing.

To verify that the appearance of splittings in the ^{13}C NMR spectra of the adsorbed copolymer are due to a surface interaction, the same method to prepare the copolymer loadings was used without adding any zirconia. The ^{13}C CP-MAS spectrum of the polymer after this treatment (PPA6%-control) gave broad lines very similar to those of the as received polymer (Figure 5.1). This shows that the narrowing of lines and the more resolved splittings upon adsorption are related to the interaction of the copolymer chains with the metal oxide.

The possibility that the samples contain a large fraction of unadsorbed chains, which recrystallized during preparation, thus giving rise to more resolved splittings, is ruled out since the FTIR-PAS spectra confirm that the copolymer is chemisorbed to the zirconia surface via carboxylate bonds. However, a certain fraction of the acrylic acid segments are not directly adsorbed to the zirconia since the lowest loadings show a shoulder corresponding to free acid groups at ~ 1710 cm^{-1} in addition to the zirconium carboxylate peaks at 1460 and 1558 cm^{-1}. Incomplete reaction of the carboxylic acid groups may create unbound PP segments between the sticker groups which are long enough to somehow rearrange or "re-crystallize" giving rise to the ^{13}C NMR spectra with better resolved splittings as compared to the bulk copolymer. Taken together, this data indicates that the narrow lines of the ^{13}C spectra of the adsorbed PPA are not due to unadsorbed bulk material but may due to some sort of ordering process of the unattached PP segments between the surface bound sticker groups.

The contrasting variable temperature ^{13}C NMR data of bulk and adsorbed PPA provides additional evidence for a surface interaction. As evident from the appearance of the splittings in the ^{13}C NMR spectra, heating the bulk copolymer above the melt and cooling resulted in a more ordered chain packing. This thermal treatment of the bulk copolymer produced a ratio of 1.22:1 for the downfield to upfield resonances of methyl and methylene carbon splittings. This value deviates significantly from the expected 2:1 ratio normally observed for α-monoclinic iPP, and is most likely due to incomplete recrystallization. Caldas and coworkers[15] obtained a ratio of 1.33:1 rather than 2:1 for the downfield to upfield resonances for the methyl group for an annealed sample of α-monoclinic iPP. They attributed this to the fact that annealing is not sufficient to attain this ratio and the splitting of these resonances is more complex than has been suggested to date.[12] The splittings observed in the NMR spectra in the crystalline portion of bulk annealed samples might not be due only to the packing of right- and left-handed helices.

Some studies suggest that these splittings are related to changes that occur in the 'up' and 'down' ordering of chain direction, associated with the projected direction of the $CH-CH_3$ bonds onto the c-axis.[16, 17]

While the crystalline regions of the bulk copolymer became more ordered after cooling from the melt, an identical thermal treatment of the adsorbed copolymer produced a more disordered chain packing, as indicated by the loss of the splittings in the ^{13}C NMR spectrum. The original packing of the adsorbed polymer chains in the presence of the metal oxide is irreversibly disrupted by heating. Recrystallization of the PP segments in the presence of zirconia appears to be constrained by the partial attachment of the copolymer chains to the surface.

The conformational and thermal behavior of the adsorbed polypropylene copolymers contrasts sharply with that of another closely related semicrystalline copolymer, poly(ethylene-co-acrylic acid) (PEA), which had an acrylic acid content similar to the PPA copolymer. First, PEA adsorbed on the same zirconia substrate showed no unbound acid groups. Secondly, the PEA copolymers became more disordered upon adsorption rather than more ordered. The ^{13}C NMR spectra of adsorbed PEA showed broadened resonances with chemical shifts indicating a higher population of gauche defects in the ethylene segments as compared to the bulk PEA copolymer. As more PEA is adsorbed, the average chain conformation of the ethylene segments remains unchanged until all surface sites are occupied, as indicated by the appearance of a band for unbound carboxylic acid groups in the FTIR-PAS spectra. At very high loadings, similar to those used here for PPA, the adsorbed PEA became essentially bulk-like with the room temperature ^{13}C NMR spectrum identical to that of the bulk copolymer. In contrast, the splittings uncharacteristic of bulk PPA were still persistent for high loadings of PPAC6%. Finally, the thermal behavior is quite different. Adsorbed PEA samples with a 5% acrylic acid content display both an ordered component (transoid chain segments similar to chains in the crystalline regions of bulk PEA) and a disordered component (gauchoid chain segments similar to chains in the amorphous regions of bulk PEA). Upon heating, the trans component is lost but this thermal disordering process is completely reversible, the ^{13}C NMR spectra returned to their previous state upon cooling.

The two systems are similar when comparing their dynamics, in that both copolymers became more mobile upon adsorption. Amorphous homopolymers, which tend to form flat conformations to maximize their interaction with the surface, often become less mobile than in the bulk state. In the case of the ethylene-acrylic acid copolymer, where the acrylic acid segments adsorb strongly while the ethylene segments loop out into a favorable solvent environment, a looped conformation is left upon drying. The polyethylene or polypropylene chain segments in such a looped structure have more free volume available for chain motion as compared to the bulk state.

The dramatic differences in the adsorption behavior of the two copolymers are surprising given that surface bonding, the substrate and the sticker groups density (acrylic acid content) are virtually identical. Nevertheless, they have different polyolefin segments, PE for PEA5% and PP for PPA6% with the difference being the extra methyl group for the latter. It has been suggested from molecular dynamics simulations that the polymer adsorption energy and hence adhesion is dependent on the geometrical structure of the monomers, and decreases for polymer chains with alkyl side-groups in the backbone.[18] Alkyl groups are believed to shelter the functional groups from optimal orientation when approaching the metal oxide surface, lowering the adsorption energy. Van der Beek et al.[19] showed experimentally that polymer chains with alkyl side-groups have a lower adsorption energy and thus weaker adhesion. Although no adhesion data is available for PPA6%, given the above trends, the polypropylene copolymer may have weaker adhesion as compared to the polyethylene copolymer. The presence of some unbound carboxylic acid sticker groups at low loadings, as well as lower amounts of adsorbed PPA as compared to PEA for the same initial loading, provide some evidence for a weaker interaction of PPA with zirconia. The PEA study showed that the average chain conformation is dictated by the topological constraints created by the irreversible surface binding of the carboxylic acid sticker groups, thus the conformation depended on the acrylic acid content rather than the coverage. Weaker topological constraints in the case of PPA may allow for re-crystallization of the PP segments during the adsorption process.

As for the different thermal behavior, a direct comparison may not be valid since the adsorbed PEA samples were only heated until the ordered (trans) component vanished at 70°C, far below the melting temperature of the bulk copolymer at ~ 100°C. Earlier studies showed that the surface-bound carboxylate remains immobilized in this temperature range. The adsorbed PPA samples were heated to the melting point of the bulk copolymer and signals corresponding to a molten state appeared. The extent to which the sticker groups remain attached to the metal oxide surface at these temperatures is unknown. In addition, different interactions are responsible for the splittings of the ^{13}C NMR signals, which are thermally reversible for adsorbed PEA and irreversible for adsorbed PPA. Whereas the 2 ppm splitting of the methylene signal of PEA is due to chain conformation (trans versus gauche), the splittings of the PPA resonances, much smaller in size, are due to chain packing. The actual chain conformation of the adsorbed PPA, as reflected by the chemical shifts, is recovered upon cooling from the melt, but the chain packing, a much more fragile feature, is irreversibly disrupted. Variation of the sticker group density of PPA may shed some light on the factors responsible for the contrasting adsorption behavior of PPA and PEA, but PPA copolymers with a range of acrylic acid contents are not currently commercially available.

5.6 Conclusions

The chain conformation, packing, and dynamics of bulk and adsorbed polypropylene-co-acrylic acid (PPA) random copolymer are investigated. FTIR-PAS spectra show that the acrylic acid segments of PPA form surface carboxylate bonds. Upon adsorption, the chain packing of PPA became more ordered, as reflected by the appearance of splittings in the ^{13}C NMR spectra, which are associated with chain-chain interactions. Such an increase in order is unexpected given the adsorption behavior of closely related semicrystalline copolymer, poly(ethylene-co-acrylic acid) (PEA). The strong surface bonds formed by the carboxylic acid groups of PEA drastically disrupt the chain conformation from that of the bulk state. In the case of the polypropylene copolymer, weaker surface bonds and thus weaker topological constraints, may allow for the crystallization of the PP segments during the adsorption process.

5.7 References

(1) Chan, C.M., *Polymer Surface Modification and Characterization*, Ed.; Hanser/Gardner Publications: Cincinnati, OH, **1994**.

(2) (a) Lee, Y.; Char, K. *Macromolecules* **1994**, *27*, 2603. (b) Mori, M.; Uyama, Y.; Ikada, Y. *J. Polym. Sci., Part A; Polym. Chem.* **1994**, *33*, 1683.

(3) (a) Svoboda, P.; Zeng, C.; Wang, H.; Lee, L.; Tamasko, D.L. *J. Appl. Polym. Sci.* **2002**, *85*, 1562. (b) Maiti, P.; Nam, P.H.; Okamoto, M.; Hasegawa, N. Usuki, Arimitsu *Macromolecules* **2002**, *35(6)*, 2042. (c) Avella, M.; Martuscelli, E.; Raimo, M.; Partch, R.; Gancolli, S.; Pasucci, B. *J. Mat. Sci.* **1997**, *32*, 2411. (d) Rong, M.Z.; Zhang, M.Q.; Zheng, Y.; Zeng, H.M.; Walter, R.; Friedrich, K. *Polymer* **2001**, *42*, 167.

(4) (a) Gutman, L.; Chakraborty, A. K. *J. Chem. Phys.* **1994**, *101*, 10074. (b) Simmons, E.R.; Chakraborty, A. K. J. Chem. Phys. 1998, 109, 8667.

(5) (a) Komoroski, R.A. *High Resolution NMR Spectroscopy of Synthetic Polymers in Bulk*, VCH Publishers Inc., Weinheim, 1986. (b) Schimdt-Rohr, K.; Spiess, H.W. *Multidimensional Solid-State NMR and Polymers*, Academic Press, New York, 1994.

(6) (a) Lin, W.Y.; Blum, F.D. *Macromolecules* **1998**, *31*,4135. (b) Blum, F. *Ann. Rep. NMR Spectroscopy* **1994**, *28*, 277. (c) Blum, F.D. *Colloids and Surfaces* **1990**, *45*, 361.

(7) Pawsey, S.; Yach, K.; Halla, J.; Reven, L. *Langmuir* **2000**, *16*, 3294.

(8) Torchia, D.A. *J. Magn. Reson.* **1978**, *36*, 91.

(9) Beckett, D.R.; Chalmers, J.M.; MacKenzie, M.W.; Willis, H.A.; Edwards, H.G.M.; Lees, J.S.; Long, D.A. *Eur. Polym. J.* **1985**, *21(10)*, 849.

(10) Saito, S.; Moteki, Y.; Nakagawa, M.; Horii, F; Kitamaru, R. *Macromolecules* **1990**, *23*, 3256.

(11) Nasreddine, V.; Halla, J.; Reven, L. *Macromolecules* **2001**, *34*, 7403.

(12) (a) Bunn, A.; Cudby, M.E.A.; Harris, R.K.; Packer, K.J.; Say, B.J. *Polymer* **1982**, *23*, 694. (b) Gomez, M.A.; Tanaka, H.; Tonelli, A.E. *Polymer* **1987**, *28*, 2227.

(13) (a) Padden, F.J.; Keith, H.D. *J. Appl. Phys.* **1959**, *30*, 1479. (b) Bruckner, S.; Meille, S.V.; Petraccone, V.; Pirozzi, B. *Prog. Polym. Sci.* **1991**, *16*, 361.

(14) (a) Mezghani, K.; Philips, PJ. *Polymer* **1995**, *35*, 2407. (b) Turner-Jones, A. *Polymer* **1971**, *12*, 487.

(15) Caldas, V.; Morin, F.G.; Brown, G.R. *Mag. Res. Chem.* **1994**, 32, S72.

(16) (a) Mencik, J. *J. Macromol. Sci., Phys.* **1972**, *B6*, 101. (b) Hikosaka, M.; Seto, T. *Polym. J.* **1973**, *5*, 111.

(17) Auriemma, F.; de Ballesteros, O.R.; De Rosa, C.; Corradini, P. *Macromolecules* **2000**, *33*, 8764.

(18) Cheng, CY.; Lee, KJ.; Li, Y.; Wang, BC. *J. Adhesion Sci. Technol.* **1998**, *12(7)*, 695.

(19) van der Beek, G.P.; Cohen Stuart, M.A.; Fleer, G.J.; Hofman, J.E. *Macromolecules* **1991**, *24*, 6600.

Chapter Six

Dynamics and Morphology of Poly(n-butyl methacrylate) Films: A ^{13}C and ^{129}Xe Solid-state NMR study

---

6.1 Preface

The previous chapters dealt with investigating the chain conformation, dynamics, and morphology of adsorbed semi-crystalline random copolymers. In this chapter, the dynamics and morphology of bulk amorphous poly(n-butyl methacrylate) (PnBMA), adsorbed on zirconia, and filled systems are characterized by ^{13}C and ^{129}Xe solid-state NMR spectroscopy. We have chosen this polymer, since there are relatively fewer surface studies of PnBMA than PMMA, and we would like to investigate the effect of the bulky side group on adsorption. Moreover, xenon has a high solubility in PnBMA, resulting in improved sensitivity in the xenon NMR signals. ^{129}Xe NMR is used to probe the morphology of the adsorbed PnBMA and DSC-detected thermal transitions of zirconia filled PnBMA. Variable temperature experiments are used to determine the glass transition of the bulk polymer.

6.2 Introduction

The glass transition temperature of poly(n-butyl methacrylate) (PnBMA) ($T_g \sim 25^{\circ}C$) makes this polymer attractive for a variety of thin film and materials applications.

PnBMA is used as a comonomer with poly(methyl methacrylate) (PMMA) to form low-T_g polymers, since PMMA ($T_g \sim 105^\circ C$) forms very brittle coatings at room temperature. PnBMA is also used by the microelectronics industry as a ceramic binder because it decomposes at relatively low temperatures in nonoxidative environments.[1] Of the poly(n-alkyl methacrylate)s, PMMA has been the most widely studied in relation to its interfacial properties. Mallik and coworkers used inelastic electron tunneling spectroscopy (IETS) to investigate the interface between PMMA and aluminum oxide and showed that the ester functionality in the polymer undergoes hydrolysis to form a carboxylate ion which binds to alumina ionically.[2] A detailed X-ray photoelectron spectroscopy, IR-RAS, and solid-state NMR study confirmed this binding mode and indicated that the adsorbed PMMA chains lie flat on the oxide surface.[3] Grohens et al.[4] have investigated the effect of tacticity on the adsorption of PMMA on γ-alumina and aluminum mirrors. They have shown that whereas i-PMMA adsorbs in a flat conformation and has a higher T_g than the bulk, s-PMMA and a-PMMA adsorb in a brush-like configuration with most attached segments adsorbing in loops and tails and the T_g remaining constant.

In addition to studies of the binding mechanism and configuration of PMMA at surfaces, the effect of the interface on the dynamic properties is a very active area of research. There have been numerous efforts to measure the glass transition temperatures of PMMA thin films and the effect of the film thickness and substrate on the T_g of standing and supported films.[5] Keddie and Jones[5a] performed the first study of the relative influence of two different substrates, gold and silicon oxide, on the T_g of ultrathin films of PMMA. Using ellipsometry to measure the thermal expansion of PMMA, they observed that the T_g of PMMA decreased on gold substrates but increased on silicon oxide due to hydrogen bonding with the surface silanol groups.

The interfacial properties of poly(n-butyl methacrylate)[6] have not been widely studied as compared to PMMA. The effect of the alkyl side chain, responsible for the relatively low T_g of PnBMA, on the surface binding, chain configuration and dynamics of adsorbed PnBMA is of interest for thin film applications of this polymer. In this chapter, the dynamics and morphology of poly(n-butyl methacrylate) adsorbed on zirconia and zirconia-filled PnBMA are studied by ^{13}C and ^{129}Xe solid-state NMR and FTIR-PAS (Fourier transform infrared photoacoustic spectroscopy). In combination with FTIR-PAS, ^{13}C NMR gives information on the surface binding, chain conformation and the local segmental motions. The ^{129}Xe chemical shift, linewidth, and spin-lattice relaxation times are used to probe the morphology of PnBMA adsorbed on zirconia. Variable temperature ^{129}Xe NMR experiments on the bulk polymer and on filled samples were used to investigate changes in the region where thermal transitions are observed by differential scanning calorimetry.

6.3 Experimental section

Sample preparation. Poly(n-butyl methacrylate) (PnBMA) was used as received (Scientific Polymer Products, Inc.). It has a glass transition temperature ~ 25°C, and a molecular weight of 180,000 g/mol. From ^{1}H and ^{13}C solution NMR analysis, the polymer was estimated to have 62.5% rr, 35% mr, and 2.5% mm triads showing that it is mainly syndiotactic. Its T_g, which is around 25°C, is also indicative of dominantly syndiotactic PnBMA. Nonporous zirconia (ZrO_2) powder (monoclinic, VP zirconium dioxide, Degussa Corp.) was calcinated at 400°C to eliminate any residual organic impurities. The reported average primary particle size of this ZrO_2 is 30 nm, and the BET surface area is 40 m^2/g. Zirconia powder (1.5 grams) was dispersed in 250 ml THF or Cyclohexane (CH) by sonication for 15 minutes. The polymer solutions were prepared by dissolving the appropriate amount of polymer in 50 ml of solvent. Three loadings were prepared from THF using 100, 200, and 750 mg of polymer. These will be referred to as: 50PnBMA-THF, 250PnBMA-THF, 750PnBMA-THF respectively. Four loadings were prepared from CH using 60, 200, 750, 1000 mg of polymer. These will be referred to as: 60PnBMA-CH, 200PnBMA-CH, 750PnBMA-CH, 1000PnBMA-CH. The copolymer solutions were added to the dispersed zirconia powder under stirring. The resulting mixture was refluxed with stirring for one day and annealed for one day. The samples were centrifuged and washed a total of six times each by redispersing the powder in 50 ml solvent with gentle heating, filtering, and then drying under vacuum after the final washing step.

Four filled samples were prepared with 5, 14, and 25 % zirconia, and 14% nano zirconia. The nano-crystalline zirconia powder (separated equiaxial single crystals, cubic zirconium dioxide, Advanced Powder Technology Pty. Ltd) with a particle size of 5 nm and a BET surface area of 140 m^2/g was used without further modification. These will be referred to as 5%Z-PnBMA, 14%Z-PnBMA, 14%nZ-PnBMA, and 25%Z-PnBMA respectively. These samples were prepared by dissolving the polymer in 50 ml THF, and the zirconia was then added to the polymer solution. The solutions were stirred until all the solvent was evaporated. The samples studied, the carbon content in percent weight

(%C), and the amount adsorbed as determined from elemental analysis are summarized in Table 6.1.

Table 6.1 Samples, preparation loadings, and adsorbed amounts.

Sample name	Preparation loadings mg polymer/1.5 g ZrO_2	Adsorbed amount (mg polymer/m^2 ZrO_2)
60PnBMA-CH	60	1.1
200PnBMA-CH	200	2.1
750PnBMA-CH	750	2.8
1000PnBMA-CH	1000	3.2
100PnBMA-THF	100	0.7
200PnBMA-THF	200	0.7
750PnBMA-THF	750	1.0

DSC. The thermal behavior of the four filled samples were investigated using a Perkin-Elmer differential calorimeter, DSC-7. Thermal transitions which were assigned to glass transitions were detected at 112°C for 14%Z-PnBMA, 120°C for 14%nZ-PnBMA, and 52°C for 25%Z-PnBMA. 5%Z-PnBMA did not show any evidence of a glass transition.

NMR. Spectra were acquired on a Chemagnetics CMX-300 NMR spectrometer using a Chemagnetics PENCIL probe with 7.5 mm zirconia rotors. Proton pulse widths between 4.0 and 4.5 μs, a contact time of 3 ms, a MAS rate of 3 kHz, and a pulse delay of 2 s were used for both bulk (100 scans) and adsorbed (4000 scans) samples and a CP-MAS TOSS (Total Suppression of Spinning Sidebands) sequence was used to acquire all 1D ^{13}C NMR spectra. For the variable-temperature experiments, the sample temperature was controlled to within ± 1° by a Chemagnetics temperature controller. ^{13}C spin-lattice relaxation times were measured using the Torchia pulse sequence[7] with a pulse delay of 5 s. ^{1}H spin-lattice relaxation in the rotating frame ($T_{1\rho H}$) were measured by varying an interval, τ, before cross polarization and a spin-locking field of 50 kHz was used.

The xenon gas used in these experiments was ^{129}Xe at natural abundance (26.44%) from Air Liquide Canada Inc. The samples were placed in a specially designed sample holder which is connected to a vacuum system. All the samples were heated under vacuum overnight and loaded with xenon gas sealed and left overnight for the xenon to equilibrate before the experiment was started. Samples masses were around 0.2 g. The xenon pressure in the sample after sealing was 100-120 psi.

74.71 MHz ^{129}Xe single pulse Bloch decay spectra were acquired on a Chemagnetics CMX-270 NMR spectrometer using a variable temperature static probe with a coil diameter of 9 mm internal diameter. A pulse width of 2.40 μs (90° pulse = 7.20 μs) and a pulse delay of 50 s were used. ^{129}Xe spin-lattice relaxation times were measured using a saturation recovery pulse sequence. Variable temperature experiments were acquired at 138.3 MHz with a 16.3 μs 90° pulse and a pulse delay of 50 s on a Varian Unity 500 NMR spectrometer. A two-channel 10 mm broad-band probe was employed. The experiments were performed in heavy-walled, 10 mm NMR tubes (with a 7 mm internal diameter) and packed to a depth of 4-5 cm. This corresponds to sample masses between 0.6 and 0.8 g, with 100-120 psi xenon pressure.

FTIR-PAS. All spectra were run on powder samples of bulk and adsorbed polymers using a Fourier transform Mattson Research series 1 spectrometer equipped with a photoacoustic cell (MTEC model 300) at 1.0 cm^{-1} nominal resolution.

6.4 Results

6.4.1 ^{13}C Solid-state NMR and FTIR

The ^{13}C CP-MAS NMR and FTIR-PAS spectra of bulk PnBMA are shown in Figure 6.1. The polymer has seven well-resolved peaks corresponding to main chain, side chain and carbonyl carbons. The carbon atoms are labeled from **a** through **h**, using the same convention as in reference 8. The only overlapping resonances correspond to the backbone and side chain methyl peaks at ~ 14.5 ppm (**c** and **h**). The chemical shifts for the backbone carbons, **a** and **b** are 56 and 45 ppm respectively. The side chain carbons **e**, **f**, **g** are at 65, 31, and 20 ppm respectively and the carbonyl carbon **d** appears at 177 ppm.

Both tetrahydrofuran (THF) and cyclohexane (CH) are good solvents for PnBMA (solubility parameter δ: 8.75 (cal/cm^3)$^{1/2}$) with THF ($\Delta\delta$ = 0.35 (cal/cm^3)$^{1/2}$) providing a more favorable environment than CH ($\Delta\delta$ = 0.55 (cal/cm^3)$^{1/2}$).[9] Figure 6.2a shows the ^{13}C CP-MAS NMR and FTIR-PAS spectra of PnBMA adsorbed from CH onto zirconia. The lines are noticeably broadened as compared to the bulk polymer. In the FTIR-PAS spectra of the four polymer loadings, the C=O stretching peak at 1728 cm^{-1} decreases in intensity and a new weak peak appears at 1547 cm^{-1}, assigned to a surface carboxylate bond.[10] There is also a new methyl peak in the ^{13}C CP-MAS spectrum of the lowest loadings appearing at ~ 12.3 ppm. The intensity of the new methyl peak decreases as a function of polymer loading and disappears for high loadings that display bulk behavior. Figure 6.2b shows clearly the surface effect where a new peak at 12.3 ppm appears for the adsorbed polymer compared to bulk PnBMA. The presence of a strong carbonyl carbon peak at ~ 177 ppm in the NMR spectra and the dominant band at 1728 cm^{-1} for the ester groups in the IR spectra for the lower loadings indicate that the majority of the polymer segments do not interact with the zirconia via the formation of a surface carboxylate bond. For 60PnBMA-CH, the ratio of the peak intensities of **e** (-OCH_2) to **a** (backbone -CH_2) decreases relative to the bulk indicating that only partial hydrolysis (~ 18%) of the ester group has occurred.

Figure 6.3 shows the ^{13}C CP-MAS NMR and FTIR spectra of the adsorbed PnBMA samples prepared from THF solutions. ^{13}C NMR spectra of loadings prepared with THF had a lower signal to noise ratio than those prepared with CH. From elemental analysis results (Table 6.1), it is observed that for the same initial loading of polymer, a lower coverage is always obtained from a solution of THF since it is a better solvent for PnBMA. For low loadings prepared from THF, the ^{13}C CP-MAS NMR spectrum has a diminished peak intensity for the OCH_2 peak relative to the bulk. This indicates that partial hydrolysis of the ester group has also occurred. Similar to the loadings prepared with CH, there is an additional peak at ~ 12.3 ppm, diminishing as the polymer loading increases. The spectrum also has a peak around 40 ppm which did not show up for the loadings prepared with CH and may be due to the interaction of THF with ZrO_2.

All the peaks and chemical shifts in the ^{13}C CP-MAS spectra of the four filled samples 5%Z-PnBMA, 14%Z-PnBMA, 14%nZ-PnBMA, and 25%Z-PnBMA are similar to bulk PnBMA except that the lines are slightly broadened. Their IR spectra are also bulk-like and have an intense peak at 1732 cm^{-1} for free ester groups and no visible carboxylate bands.

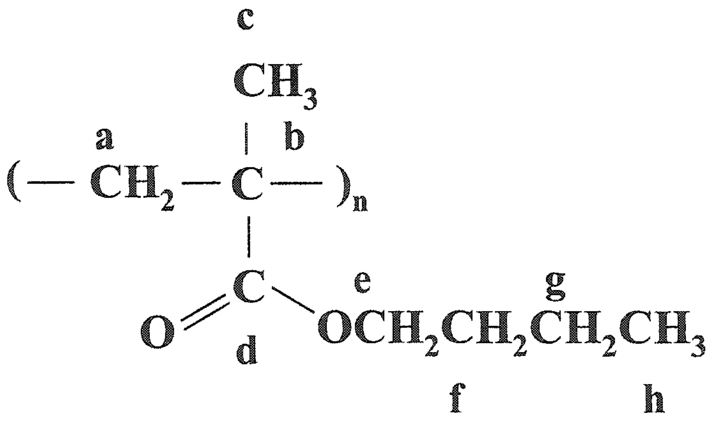
c
CH3
a
b
(— CH2 — C —)n
C
O
d
e
g
OCH2CH2CH2CH3
f
h

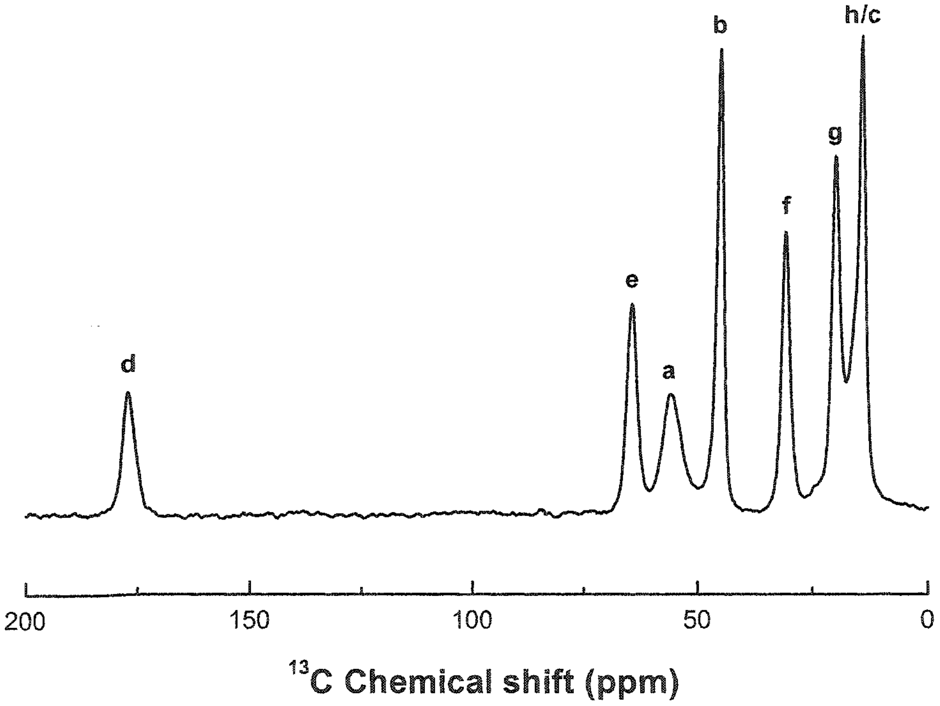
b
h/c
g
f
e
a
d
200
150
100
50
0
13C Chemical shift (ppm)

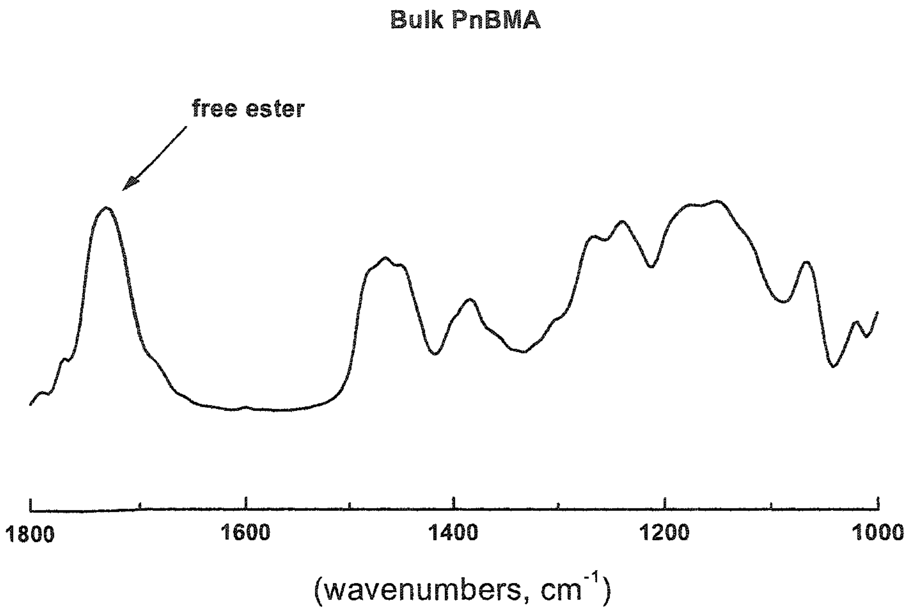

Figure 6.1 FTIR and ^{13}C CP-MAS spectra of bulk PnBMA.

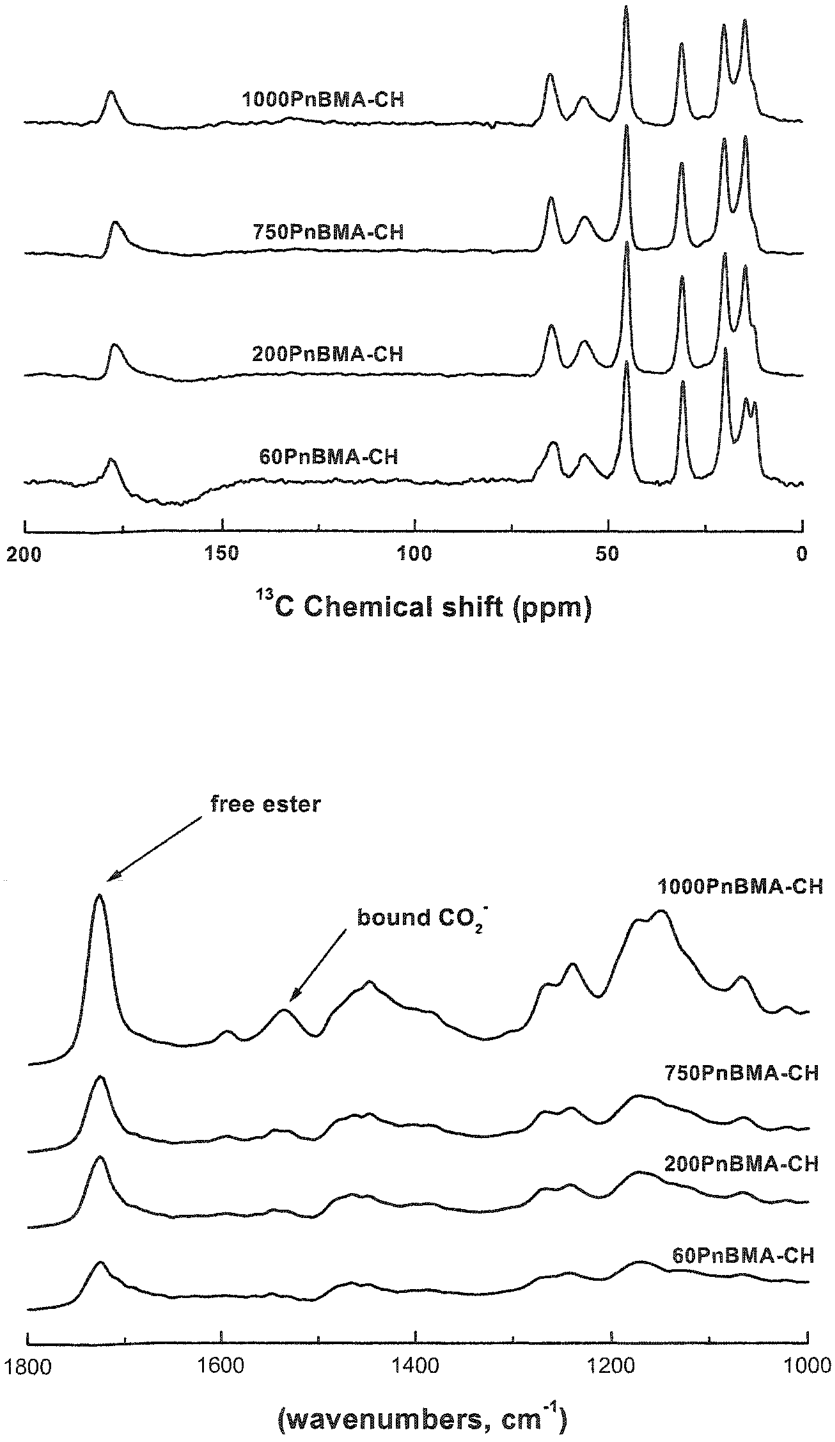

Figure 6.2 (a) FTIR and ^{13}C CP-MAS spectra of PnBMA loadings adsorbed from CH.

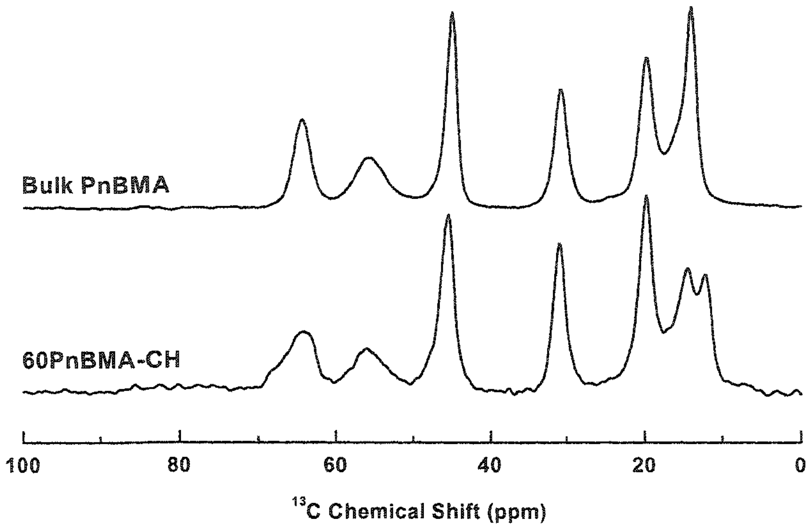

Figure 6.2 (b) ^{13}C CP-MAS spectra of bulk PnBMA and 60PnBMA-CH.

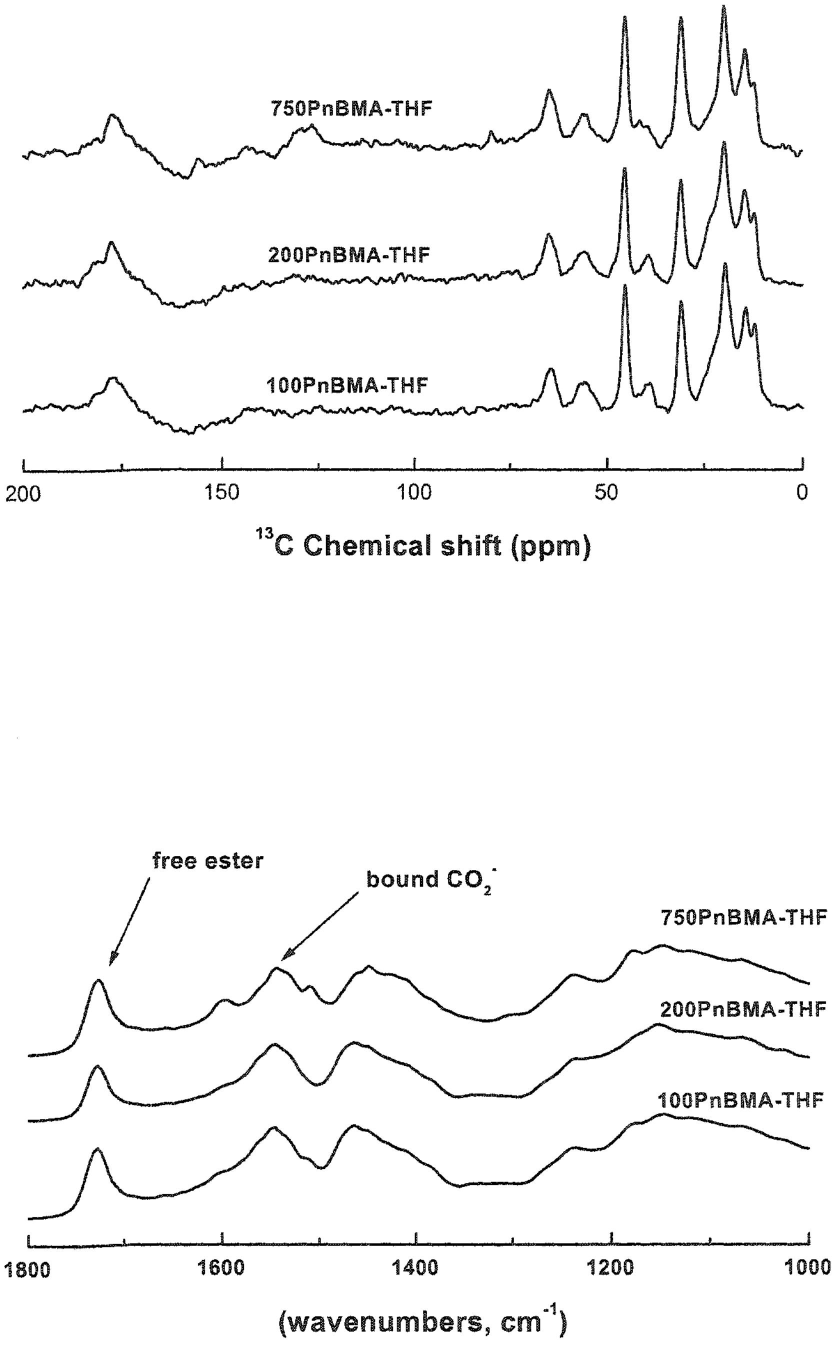

Figure 6.3 FTIR and ^{13}C CP-MAS spectra of PnBMA loadings adsorbed from THF.

6.4.2 Relaxation Measurements

^{13}C spin-lattice relaxation times were measured using the Torchia pulse sequence[7] and values are listed in Table 6.2. Carbons **a** and **b** are diagnostic of backbone mobility. For the bulk polymer, the T_{1C} values for carbons **f**, **g**, and **h** (0.4 s, 0.6, and 1.1 ± 0.1 s) show that the mobility of the side-chain carbons increases with distance from the main chain. As temperature increased, the relaxation times of backbone carbons decreased and those of the side chain increased indicating that the former are in the slow motional regime ($\omega_o^2\tau^2 >> 1$) while the latter are in the extreme narrowing condition.

Upon adsorption, only the side chain carbons of PnBMA showed significant changes in T_{1C}. The increase of the T_{1C} values of carbons **e**, **f**, and **g** in the adsorbed samples indicates an enhanced mobility of the side chains since these carbons are in the fast motional limit where the spin lattice relaxation time is inversely proportional to the correlation time. The T_{1C} of the new methyl peak at 12.3 ppm is 2.3 s while that of the methyl peak at 14.5 ppm is 1.2 s, indicating higher mobility of the former.

In contrast to the adsorbed PnBMA samples, only the backbone methylene, carbon **a**, of the zirconia-filled PnBMA samples showed any differences from the bulk polymer values. T_{1C} of carbon **a** decreased from 9 s with increasing amounts of filler to 6.3 and 5.1 s for the 14% and 25% filled samples (uncertainities ~ 0.5 sec). Since the backbone carbons are in the slow motional regime, the decrease in T_{1C} indicates enhanced motion.

Since spin-lattice relaxation in the laboratory frame, T_1, probes motional frequencies in the MHz range, it is normally more sensitive to changes in the more mobile polymer side chains rather than the slower backbone reorientations. Changes in the backbone motion are usually detected by spin-lattice relaxation in the rotating frame, $T_{1\rho}$, which probes motional frequencies in the kHz range. ^1H spin-lattice relaxation measurements in the rotating frame ($T_{1\rho H}$) were carried out on the bulk, adsorbed and filled systems. Since spin diffusion will equalize the $T_{1\rho H}$ values for the different proton sites, only an averaged change in motional frequencies can be detected and changes in the side chain versus the backbone cannot be distinguished. The $T_{1\rho H}$ values at 25°C for 60PnBMA-CH and 750PnBMA-CH are 10.0 and 13.0 (± 0.5) ms respectively with the latter having the same value as bulk PnBMA. The $T_{1\rho H}$ values of the filled samples showed much larger changes from that of bulk PnBMA, decreasing from 13.0 ms to 8.0, 7.0, 6.0, and 6.0 ms for 5%Z-PnBMA, 14%Z-PnBMA, 14%nZ-PnBMA, and 25%Z-PnBMA respectively (uncertainities ~ 0.5 ms). Since $T_{1\rho H}$ decreased with increasing temperature for adsorbed and filled PnBMA samples, these systems are in the slow motional regime where $T_{1\rho H}$ increases with decreasing mobility. Thus the shorter $T_{1\rho H}$ values of the adsorbed and filled samples with respect to those of the bulk PnBMA, indicate enhanced mobility in the kHz frequency range.

Table 6.2 ^{13}C Spin-lattice relaxation times of adsorbed and filled PnBMA.

Sample	**T_{1C} (sec)**						
	12.3 ppm	**14.5 [h/c]**	**20.2 [g]**	**31.3 [f]**	**45.3 [b]**	**56.1 [a]**	**65.0 [e]**
PnBMA	-	1.1	0.6	0.4	5.0	9.0	0.6
750PnBMA-THF	2.5	1.5	1.0	0.5	5.8	-	1.7
750PnBMA-CH	1.5	1.3	0.7	0.5	4.4	7.2	0.8
60PnBMA-CH	2.3	1.2	1.0	0.6	5.2	8.0	1.6
14%Z-PnBMA	-	1.3	0.5	0.4	4.4	6.3	0.6
14%nZ-PnBMA	-	1.4	0.6	0.4	4.3	7.8	0.5
25%Z-PnBMA	-	1.3	0.5	0.3	4.4	5.1	0.6

6.4.3 ^{129}Xe NMR

6.4.3.1 1D and Variable Temperature ^{129}Xe NMR of PnBMA

Figure 6.4 shows the ^{129}Xe NMR spectrum of bulk PnBMA. The peak at 0 ppm corresponding to unadsorbed xenon gas and the second peak at 196 ppm is due to xenon adsorbed in the polymer. The room temperature ^{129}Xe chemical shift of xenon gas adsorbed in amorphous polymers typically ranges between 200-230 ppm.[11] This variation is due to the density dependence of the ^{129}Xe chemical shift, the shift being inversely proportional to the available free volume. The xenon interacts with the polymer chains via dispersive van der Waals interactions and its chemical shift and linewidth reflect the extent of the interaction of xenon atoms with different sites and their residence time at these sites. Xenon dissolves only in the amorphous components of polymers where chain motion creates free volume. Unlike porous materials, where the void space is much larger than that of the xenon atom, the free volume between polymer chains is of a comparable size to the xenon atom, thus making xenon a probe of polymer chain mobility. At 25°C, PnBMA is around its glass transition temperature so the polymer chains will have some degree of mobility. The xenon atoms will thus experience an averaged environment due to increased chain mobility giving rise to narrow lines.

Variable temperature ^{129}Xe NMR experiments were performed on PnBMA to observe the changes at the glass transition temperature. Figures 6.5a and b show the plot of the chemical shift and linewidth of the bulk xenon peak as a function of temperature from 0°C to 80°C. As the temperature increases, the free volume increases resulting in an upfield shift. At low temperatures, the mobility of the xenon diminishes due to densification of the polymer leading to line broadening and to a downfield shift. Plots of the xenon linewidth versus temperature, like those of Figures 6.5a and b, have been used to determine the glass transition temperature (T_g) of amorphous polymers by fitting the set of data to two straight lines that intersect at T_g.[12] A break at T_g occurs because the xenon linewidth is sensitive to the surrounding medium, which changes from glassy (rigid) to rubbery (mobile). A smaller break at T_g, sometimes observed for the chemical shift, was not detected for PnBMA. However the linewidth data, shown in Figure 6.5b, can be fit to two straight lines which intersect near 25°C, identical to the reported calorimetric T_g of PnBMA.

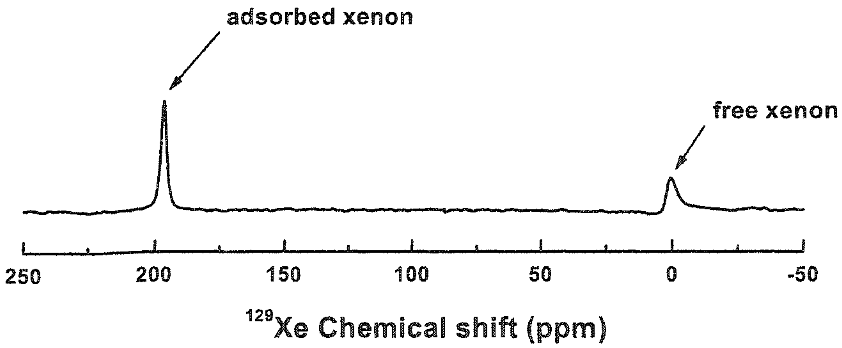

Figure 6.4 ^{129}Xe NMR spectrum of bulk PnBMA.

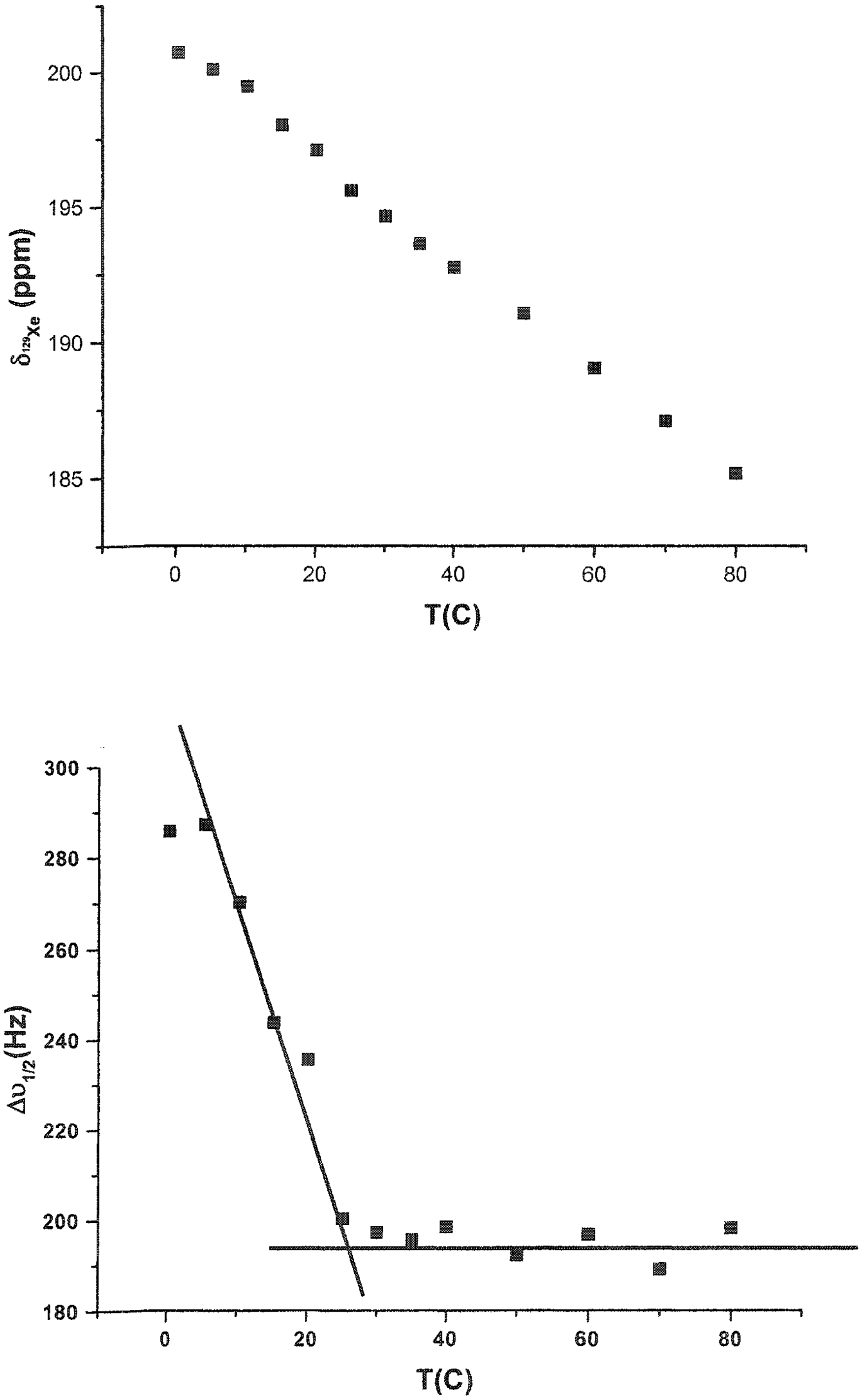

Figure 6.5 Plots of the variation of the ^{129}Xe chemical shift and linewidth for PnBMA.

6.4.3.2 ^{129}Xe NMR of adsorbed PnBMA

The ^{129}Xe NMR spectra of the different copolymer loadings adsorbed from cyclohexane are shown in Figure 6.6. Xenon adsorbed on the surface of bare zirconia has a peak at 5.3 ppm. For the adsorbed polymer samples, the xenon is adsorbed into the microvoids created by the aggregation of zirconia. Two peaks are observed for all loadings, one at 0 ppm for free unadsorbed xenon gas and the second downfield peak for adsorbed xenon gas. For the 60PnBMA-CH sample, which has a coverage of 1.1 mg/m^2 (Table 5.1), a broad resonance at 12.8 ppm is observed for xenon occupying the microvoids of the aggregated particles. The xenon chemical shifts for 60PnBMA-CH, 200PnBMA-CH, 750PnBMA-CH, and 1000PnBMA-CH are 12.8, 21.7, 29.6, and 30.1 ppm respectively. This is an indication that xenon becomes more restricted as more polymer is adsorbed due to diminishing microvoid size. No peak corresponding to xenon absorbed in a bulk-like polymer environment (196 ppm for PnBMA) was observed for these loadings.

^{129}Xe spin-lattice relaxation times T_1(Xe) were measured in an effort to probe the uniformity of the polymer coating. Xenon relaxes more rapidly on uncoated zirconia due to interactions with surface hydroxyls or paramagnetic centers. When PnBMA is adsorbed on the zirconia, the hydrophobic polymer chains shield the xenon from the surface, resulting in slower relaxation and longer T_1(Xe) values. T_1(Xe) increased as a function of coverage for the same solvent system, and loadings prepared from THF had generally shorter T_1(Xe) values than those prepared from CH due to lower coverages. For example, the T_1(Xe) values of 150PnBMA-THF (coverage = 0.7 mg/m^2) versus 60PnBMA-CH (coverage = 1.1 mg/m^2) were 1.2 and 4 s respectively. The T_1(Xe) for free and adsorbed xenon resonances were very similar indicating that xenon is rapidly exchanging between these states. Coverages higher than 1.1 mg/m^2 showed similar T_1(Xe) values, indicating that the zirconia surfaces sites responsible for relaxation of the Xe spins are mostly occupied above this coverage.

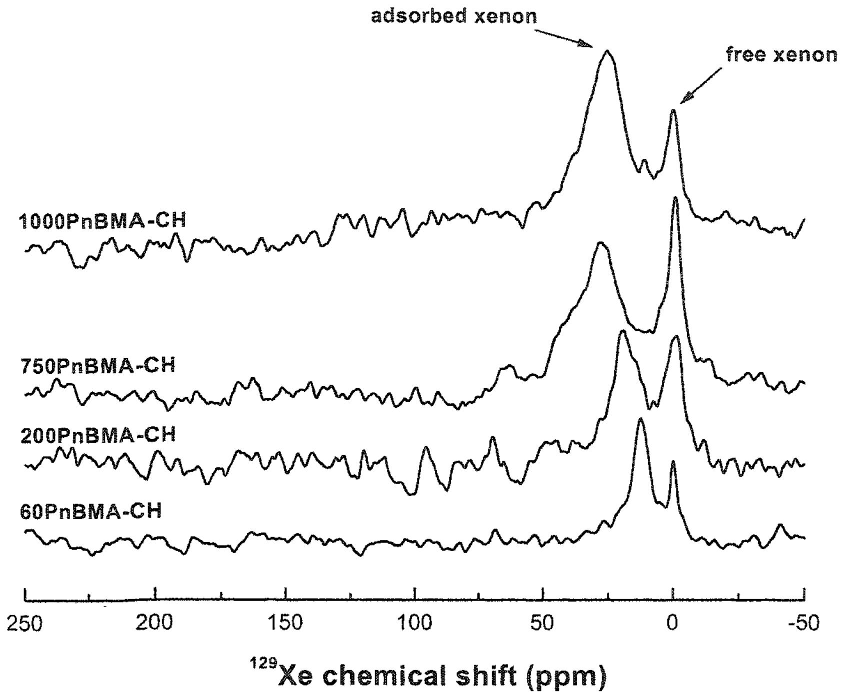

Figure 6.6 ^{129}Xe NMR spectra of PnBMA loadings prepared from CH.

6.4.3.3 Variable Temperature ^{129}Xe NMR of filled PnBMA.

Calorimetric and variable temperature ^{129}Xe NMR studies were carried out on the zirconia filled PnBMA samples to study the effect of the interaction of PnMBA with zirconia on the glass transition. Figure 6.7 shows the ^{129}Xe NMR spectra of the 5%Z-PnBMA, 14%Z-PnBMA, 14%nZ-PnBMA, and 25%Z-PnBMA samples. Each sample has a peak for free xenon gas as well as one for xenon adsorbed in a bulk-like polymer medium. The peaks for xenon adsorbed in the polymer matrix are at 192 ± 2 ppm for the four filled samples, slightly lower than that of bulk PnBMA. However, the linewidths, ranging from 380 to 640 Hz, are broader than the xenon peak for bulk PnBMA either due to more restricted chain mobility and/or a more heterogeneous environment of the polymer chains in the filled samples. From calorimetry, 5%Z-PnBMA did not display any transitions below the onset of thermal decomposition. The thermal transitions for 14%Z-PnBMA, 14%nZ-PnBMA, and 25%Z-PnBMA were detected at 112°C, 120°C, and 52°C respectively and no weight loss was observed at these temperatures. However, these transitions were only detected upon the initial heating of the filled samples and were absent when the samples were reheated. The breadth of the transitions was ~ 7, 20, 20, and 8°C for bulk PnBMA, 14%Z-PnBMA, 14%nZ-PnBMA, and 25%Z-PnBMA respectively. Variable temperature ^{129}Xe NMR experiments were performed on the 25%Z-PnBMA, in the range of 25-90°C, to probe the dynamics of polymer chains in the region where the DSC-detected thermal transition occurs. Similar to bulk PnBMA, the plot of xenon chemical shift versus temperature gave a straight line of negative slope (~ -1) as shown in Figure 6.8, indicating that the rate of decrease in the chemical shift with temperature is the same for bulk PnBMA and 25%Z-PnBMA. As shown in Figure 8b, the xenon linewidth decreased from 470 Hz at 25°C to 388 Hz in the range 50-60°C but then increases. However there are large fluctuations in the xenon linewidth above 70°C. The variable temperature ^{129}Xe NMR experiments were not performed for the 14%Z-PnBMA and 14%nZ-PnBMA samples since the DSC-detected thermal transitions occur at temperatures where pressure buildup of xenon could cause rupture of the NMR tubes.

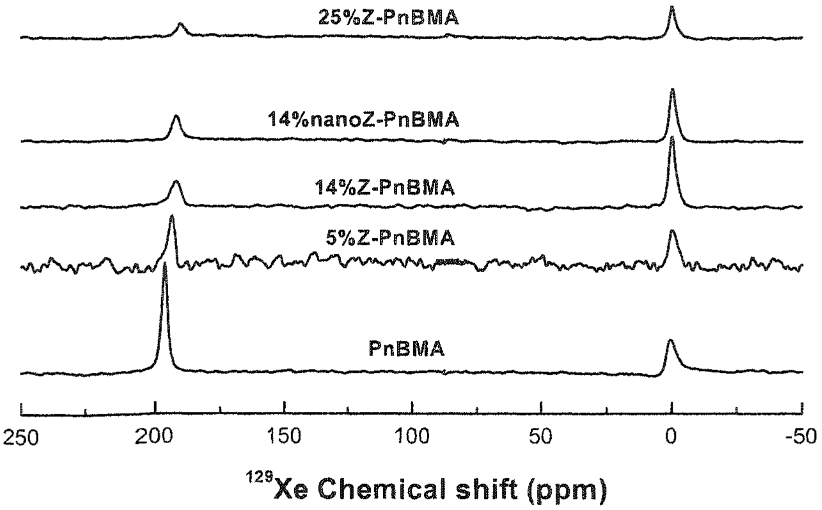

Figure 6.7 ^{129}Xe NMR spectra of zirconia-filled PnBMA samples.

Table 6.3 ^{129}Xe NMR chemical shifts, linewidths at 25 °C, and thermal calorimetric transitions of bulk PnBMA and filled samples.

Sample Name	% ZrO_2	^{129}Xe linewidth (Hz)	DSC T(°C)
Bulk PnBMA	0	200	25
5%Z-PnBMA	5	380	-
14%Z-PnBMA	14	610	112
14%nZ-PnBMA	14 (nano)	640	120
25%Z-PnBMA	25	470	52

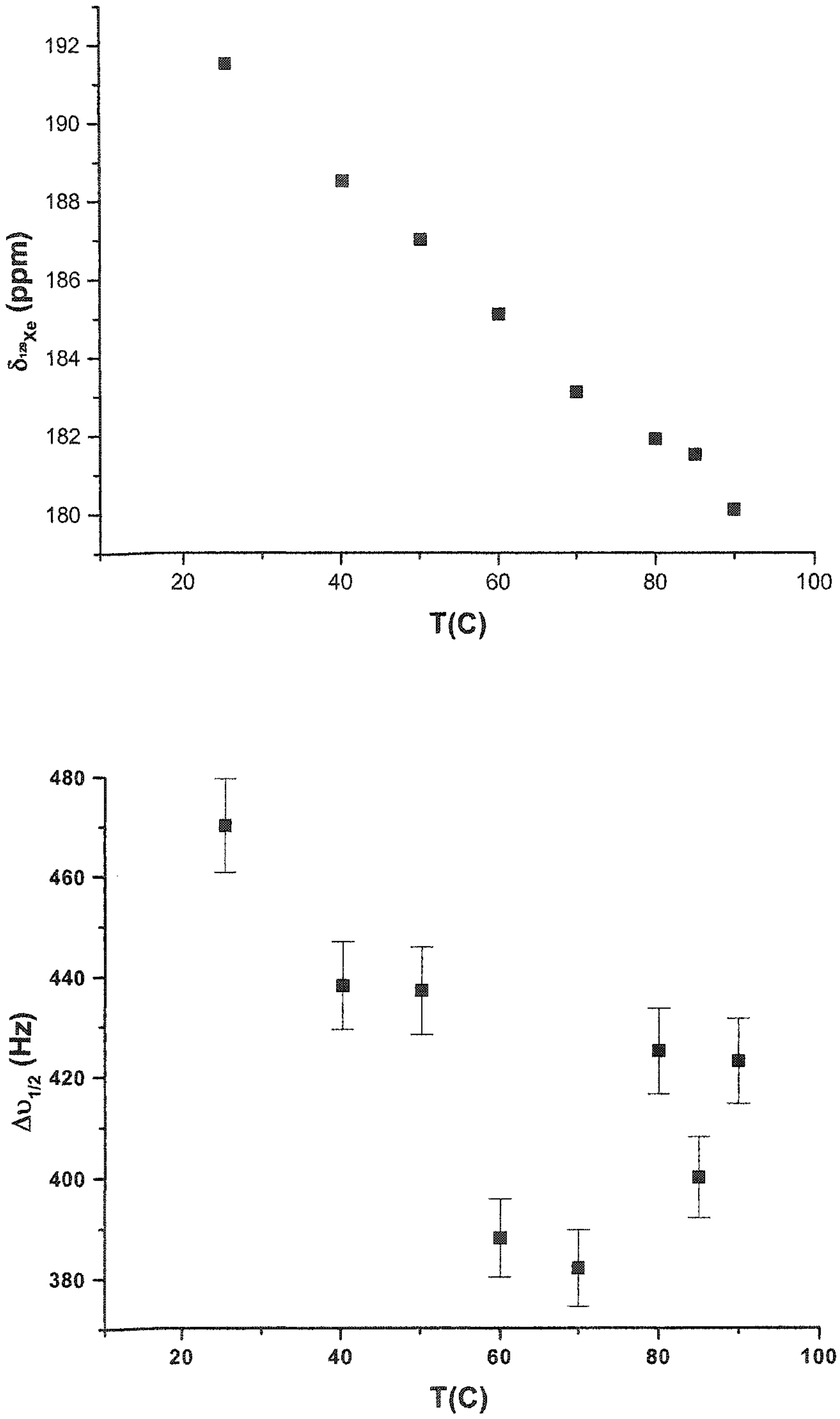

Figure 6.8 Plots of the variation of the ^{129}Xe chemical shift and linewidth for 25%Z-PnBMA.

6.5 Discussion

6.5.1 Surface Bonding, Chain Conformation and Mobility of Adsorbed PnBMA

PnBMA binds to zirconia by partial hydrolysis of the ester groups. The relative intensities of the backbone and sidechain carbons in the ^{13}C NMR spectra indicate that only ~ 18% of the ester groups are hydrolyzed for the lowest loadings. This hydrolysis results in the formation of surface carboxylate bonds, as indicated by the weak band at ~ 1547 cm^{-1} in the FTIR-PAS spectra, corresponding to the asymmetric C-O stretch of a chelating bidentate zirconium carboxylate bond.[10] This low rate of hydrolysis, as compared to PMMA on alumina where 70% of the ester groups are hydrolyzed, may be due to the lower reactivity with zirconia and/or the more bulky ester side chains. The adsorption of PnBMA on high surface area alumina powder was studied by FTIR-PAS.[6b] The solvent and polymer concentration were varied and a maximum hydrolysis rate of 33 % was found, also much lower than for PMMA on alumina. Similar to the adsorption of PnBMA on zirconia, at higher polymer concentrations the ester C=O band increased in intensity due to increasing amounts of free loops and tails or due to deposition of secondary layers of polymer chains onto the previously adsorbed layer.[6b]

Another possible mechanism for the binding of PnBMA onto zirconia can occur through hydrogen bonding between the ester groups and the surface hydroxyls. Fontana and Thomas[13] reported that the ester carbonyl stretching vibration frequency of PMMA is shifted to lower frequencies by 14 to 29 cm^{-1} upon adsorption due to hydrogen bonding with the surface hydroxyl groups. We did not observe any shift of the ester band to lower frequencies upon adsorption, indicating that hydrogen bonding is not the dominant mechanism. Likewise, no such shift was reported for PnBMA adsorbed on alumina.[6b]

Van der Beek et al. determined that PMMA adsorbed better than PnBMA on both silica and alumina because polymer chains with larger alkyl side-groups have a lower adsorption energy and thus weaker adhesion.[14] They found that adsorption is stronger on silica than on alumina for all polymers, since many of the Lewis acid sites on alumina are not accessible to the basic functionalities of the polymers especially for polymers with a bulky side chain. They also pointed out that the size of a polymer segment affects adhesion. The smaller the polymer segment, the larger the number of specific interactions per surface area, and the stronger the adhesion to the substrate. While both are polyesters, the former has a bulky butyl side group which leads to steric hindrance for the ester functionality to interact with the substrate.

For all low loadings of PnBMA prepared from both THF and CH, there is a new methyl peak at 12.3 ppm in the ^{13}C CP-MAS spectra. This peak diminished in intensity as the coverage increased and was more intense for loadings prepared from THF due to the overall lower coverages. Whereas the other methyl resonance at 14.5 ppm is in the typical chemical shift range observed for bulk-state hydrocarbons, the ^{13}C chemical shift of the new methyl peak is anomalously low. A conformational change as the source of the unusually low methyl shift is ruled out based on a previous ^{13}C NMR study of PMMA adsorbed on alumina. Konstadinidis et al.[3] observed an upfield shift for the α-CH_3 and a corresponding downfield shift for the backbone -CH_2 upon adsorption of PMMA on amorphous alumina. They interpreted this as a γ-gauche effect where the α-CH_3 goes from trans to gauche (upfield shift) and the -CH_2 from gauche to trans (downfield shift) resulting in a relatively flat configuration of the extensively hydrolyzed molecules on the alumina surface. In our case, the appearance of a new methyl peak at 12.3 ppm was not accompanied by a downfield shift of carbon **a,** which remained unchanged upon adsorption. Furthermore, the extent of hydrolysis of PnBMA (~ 18%) is small compared to PMMA on alumina (~70%) and as discussed below, PnBMA does not adsorb in a flat conformation.

Such low methyl shifts (11-13 ppm) have been observed for single monolayers of long chain organic acids adsorbed on zirconia and other metal oxides and is characteristic of methyl groups located at the monolayer/air interface.[15] Wang et al.[16] studied the molecular structure of PnBMA at the PnBMA/air and PnBMA/water interfaces by sum frequency generation (SFG) vibrational spectroscopy. They found that PnBMA surfaces in both air and water are dominated by methyl groups of the ester side chains. Thus we assign the new methyl peak to the unhydrolyzed ester sidechains segregating to the polymer/air interface. This assignment is further supported by the T_{1C} measurements which show an enhanced mobility of the methyl groups at 12.3 ppm as compared to the other methyl groups.

In regards to the chain configuration of adsorbed PnBMA, the lack of a conformational change akin to the case of PMMA on alumina, an enhanced chain mobility, and the low rate of hydrolysis, points towards the formation of loops and tails rather than a flattened train structure. Homopolymers adsorbed in a flat conformation tend to show a more restricted mobility as compared to the bulk state.[17] The NMR relaxation measurements of adsorbed PnBMA indicate an enhanced mobility of the sidechains in the MHz frequency range (T_{1C}) and perhaps also of the backbone in the kHz range ($T_{1\rho H}$). Grohens et al.[4a] showed that isotactic PMMA adsorbs in a more flattened way than atactic and syndiotactic PMMA. They attributed this to the flexibility of meso (tg) chain segments in i-PMMA, which can rearrange, unlike syndiotactic PMMA, whose local stiffness due to tt sequences hinders this rearrangement. The PnBMA used for this study has a high fraction of trans conformers (~ 20% gauche conformers), typical of poly(n-alkyl methacrylates) with long alkyl side groups.[18] The local stiffness due to the syndiotacticity of the PnBMA chains will hinder adsorption, leading to a low hydrolysis rate and formation of a more loopy rather than flat structure.

6.5.2 Morphology of Adsorbed PnBMA and zirconia-filled PnBMA

The variation of the xenon linewidth with temperature provides information about polymer chain mobility. Below the glass transition the xenon lines are broad, indicating restricted dynamics in the glassy state and above it the lines become narrower, reflecting the enhanced mobility in the rubbery state. The ^{129}Xe linewidth data for PnBMA can be fit to two straight lines that intersect in the range 20-25°C, corresponding to the calorimetric T_g. The discontinuity of the chemical shift as a function of temperature is not evident due to lower sensitivity to mobility changes and a straight line of negative slope is obtained for these plots. In a ^{129}Xe NMR study of poly(ethyl methacrylate)[12], only a small break in the slope of the chemical shift versus temperature at T_g was detected. The authors observed that the discontinuity in the ^{129}Xe linewidth versus temperature plot of poly(ethyl methacrylate) was much larger. For poly(n-alkyl methacrylate)s, the extent to which the dissolved xenon peak persists below T_g depends on the length of the side chains. The bulkier the side chain, the larger the free volume available for xenon to occupy, and the gas can permeate the polymer far below T_g. This trend holds as long as the side chains do not crystallize and prevent the gas from permeating the polymer. For example, no adsorbed xenon peaks were observed for poly(octadecyl methacrylate) whose long side chains (18 carbons) are crystallized.[19]

For the adsorbed PnBMA samples, we observed an increase in the chemical shift of xenon as a function of polymer loading due to diminishing microvoid size. The large linewidths of these signals reflect the distribution of microvoid size. The xenon spin-lattice relaxation times increase with coverage due to blocking of the surface relaxation sites of the zirconia by the hydrophobic polymer. The results obtained in this study on amorphous films of PnBMA are similar to what we have previously observed for zirconia coated with poly(ethylene-co-acrylic acid) (PEA), a semicrystalline copolymer.[20] However, the highest loadings of PEA showed signals for xenon adsorbed in the polymer matrix in addition to the peak for xenon residing in the microvoids created by aggregation of the zirconia particles. For PnBMA, we observed such peaks only for the zirconia-filled PnBMA samples. PEA adsorbed much more strongly on zirconia, with all the carboxylic acid groups forming surface carboxylate bonds. The amount of adsorbed PnBMA is insufficient for detection of signal, or the signal is very broad and cannot be detected.

The ^{129}Xe chemical shifts of the four zirconia filled PnBMA samples were similar, 192 ± 2 ppm, slightly lower than the value for the pure polymer. The ^{129}Xe NMR linewidths of the filled samples are larger than that of bulk PnBMA and increase as a function of filler content and then decreased for 25%Z-PnBMA. Similar increases in the ^{129}Xe linewidths have been observed for filled elastomers. Veeman et al.[21] observed that the linewidth increased from 164 Hz for EPDM to 250 Hz for carbon black (CB)-filled EPDM. Although the ratio of surface areas of nano zirconia to zirconia is 3.5, the linewidth of 14%nZ-PnBMA (640 Hz) was only slightly larger than that of 14%Z-

PnBMA (610 Hz), indicating that the zirconia particle size does not have a profound effect on the linewidth. While we were able to determine T_g for bulk PnBMA from the variation of the ^{129}Xe linewidth with temperature, this was not possible for the zirconia-filled PnBMA. The plot of the linewidth versus temperature did not yield a set of data that can be fit to two straight lines as for the bulk and the xenon linewidth fluctuated above 70°C. These fluctuations could be possibly due to the onset of thermal decomposition in the form of further hydrolysis of the ester sidechains.

The transition temperatures detected for 14%Z-PnBMA, 14%nZ-PnBMA, and 25%Z-PnBMA are 87, 95, and 27°C higher respectively than the T_g of pure PnBMA. These temperature differences are much larger than the typical increase in T_g when fillers are added to polymers. For example, the T_g of 20 % carbon black-filled PnBMA is only 9 °C higher than pure PnBMA. The T_g of PnBMA latex films increases by 14°C for a 22.5 % silica content.[22] The increase in T_g for silica-filled poly(methyl methacrylate) and poly(ethyl methacrylate) ranged from 1 to 18°C.[23] Dynamic mechanical studies performed by Tsagaropoulos and Eisenberg showed that colloidal silica-filled polymers exhibit a second, highly elevated T_g (> 100 C), attributed to the overlap of regions of restricted mobility.[24] They found that these transitions were broader than those in the bulk and that higher filler content and smaller filler size resulted in higher T_g values. Above a critical concentration of silica particles, these overlap regions decrease resulting in a drop in the total area under the tan δ (loss tangent) peaks and the second T_g was lowered. Due to the small size of the regions of restricted mobility, the second glass transition could not be detected by DSC. The average particle size of the zirconia (30 nm) powder is much larger than the silica particles used in the study by Tsagaropoulos and Eisenberg and only one set of transitions which could possibly be attributed to glass transitions in terms of enthalpy changes are detected. Furthermore, these transitions are observed only for the initial heating and were absent upon reheating the zirconia-filled PnBMA samples.

Although we cannot assign the DSC-detected transitions of the zirconia-filled PnBMA samples to glass transitions, it is interesting to note that the trend in the ^{129}Xe linewidths with filler content mirrors the trend in the temperatures of these transitions. Both a smaller linewidth and a lower transition temperature were detected for the sample with the highest filler content, 25%Z-PnBMA. It has been observed that the glass transition temperature of filled polymer samples increases with filler content up to a critical value, above which the T_g becomes lower. This can be attributed to aggregation of filler particles at high contents, resulting in a smaller effective surface area for interaction with the polymer.[23] The agglomeration of the filler particles at high contents results in an increased free volume of the polymer matrix surrounding the agglomerates.[25] Although the ^{13}C relaxation data shows that the local segmental mobility of PnBMA increases with filler content, the ^{129}Xe NMR linewidths, and possibly the calorimetric data, indicate restricted dynamics on a larger length scale. We speculate here that this variation of the chain mobility with length scale can be interpreted in terms of a physical network. The enhanced local mobility is due to the nature of the surface bonding of PnBMA where the low hydrolysis rate and tacticity of PnBMA prevent adsorption in a flat conformation as in the case of PMMA, leading to a predominance of mobile loops and tails. The zirconia particles are well dispersed in the PnBMA matrix but due to the large molecular weight of the PnBMA used here, they can be bridged by loops and tails to form a network. The combination of long loops and tails with particle bridging would account for the coexistence of enhanced local mobility and restricted mobility on a larger length scale.

6.6 Conclusions

^{13}C and ^{129}Xe solid-state NMR experiments have been performed to probe the dynamics and morphology of bulk, adsorbed, and zirconia-filled PnBMA. The ^{13}C CP-MAS and FTIR-PAS spectra of all adsorbed PnBMA samples have a free ester peak indicating loop/tail formation. The adsorption occurs with partial hydrolysis of the ester groups (~18%) and with no conformational changes. The ^{13}C CP-MAS spectra of the adsorbed PnBMA samples have a new peak at 12.3 ppm, assigned to the methyl groups of the non-hydrolyzed ester sidechains, which segregate to the polymer/air interface.

^{129}Xe NMR experiments showed that xenon experiences two environments: microvoids in low loadings and bulk-like medium in zirconia-filled samples. The xenon chemical shift increased as a function of loading due to diminishing microvoid size and ^{129}Xe spin-lattice relaxation times became longer due to weaker interaction between xenon and zirconia. Although ^{13}C relaxation measurements indicate an enhanced local segmental mobility of both the adsorbed and filled PnBMA samples, the ^{129}Xe NMR parameters of the filled samples are consistent with restricted chain mobility on a larger length scale. The xenon linewidths of the zirconia filled samples are correlated with the temperatures of DCS-detected thermal transitions which increase as a function of filler content and then decrease for the highest filler content measured. The coexistence of local enhanced mobility with restricted long range chain motion may be due to particle bridging by the long loops and tails of adsorbed PnBMA.

6.7 References

(1) Stetson, H.W. *High Technology Ceramics-Past, Present and Future, Ceramics and Civilization*, Ser. Vol. 3, American Ceramic Society, Westerville, OH, 1986, p: 307.

(2) Mallik, R.R.; Pritchard, R.G.; Horley, C.C.; *Polymer* **1985**, *26*, 551.

(3) Konstadinidis, K.; Thakkar, B.; Chakraborty, A.; Potts, L.W.; Tannenbaum, R.; Tirrell, M. *Langmuir* **1992**, *8*, 1307.

(4) (a) Grohens, Y.; Brogly, M.; Labbe, C.; Schultz, J. *Polymer* **1997**, *38(24)*, 5913. (b) Grohens, Y.; Schultz, J.; Prud'Homme, R.E. *Int. J. Adhesion and Adhesives* **1997**, *17*, 163. (c) Grohens, Y.; Auger, M.; Prud'Homme, R.E.; Schultz, J. *J. Polym. Sci.: Part B: Polym. Phys.* **1999**, *37*, 2985.

(5) (a) Keddie, J.L.; Jones, R.A.L.; Cory, R.A. *Faraday Discuss.* **1995**, *98*, 219. (b) Forrest, J.A; Dalnoki-Veress, K.; Dutcher, J.R. *Phys. Rev. E* **1997**, *56*, 5705. (c) Jones, R.A.L. *Current Opinion in Colloid and Interface Science* **1999**, *4*, 153. (d) Grohens, Y.; Hamon, L.; Reiter, G.; Soldera, A.; Holl, Y. *Eur. Phys. J. E* **2002**, *8*, 217.

(6) (a) Gandhi, K.; Salovey, R. *J. Appl. Polym. Sci.* **1990**, *41*, 2103. (b) Pekel, N.; Guven, O. *J. Appl. Polym. Sci.* **1998**, *69*, 1669. (c) Feng, J.; Odrobina, E.; Winnik, M.A. *Macromolecules* **1998**, *31*, 5290. (d) Kobayashi, M.; Rharbi, Y.; Brauge, L.; Cao, L.; Winnik, M. *Macromolecules* **2002**, *35*, 7387.

(7) Torchia, D.A. *J. Magn. Reson.* **1978**, *36*, 91.

(8) Qiu, X.; Mirau, P. *J. Magn. Res.* **2000**, *142*, 183.

(9) Brandrup, J.; Immergut, E.H. Polymer Handbook 3rd Ed., John Wiley and Sons Inc., New York, 1989.

(10) Pawsey, S.; Yach, K.; Halla, J.; Reven, L. *Langmuir* **2000**, *16*, 3294.

(11) Raftery, D; Chmelka, B.F. *NMR Basic Principles and Progress* **1994**, *30*, 111.

(12) Stengle, T.R.; Williamson, K.L. *Macromolecules* **1987**, *20*, 1430.

(13) Fontana, B.J.; Thomas, J.R. *J. Phys. Chem.* **1961**, *65*, 480.

(14) van der Beek, G.P.; Cohen Stuart, M.A.; Fleer, G.J.; Hofman, J.E. *Macromolecules* **1991**, *24*, 6600.

(15) Gao,W.; Dickinson, L.; Grozinger, C.; Morin, F.G. ; Reven, L. *Langmuir* **1996,** *12,* 6429-6435.

(16) Wang, J.; Paszti, Z.; Even, M.A.; Chen, Z. *J. Am. Chem. Soc.* **2002**, 124(24), 7016.

(17) Fleer, G.J.; Stuart, M.A.; Scheutjens, J.M.H.M.; Cosgrove, T.; Vincent, B. *Polymers at Interfaces*; Chapman & Hall: London, 1993.

(18) Zhongde, X.; Hadjichristidis, N.; Fetters, L.J. *Macromolecules* **1984**, *17*, 2303.

(19) Dickinson, L. Ph.D. Thesis, McGill University, 1998.

(20) Nasreddine, V.; Chijiwa, S.; Reven, L. *Manuscript in preparation.*

(21) Sperling-Ischinsky, K.; Veeman, W.S. *J. Braz. Chem. Soc.* **1999**, *10(4)*, 299.

(22) Kobayashi, M.; Rharbi, Y.; Brauge, L.; Cao, L.; Winnik, M. *Macromolecules* **2002**, *35*, 7387.

(23) Reid, C.G.; Greenberg, A.R. *J. Appl. Polym. Sci.* **1990**, *39*, 995.

(24) Tsagaropoulos, G.; Eisenberg, A. *Macromolecules* **1995**, *28*, 6067.

(25) Xiong, M.; Wu, L.; Zhou, S.; You, B. *Polym. Int.* **2002**, *51*, 693.

Chapter Seven

Conclusions, Contributions to Knowledge, and Future Work

7.1 Preface

This is the last chapter of the thesis and consists of the conclusions and contributions to knowledge, suggestions for future work for the three adsorbed polymers: PEA, PPAC, and PnBMA, and a list of publications and conference presentations.

7.2 Poly(ethylene-co-acrylic acid) (PEA)

7.2.1 Conclusions and Contributions to Knowledge

This is the first solid-state NMR study of an adsorbed semi-crystalline random copolymer where the copolymer belongs to an important class of materials used as adhesion promoters. For this system we have shown that the chain conformation is a function of sticker density and not coverage. NMR dynamics studies support our proposed picture of the microscopic structure of this strongly bound random copolymer: The ordered component observed in the ^{13}C CP-MAS spectrum of adsorbed PEA5% is due to chain folding and looping of the PE segments rather than segments lying flat on surface. ^{129}Xe NMR spectroscopy has traditionally been used to characterize bulk polymers, but we have demonstrated that xenon chemical shifts and spin-lattice relaxation times can yield morphological information about adsorbed polymers. Xenon probes two different environments in these samples: microvoids for low polymer loadings and a bulk-like polymer medium for high loadings.

7.2.2 Suggestions for Future Work

The study of the chemisorption of PEA on zirconia provided a model system to investigate how sticker concentration affects the chain conformation of adsorbed random copolymers. An extension to this work would involve studies of similar copolymers adsorbed on alumina (the substrate more commonly used in industry) and a comparison of the results with the adhesion data found in the literature. Such a comparison is needed to better understand the correlation between microscopic properties of adsorbed polymers and their optimum adhesive properties. The effect of the binding strength on the dependence of the surface conformation on sticker density rather than coverage should be tested. Poly(ethylene vinyl acetate) (EVA), another commonly used adhesion promoter, would be a good candidate for such a study since EVA is expected to bind more weakly to metal oxides than acrylic acid based copolymers. It would also be of interest to compare the adsorption behavior of the random copolymers with that of the block copolymer analogues. Performing ^{129}Xe NMR studies on these systems could also provide useful morphological information.

7.3 Poly(propylene-co-acrylic acid) (PPAC)

7.3.1 Conclusions and Contributions to Knowledge

The study of adsorbed PPAC, also a semi-crystalline, acrylic acid based random copolymer, was carried out to determine the effect of the hydrophobic component, in this case polypropylene (PP), on the surface chain conformation and mobility and how it differs from PEA, adsorbed on the same substrate. We observed that the ^{13}C CP-MAS spectra of adsorbed PPAC contain splittings normally attributed to chain-chain interactions in certain polymorphs of crystalline PP. These splittings in the ^{13}C NMR spectra of adsorbed PPAC were more resolved that in the spectrum of the bulk copolymer. We attribute this to recrystallization of unbound PP segments between sticker groups. The weaker surface bonds and thus weaker topological constraints as compared to PEA adsorbed on zirconia, may allow for the crystallization of the PP segments during the adsorption process.

7.3.2 Suggestions for Future Work

A more detailed investigation is needed to better understand the changes in the chain packing accompanying the adsorption of PPAC, especially since it is unexpected that the polymer chain order would increase upon adsorption. Our suggestion that this behavior is associated with the relatively weak binding strength of PPAC can be tested by increasing sticker groups density (acrylic acid content) or the type of sticker group to promote stronger binding to prevent any recrystallization of the PP component. Investigating the adsorption of copolymers of atactic PP would also be preferable due to the absence of crystallization, which complicates the analysis.

7.4 Poly(n-butyl methacrylate) (PnBMA)

7.4.1 Conclusions and Contributions to Knowledge

This work represents the first solid-state NMR study of adsorbed PnBMA. We have chosen this polymer to examine the effect of the bulky butyl side-chain on the structure and dynamics of the adsorbed polymer for comparison with PMMA, whose adsorption behavior has been extensively studied. Adsorption of PnBMA from both THF and CH occurred with partial hydrolysis of the ester groups and with no conformational changes. This is attributed to the local stiffness arising from the high fraction of trans sequences in bulk PnBMA, which is mainly syndiotactic. We have observed that the non-hydrolyzed ester side-chains segregate to the polymer/air interface, as indicated by the appearance of a new methyl peak in the ^{13}C NMR spectra of adsorbed PnBMA. ^{129}Xe NMR experiments showed that at low loadings, xenon fills the microvoids created by the aggregation of zirconia, whereas in filled samples, a signal for xenon adsorbed in the polymer appears. The xenon linewidths of the zirconia filled PnBMA samples are correlated with the temperatures of DSC-detected thermal transitions, which increase as a function of filler content and then decrease for the highest filler content measured. Whereas NMR relaxation data of adsorbed and filled samples indicated enhanced mobility compared to bulk PnBMA, the ^{129}Xe NMR parameters of the filled samples are consistent with restricted chain mobility on a larger length scale. This is suggested to be due to particle bridging by the long loops and tails of adsorbed PnBMA.

7.4.2 Suggestions for Future Work

The ^{129}Xe NMR study of the zirconia-filled PnBMA was preliminary. The morphological changes of the zirconia filler should also be investigated by transmission electron microscopy (TEM). Variable temperature ^{13}C NMR studies of the filled PnBMA samples heated above the transition temperatures would help determine if the DSC-detected transitions are associated with any chemical changes, such as further hydrolysis of the ester side-chains.

There has been only one ^{129}Xe NMR study of a filled polymer system reported in the literature and this study was also preliminary in nature and did not address the effect of the filler on the glass transition. A study of a system where the effect of the filler on the thermal behavior of the polymer is well known is needed to evaluate the usefulness of the ^{129}Xe NMR experiment to characterize filled polymers. A ^{129}Xe NMR systematic study, with variation of the particle size and filler content, should be complemented by other techniques, which detect the glass transition such as dynamic mechanical measurements.

7.5 Work published, in preparation, and presented in Conferences

*7.5.1 Publications**

1) Nasreddine, V.; Morin, F.; Reven, L. "Dynamics of Adsorbed Polyethylene-Acrylic Acid Copolymers: A Solid-State NMR Study" *submitted to Polymer.*

2) Nasreddine, V.; Chijiwa, S.; Reven, L. "Probing the Morphology of Adsorbed Random Copolymers: A ^{129}Xe NMR study" *submitted to Langmuir.*

3) Nasreddine, V.; Morin, F.; Reven, L. "^{13}C Solid-State NMR of Adsorbed Polypropylene-Acrylic acid Copolymers" *to be submitted.*

4) Nasreddine, V.; Genereux-Vincent, T.; Reven, L. "Dynamics and Morphology of Poly(n-butyl methacrylate) Films: A ^{13}C and ^{129}Xe Solid-state NMR study" *to be submitted.*

5) Nasreddine, V. "Being a Teaching Assistant: There is More to It Than Just Teaching" ***(Invited Paper)*** (Student Affiliates, American Chemical Society) *InChemistry* **2002,** *12(2)*, 22.

6) Nasreddine, V; Reven, L. "Chain conformation and dynamics of polypropylene/acrylic acid copolymer films" *Polymer Preprints* (American Chemical Society, Division of Polymer Chemistry) **2002,** *43(2)*, 1392.

7) Nasreddine, V; Chijiwa, S; Reven, L. "^{129}Xe NMR of adsorbed random copolymers" *Polymer Preprints* (American Chemical Society, Division of Polymer Chemistry) **2002,** *43(1)*, 390.

8) Nasreddine, V; Reven, L. "Chain conformation, dynamics, and morphology of adsorbed random copolymers" *Polymer Preprints* (American Chemical Society, Division of Polymer Chemistry) **2002,** *43(1)*, 373.

9) Nasreddine, V.; Halla, J.; Reven, L. Conformation of Adsorbed Random Copolymers: A Solid-State NMR and FTIR-PAS Study. Department of Chemistry, McGill University. *Macromolecules* **2001,** *34*, 7403.

7.5.2 Conferences

1) Victor Nasreddine **"General chemistry tutorials: For a better understanding of chemical principles"** Abstracts of Papers, *224th ACS National Meeting*, Boston, MA, United States, August 18-22, 2002 (2002), CHED-319.

2) Victor Nasreddine, Tobie Genereux-Vincent, and Linda Reven **"Dynamics and morphology of poly(n-butyl methacrylate) films"** Abstracts of Papers, *224th ACS National Meeting*, Boston, MA, United States, August 18-22, 2002 (2002), COLL-175.

3) Victor Nasreddine, Sachiko Chijiwa, and Linda Reven **"^{129}Xe NMR of Adsorbed Random Copolymers"** Abstracts of Papers, *223rd ACS National Meeting*, Orlando, FL, United States, April 7-11, 2002 (2002), POLY-058.

4) Victor Nasreddine and Linda Reven **"Chain Conformation, Dynamics, and Morphology of Adsorbed Random Copolymers"** Abstracts of Papers, *223rd ACS National Meeting*, Orlando, FL, United States, April 7-11, 2002 (2002), POLY-041.

5) Victor Nasreddine, Sachiko Chijiwa, and Linda Reven **"Dynamics and Morphology of Adsorbed Random Copolymers: A Solid-State NMR Study"** *2nd Alpine Conference on Solid-State NMR,* Sept. 9-13 2001, Chamonix-Mont Blanc, France. Poster Presentation. (Alma Matter Travel Award)

6) Victor Nasreddine, Sachiko Chijiwa, and Linda Reven **"Dynamics and Morphology of Adsorbed Random Copolymers: A Solid-State NMR Study"** *84th CSC Conference and Exhibition,* May 26-30 2001, Montreal, Quebec. Oral Presenation.

7) Linda Reven[1], Susan M. DePaul[2], Hans W. Spiess[2], Victor Nasreddine[1], Leonard N. J. Rodriguez[1], and Christopher J. Barrett[1] **"High Resolution Solid-State NMR of Adsorbed Polymer Films"** *Experimental NMR Conference*, Orlando, Florida, 2001. [1]McGill University, Canada. [2]Max Planck Institute for Polymer Science, Mainz, Germany.

8) Victor Nasreddine, Sachiko Chijiwa, and Linda Reven **"Probing the Dynamics of Adsorbed Random Copolymers: A Solid-State NMR study"** *30th Canadian High Polymer Forum*, August 13-16 2000, Aylmer, Quebec. Poster Presentation.

9) Victor Nasreddine, Sachiko Chijiwa, and Linda Reven **"A Solid-State NMR Study of Adsorbed Polyethylene-co-Acrylic Acid Random Copolymers"** *42nd Rocky Mountain Conference on Analytical Chemistry, NMR Symposium*, July 30-August 3 2000, Broomfield, Colorado, USA. Poster Presentation.

7.6 Appendices

7.6.1 Calculation of domain sizes

This is a sample calculation of the domain sizes of bulk PEA5% using spin diffusion data obtained from the Dipolar filter experiment.

$\Delta\upsilon_{1/2}$ (rigid) = 57000 Hz, $\Delta\upsilon_{1/2}$ (mobile) = 20000 Hz, $F_{\text{rigid}} = 0.52$, $F_{\text{mobile}} = 0.48$,

$\sqrt{t_M^S} = 5.6\ \text{ms}^{1/2}$ (the intersection point of the rising linear part and the plateau),

$\alpha = 45000$ Hz.

The spin diffusion coefficients D_R and D_M of the rigid and mobile components have the following expressions:

$$D_R = \frac{1}{12}\sqrt{\frac{\pi}{2\ln 2}}\left\langle r^2\right\rangle \Delta\upsilon_{1/2}$$

and

$$D_M = \frac{1}{6}\left\langle r^2\right\rangle [\alpha\,\Delta\upsilon_{1/2}]^{1/2}$$

and the r value used is 0.225 nm. Substituting all the values in these expressions will yield the values of the spin diffusion coefficients: D_R = 0.36 nm^2/ms and D_M = 0.25 nm^2/ms. The square root of the effective spin diffusion coefficient is defined as:

$$\sqrt{D_{eff}} = \frac{\sqrt{D_{mobile}\, D_{rigid}}}{(\sqrt{D_{mobile}} + \sqrt{D_{rigid}})/2}$$

$\sqrt{D_{eff}} = 0.55$ nm^2/ms. The domain size of the mobile component is:

$d_{mobile} = 2\varepsilon(D_{eff}\,\tau^{s}{}_{m}/\pi)^{1/2}/F_{rigid}$ where $F_{rigid} = 1 - F_{mobile}$

resulting in a value of 7 nm as shown in Table 2.2. The value of the domain size of the rigid component of bulk PEA5% is obtained from the same expression but replacing F_{rigid} by F_{mobile}.

This same calculation is used to determine the domain sizes of the adsorbed loadings 450PEA5% and 100PEA5%. Domain sizes determined by using this expression:

$$D = \frac{\Delta\nu_{1/2}\,(r_{HH})^2}{3}$$

for the spin diffusion coefficients for both components yielded similar values within the limit of experimental error.

7.6.2 ^{13}C Spin-lattice relaxation data

A. <u>PEA5%:</u>

The spin-lattice relaxation times were determined by fitting the data to a monoexponential function.

i) T_{1C}(disordered) PEA5% = 0.5 sec.

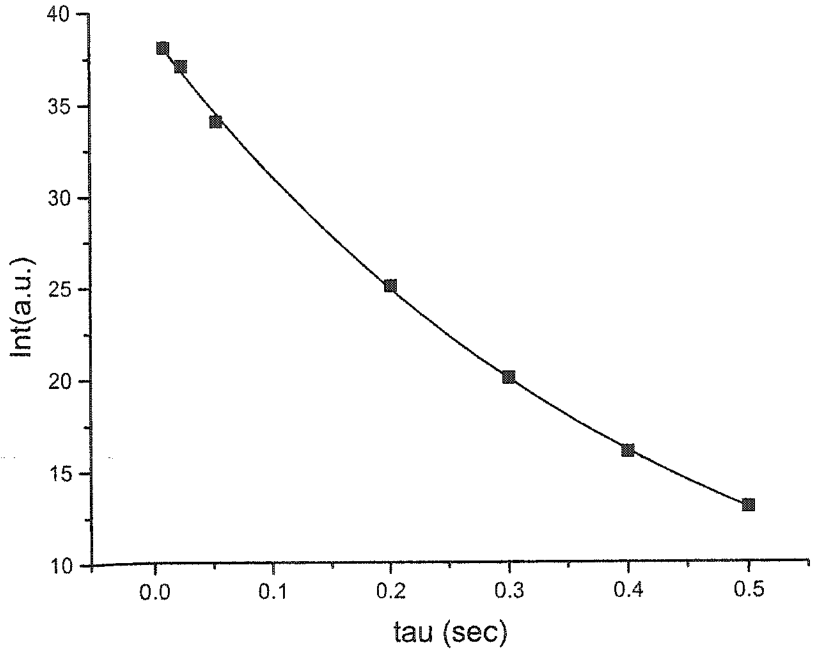

ii) T_{1C}(ordered) PEA5% = 115 sec.

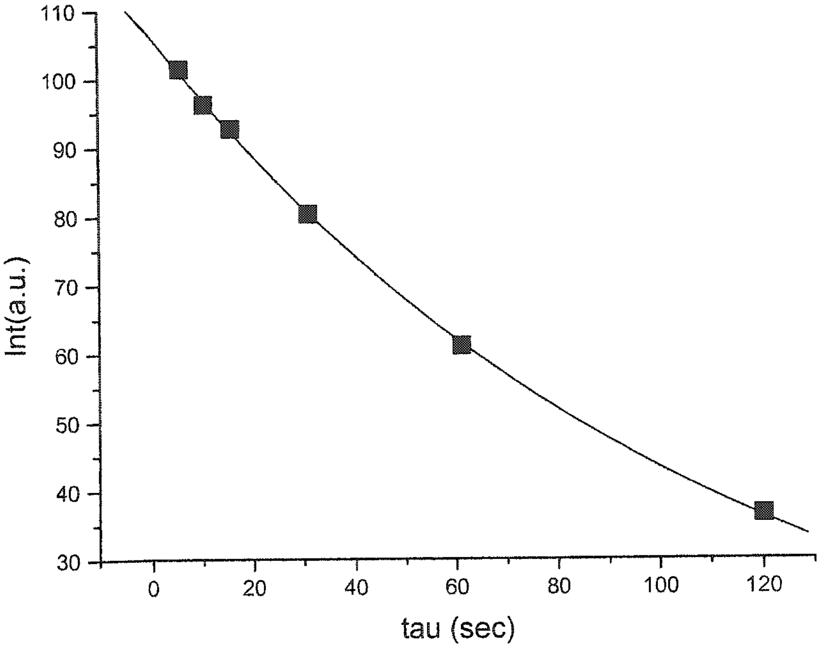

B. <u>100PEA5%:</u>

i) T_{1C}(disordered) 100PEA5% = 0.6 sec.

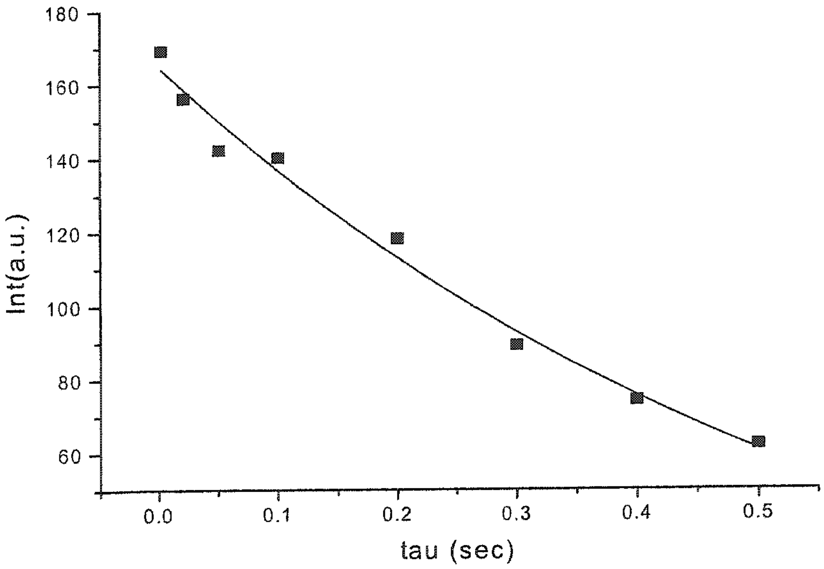

ii) T_{1C}(ordered) 100PEA5% = 103 sec.